TRIBHUVAN UNIVERSITY

INSTITUTE OF ENGINEERING

PULCHOWK CAMPUS

THESIS NO: M-109-MSMDE-2024-2026

Influence Of Internal Heat Loads and Ceiling Heights on The Effectiveness Of Displacement and Mixing Ventilation for a Room

by

Ananda Lamichanne

A THESIS

SUBMITTED TO THE DEPARTMENT OF MECHANICAL AND AEROSPACE ENGINEERING IN PARTIAL FULFILLMENT OF THE REQUIREMENTS FOR THE DEGREE OF MASTER OF SCIENCE IN MECHANICAL SYSTEMS DESIGN AND ENGINEERING

DEPARTMENT OF MECHANICAL AND AEROSPACE ENGINEERING

LALITPUR, NEPAL

MAY , 2026

COPYRIGHT

TRIBHUVAN UNIVERSITY

INSTITUTE OF ENGINEERING

PULCHOWK CAMPUS

DEPARTMENT OF MECHANICAL AND AEROSPACE ENGINEERING

The undersigned certify that read and recommended to the Institute of Engineering for acceptance, a thesis report entitled **"Influence of Internal Heat Loads and Ceiling Heights on the Effectiveness of Displacement and Mixing Ventilation for a Room"** (080MSMDE002), in partial fulfillment of the requirements for the degree of Master of Science in Mechanical Systems Design and Engineering.

Supervisor: Vishwa Prasanna Amatya

Associate Professor

Department of Mechanical and Aerospace Engineering

Supervisor: Dr. Durga Bastakoti

Assistant Professor

Department of Mechanical and Aerospace Engineering

Er. Rajan Bhusal

Senior Engineer/HVAC Consultant

VIE TEC Private Limited

Tribhuvan University
Institute of Engineering
Department of Mechanical and Aerospace Engineering
Pulchowk Campus

Committee Chairman, Sudip Bhattrai, Ph.D.

Head of Department

Department of Mechanical and Aerospace Engineering

Date: April 24, 2026

ABSTRACT

This study presents a comprehensive numerical investigation of the influence of internal heat load distribution and ceiling height on the performance of mixing ventilation (MV) and displacement ventilation (DV) systems in an enclosed space. A 3D computational fluid dynamics (CFD) model was developed to simulate airflow, temperature distribution, and contaminant transport within a representative room environment under steady-state conditions. The analysis incorporates both thermal comfort and indoor air quality (IAQ) parameters, evaluated through indices such as thermal comfort number, air quality number, local mean age of air, and contaminant removal effectiveness. The study considers multiple ventilation configurations, including ceiling-based mixing ventilation, mixing ventilation with floor-level exhaust, and displacement ventilation. First, a 3m envelope space with define cooling load was chosen, and the internal heat gain values were distributed among the occupant zone and other zones in different ratios. Then the three types of ventilation arrangements were simulated under the different heat distribution cases. MV was seen as the least affected by internal heat gain distribution, with its thermal comfort number, air quality number, and ADI just having 4.35%, 7.55%, and 6%. The MV with floor outlet was moderately affected by internal heat gain distribution, with its thermal comfort number, air quality number, and ADI just having 5%, 16.87%, and 10.5%.DV was seen as the most affected by internal heat gain distribution, with its thermal comfort number, air quality number, and ADI just having 4%, 20%, and 13.7 %. Likewise, the three types of ventilation systems were also simulated under three ceiling heights: 2.6m, 3 m, and 3.4m with a constant internal heat gain. The MV was seen with decreasing thermal comfort, air quality number, and so the ADI as the ceiling height increased. On the contrary, DV was seen with increasing thermal comfort number, air quality number, and ADI as the ceiling height increased. The existence of a minimal ceiling height for DV under a given heat gain was also determined using Ri. For the chosen case of heat gain, 3m was seen as the minimal height required for stable DV. Likewise, for heat distribution as well, the existence of a plume strength limit was determined for stable stratification, which was at 76.36% heat gain from the occupant space. Thus, both MV and DV were seen to be affected by internal heat gain distribution and ceiling height. However, the sensitivity of DV to internal heat gain and ceiling height was significant when compared to MV.

ACKNOWLEDGEMENT

First and foremost, I would like to express my sincere gratitude to my supervisors, Associate Professor Vishwa Prasanna Amatya and Assistant Professor Dr. Durga Bastakoti, for their unwavering support and guidance throughout the research period. Their expertise, valuable feedback, and thoughtful suggestions have significantly contributed to completing this thesis and greatly improved the quality of my work.

I am also thankful to the members of my thesis committee for their insightful comments and suggestions, which greatly improved the quality of this work. My heartfelt thanks go to the faculty and staff of the Department of Mechanical and Aerospace Engineering, Pulchowk Campus, for providing a supportive academic environment and the necessary resources to carry out this research.

I would also like to thank my friends Binod KC and Amrtit Bhandari for unwavering support and love. Your presence has made this journey enjoyable and enlightening. Lastly, I owe my deepest gratitude to my family for their unwavering love and support. Their understanding and sacrifices have been the foundation of my academic pursuits.

TABLE OF CONTENTS

TABLE OF FIGURES

LIST OF TABLES

LIST OF ABBREVIATIONS and ACRONYMS

ACH	Air Change per Hour
ADI	Air Distribution Index
AIVC	Air Infiltration and Ventilation Center
Ar	Archimedes Number
ASHRAE	American Society of Heating, Refrigeration, and Air Conditioning Engineers
CBE	Center for Built Environment
CFD	Computational Fluid Dynamics
CLTD	Cooling Load Temperature Difference
CFM	Cubic Feet per Minute
DV	Displacement Ventilation
HVAC	Heating, Ventilation, and Air Conditioning
IAQ	Indoor Air Quality
MV	Mixing Ventilation
RTS	Radiant Time Series
Ri	Richardson Number

Chapter 1: INTRODUCTION

1.1 Background

Space ventilation has been a long-standing practice. It is a systematic process, centred on the supply and removal of air from enclosed spaces so that the temperature, humidity, and occupant comfort can be maintained within them. The concept of ventilation initially started as natural ventilation, where louvers, windows, and vents were used for supplying and removing air from a space. However, the ventilation system evolved as the need for more efficient and effective thermal comfort arose, leading to the introduction of mechanical ventilation, where ducts, fans, and HVAC systems are used in combination with a natural ventilation system. As time went by, the ventilation system also went through numerous advancements, thus leading to several highly efficient ventilation strategies, both natural and mechanical. The development became even more rapid during the times of the Industrial Revolution, as a proper HVAC system is very crucial for every industry. Coming today, HVAC is a big industry, with around 20% of global energy used for this purpose(Yadav et al., 2024). The percentage is even higher for buildings, where 50% of energy is used in HVAC. The percentage is also high for industrial sectors, where a considerable percentage of total energy consumption is shared by HVAC. This number is the result of an increasing global population and the even more increasing demand for HVAC for space ventilation.

The long evolution and advancement in the field of space ventilation, especially HVAC, have also introduced several standard procedures for ventilation design strategies. On top of that, there has also been introduced a concept like energy efficiency, indoor air quality has also been introduced, which has provided a slightly different dimension on how a ventilation system should be viewed aside from thermal comfort. Today, there are various strategies for designing a ventilation system for an occupancy room, namely, Mixing Ventilation (MV), Displacement Ventilation (DV), and unidirectional ventilation. There can also be seen a ventilation system like hybrid ventilation, which is a combination of both Mixed with HEPA local exhaust. Out of them, the MV and DV are the most used ones. This has all to do with their design simplicity and operational effectiveness. The operation of MV and DV is very different. Mixing

Ventilation (MV), as the name suggests, is a ventilation strategy where high-velocity air is supplied through the diffuser located at the ceiling, promoting uniform mixing of the room air with fresh air, thus maintaining a stable thermal condition within the room. In contrast, Displacement Ventilation (DV) is a ventilation strategy where a low velocity fresh air is supplied through a diffuser placed near the floor, which then rises vertically relying on buoyancy-driven flow, thus removing the heat and contaminants from the room. That way, the Displacement DV creates a stratified airflow, which also prevents mixing between the clear air zones and the contaminated zones.

Though ventilation is often seen as a strategy to maintain thermal comfort, a well-designed ventilation system can also add benefits like the prevention of airborne contaminants and, thus, pathogen transmission. The performance of a room is highly affected by the design of the room's ventilation system. It's the ventilation system design that determines the room's airflow contaminant removal capacity, thermal comfort, temperature distribution, etc, which are among the major parameters denoting the effectiveness of a room. Thus, a ventilation system design highly affects the effectiveness of an occupancy room, be it inlet air speed, diffuser placement, or duct sizing. So, designing an efficient ventilation system for an occupancy room is a very rigorous process with numerous factors to be considered to come out with the best possible ventilation system design. Thus, it may often be quite complex to choose a specific type of ventilation system for a given space, as there are lots of matrices to be looked after, ranging from energy efficiency, indoor air quality, thermal comfort, and many more.Figure 1 shows a basic illustration of MV and DV.

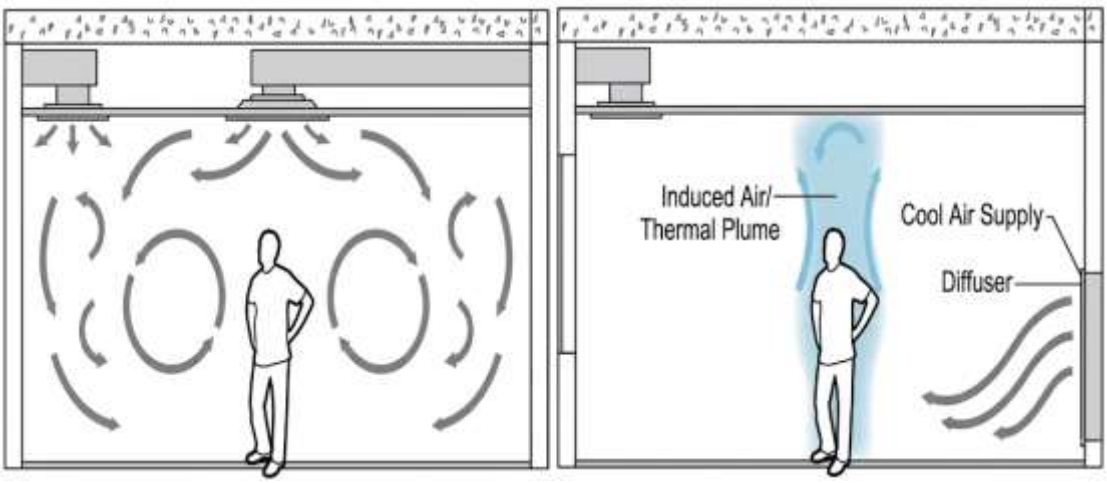

Figure 1:Mixing ventilation(left) and displacement ventilation(right)

MV and DV also differ in terms of their design. The selection between Displacement DV and MV is often determined by factors like heat load level, contaminant control, ceiling height, desired thermal comfort, temperature control, energy efficiency, room geometry, etc, as both displacement strategies come with their advantages and shortcomings. However, in many instances, MV can be chosen because of the simpler design procedure based on turbulent jet theory, straightforward design charts, predictability, etc, which isn't the case with displacement ventilation. Thus, MV is the more popular ventilation strategy as of now, despite numerous studies suggesting DV with superior indoor air quality and energy efficiency.

1.2 Statement of Problem

The most common types of ventilation today, Mixing Ventilation MV and DV, have been among the most studied and compared for a long time. MV, in particular, is among the most used ventilation systems for general-purpose space ventilation, all thanks to its simple design procedure, controllability, and lots of standardized design guidelines. It also comes with features like temperature uniformity, low ceiling height performance, flexible installation, etc. On the other side, DV, which is still considered superior in aspects like energy efficiency, indoor air quality, noise, ventilation effectiveness, air quality in the breathing zone, etc. Since MV is about facilitating a uniform thermal environment and DV is about facilitating a non-uniform thermal environment, it may often become tricky to compare their suitability for a given space. Though there are some Air Distribution Index-based frameworks for their comparison. Factors such as the spatial distribution of internal heat gain, which is a vital factor affecting IAQ and thermal comfort in systems like DV, are often not accounted. Without accounting for the uneven distribution of internal heat gain along the envelope height, comparison of MV and DV may not be reliable. With a full-scale experimental study turning out to be expensive, a Computational Fluid Dynamics (CFD) study combined with the Air Distribution Index(ADI) Method may help compare these ventilation systems. Such a comparison can give the suitability of the two ventilation systems not only based on ADI but also based on how the internal heat gains are lumped in the envelope space, which is a very common case in reality.

1.3 Objectives of Research

1.3.1 Main objective

The main objective is to compare the thermal comfort and IAQ performance of mixing and Displacement Ventilation under different vertical enclosure heights and sensible cooling loads

1.3.2 Specific objectives

The specific objectives are as follows:

i. To model and simulate a room with mixing and displacement ventilation separately
ii. To study the influence of vertical enclosure height on the thermal comfort and IAQ perfromance of mixing and displacement ventilation
iii. To analyze the influence of internal heat load distribution on the thermal comfort and IAQ performance of mixing and displacement ventilation
iv. To compare thermal comfort and IAQ perfromance of MV and DV under different scenarios
v. To determine the suitability of MV and DV under different heat load gains.

Chapter 2: LITERATURE REVIEW

2.1 Displacement Ventilation

Displacement Ventilations is defined as a method of air distribution that uses a slow-moving stream of fresh air from the floor to displace warmer, waste air, which accumulates at the ceiling and is expelled through exhaust panels(Sinopoli, 2010). This approach enhances HVAC efficiency by maintaining cooler air in the occupied lower area and promoting natural convection. This type of ventilation relies on the fundamental physics of buoyancy-driven flow, resulting in thermal stratification, which helps the warm air and pollutants rise above and exhaust through the ceiling outlet, with the cold fresh air staying at the floor. That way, the Displacement Ventilation creates a zone, an upper zone near the ceiling where all the contaminants and warm air get accumulated, and the lower zone near the occupants is left with clean, fresh air. Thus, the Displacement Ventilations very helpful towards indoor air quality and is often regarded as very energy-efficient ventilation. The process diagram for displacement ventilation is given in Figure 2.

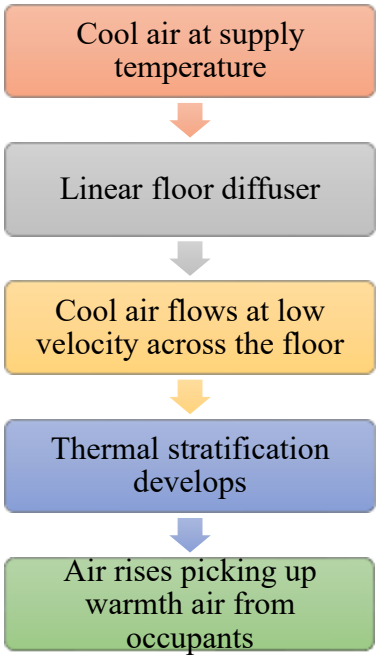

Figure 2: Illustration of the displacement ventilation mechanism

Introduced back in the mid-20th century, this method gained popularity back in 1960; however, it was taken over by Mixing Ventilation because of its simpler design process,

controllability, etc. However, the ventilation strategy gained popularity again since the 1990's, with the majority of its application seen around places with high ceilings and cooling loads due to its superior air quality and energy efficiency. Figure 3 depicts a more detailed figure of airflow in displacement ventilation.

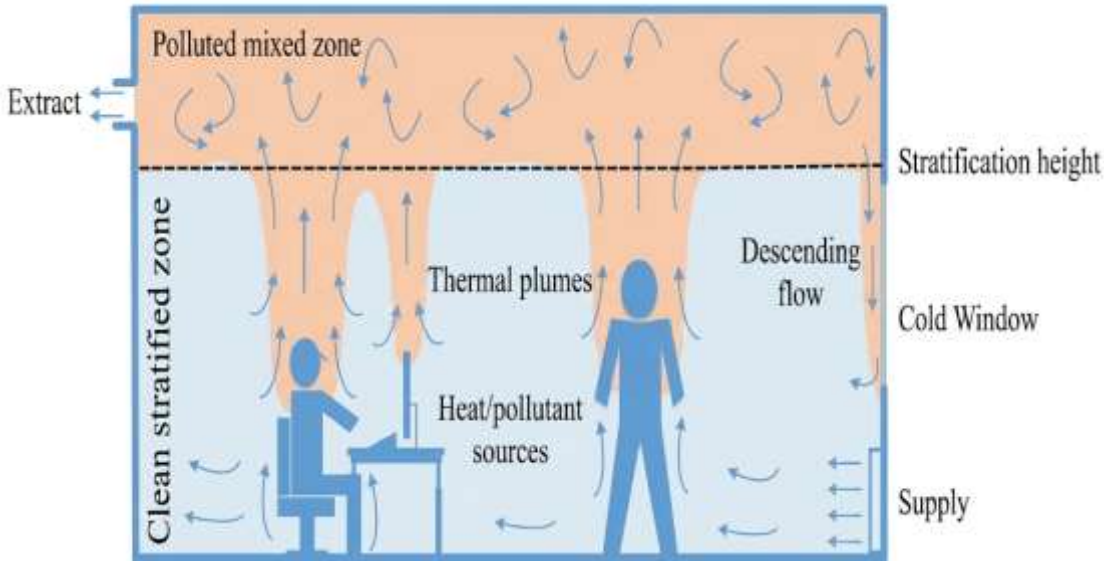

Figure 3: Pictorial illustration of displacement ventilation(Javed et al., 2021)

The application of Displacement Ventilation is still not so popular in common households as its design method is quite complex because of its reliance on buoyancy-driven flow, where even slight errors may disrupt the thermal stratification. On top of that, this type of ventilation is regarded as suitable when the ceiling has some height to it. However, there has been various research around the development of a simplified design approach for displacement ventilation, which can even be applicable in common places.

2.1.1 Design of Displacement Ventilation

A typical Displacement Ventilation system has a diffuser placed near the floor level wall(Franco & Schito, 2020), with low velocity air, 0.1-0.3 m/s (normally 1-3°C below the desired room temperature), which is determined based on ASHRAE Standard 55 draft comfort limits. The main point is the introduction of a slightly cooler air that can attain buoyancy from the occupant and heat sources rising upward. That way, the buoyancy forces lift the air to the higher side of the room, thus pushing the lighter contaminated air out of the ceiling outlet. So, it provides good air quality within the

breathing zone as the contaminants are left above the breathing zone due to thermal stratification. Still, there are factors like door opening and human movements that may often cause mixing between the stratified air layers. Figure 4 shows a basic illustration of the displacement ventilation mechanism.

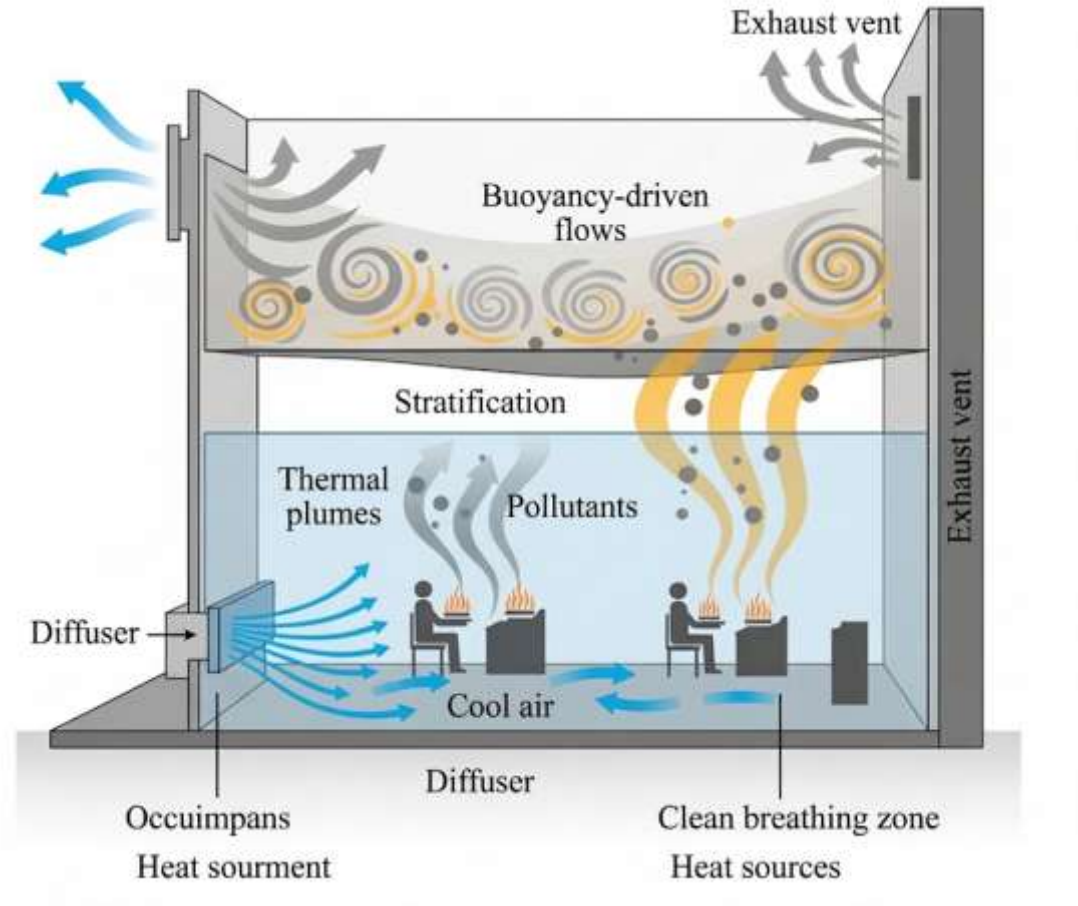

Figure 4: Displacement ventilation

A displacement ventilation in a space generally has three zones as given below:

a) Establishment Zone (I)

It is the zone in Displacement Ventilation where the velocity of air is the same as that of the air coming out of the diffuser. The air velocity at the establishment zone is dependent on the diffuser design.

b) Acceleration Zone (II)

The acceleration zone is the zone where the air velocity starts becoming higher than the supply velocity due to the temperature difference between the room and the supplied

air. As the flow drops along the floor, the thickness of the jet also decreases, and air spreads all over the floor, forming a jet-like flow. That way, the air supplied to the room spreads all over the floor space.

c) Gravity zone (III)

The gravity zone in displacement ventilation is characterized by a decrease in the velocity of the air. It is in the latter half of this zone that the air attains thermal plumes from the room occupant and equipment and starts deflecting upward before it spreads further. It is the last zone in the displacement ventilation. A detailed illustration of the different zones in DV is given in Figure 5.

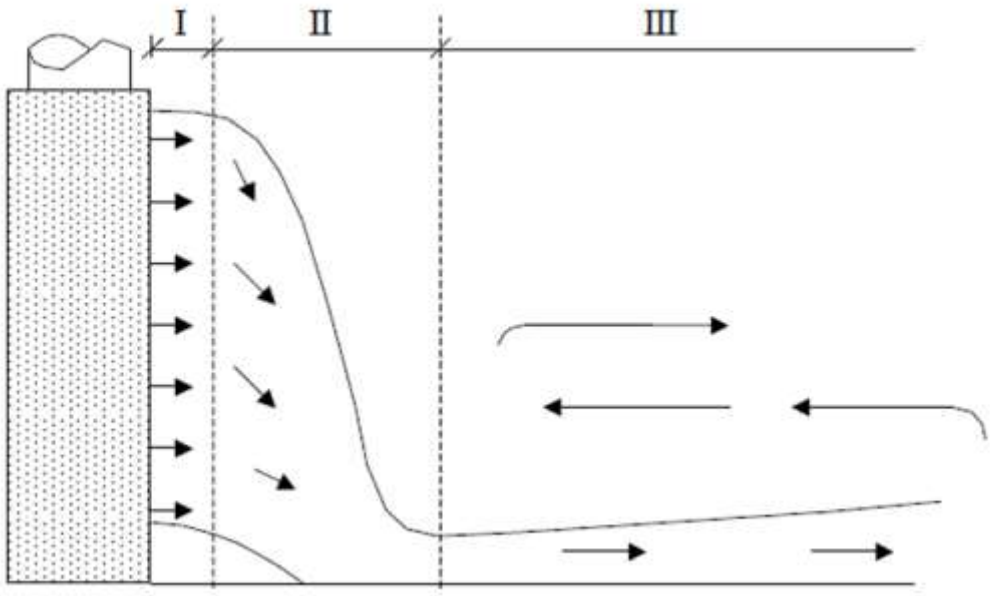

Figure 5: Different zones in displacement ventilation

2.1.2 Buoyancy Driven Flow

Buoyancy-driven flows are those groups of flows that are driven by the density difference within the fluid. These types of flows are very common in buildings where they can act as a passive ventilation, where a pressure gradient takes in colder air from the lower opening and warm air goes out of the upper located exhaust. The buoyancy force in these flows is mainly the result of the vertical difference between the inlet and outlet, and the indoor and outdoor air temperature difference. Thus, the process allows a very steady technique for space ventilation, though it may require a highly precise

location for the inlet, outplacement, and their vertical height difference. This mechanism is also the driving force behind the displacement ventilation. There is also a simplified mathematical formula relating the various factors affecting the ventilation flow rate in buoyancy-driven flows.

$$\text{Flow rate } (Q_S) = \quad Cd \times A \times \sqrt{2gH\frac{Ti-To}{Ti}} \qquad (1)$$

Where,

C_d = Discharge coefficient

A = Area of openings

Ti = Inlet air temperature

To = Outdoor air temperature

2.2 Mixing Ventilation

Mixing Ventilation is a widely used air distribution method in HVAC systems, where fresh air is introduced at high velocity into a space, promoting thorough mixing with the existing indoor air. This approach ensures uniform temperature and humidity levels throughout the room, creating a consistent and comfortable environment for occupants. In Mixing Ventilation systems, air is typically supplied through ceiling-mounted diffusers, which discharge air at high velocity. The forceful air jets induce turbulence, causing the fresh air to mix with the room's existing air. This results in a homogeneous distribution of air temperature and quality across the space. This type of ventilation system is designed based on the jet momentum theory, making it very easy to design and control, though it may sometimes be found with issues like contaminant dispersion. This type of ventilation is mainly suitable for lower ceiling rooms with variable heat loads, though it is more than capable of delivering thermal comfort at higher ceiling heights, provided the diffuser is provided with enough throw to reach the occupant zone. A basic illustration of the mixing ventilation mechanism is given in Figure 6.

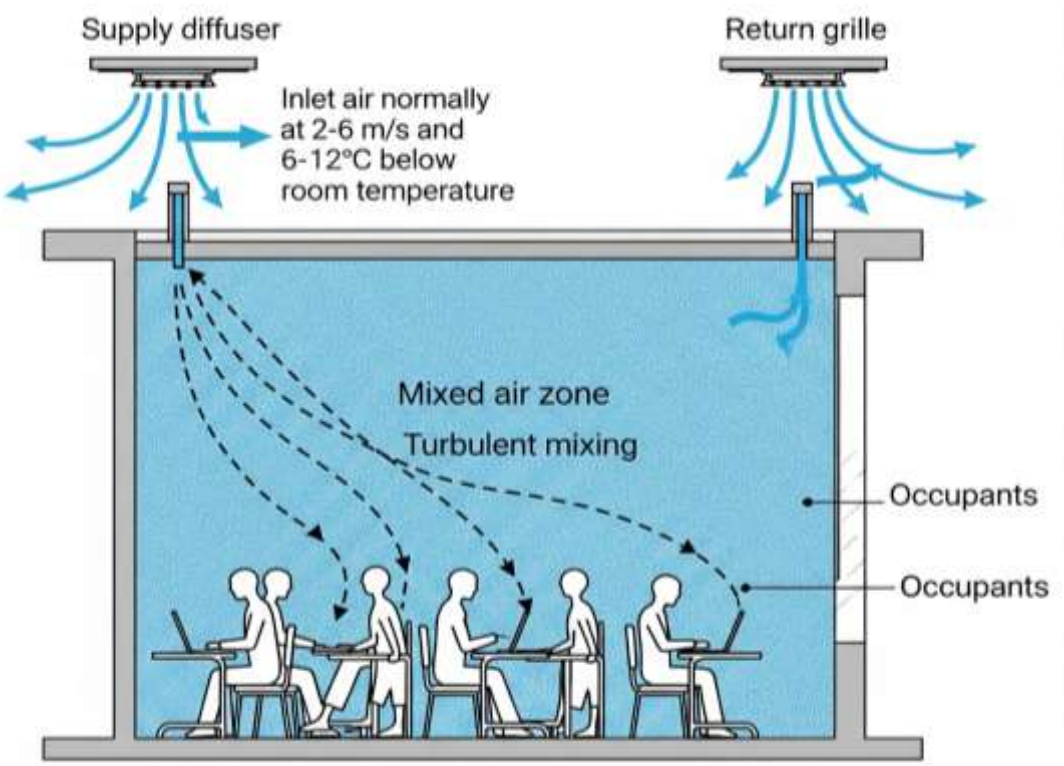

Figure 6: Mixing ventilation

Though this type of ventilation is mainly used in low-height ceiling spaces, there have been significant studies regarding its effectiveness compared to displacement ventilation for application in spaces with mid-range ceiling heights and heat loads. satisfactory results that agreed well with those available in the literature. Compared to the mixing ventilation system, the displacement ventilation system demonstrated a high draft risk at the floor level. In the breathing zone, the displacement ventilation system showcased a uniform temperature in the cubicles. A comparative illustration of contaminant distribution for mixing and displacement ventilation is given in Figure 7.

Figure 7: Contaminant distribution in mixing and displacement ventilation

2.2.1 Jet Momentum Theory

It is the basic principle that governs the operation of an MV process, explaining how an air jet with a higher velocity is introduced into a room to generate a detailed mixing. The MV design process is based on this theory to ensure uniformity in ventilation and thermal comfort throughout the space via mixing. This theory can be used in the design of MV under different scenarios, as given below:

i. Jet Behavior based on momentum:

Normally, the supply jet in the ventilation system has some momentum to it that determines the effective throw of the diffuser. The higher the momentum, the better the mixing, as it allows a deeper air penetration within the space. As the jet entrains the surrounding its expansion slows based on momentum conservation laws.

ii. Surface effect:

When a diffuser is located near the walls or ceiling surfaces, the surface effect comes into play, allowing the jet to stick to the surface and reach more horizontal distance with less entrainment. That way, using the application of a diffuser on surfaces helps reduce downward drafts and increase the coverage.

iii. Buoyancy Effects:

A substantial difference between the supplied air temperature and the room air temperature may often lead to buoyancy, thus altering the trajectory of air jets as cool air falls with the warm air rising up. Thus, a proper balance must be desired between variables like Archimedes' number, pressure, velocity outlet geometry, and temperature difference to allow consistency in the throw and direction of the jet.

iv. Balance of inlet jet momentum for control:

Under cases like side wall MV design, control can also be attained through the balancing of opposing jets' momentum to attain more stability in the airflow, thus reducing drafts or uneven distribution of air.

v. Multiple Jets Interaction

This idea is based on the combination of multiple supply jets to merge their momentum, thus causing a confluent jet capable of further penetration and much more efficient mixing compared to a single jet. This kind of approach is implemented in a ventilation system that blends both DV and MV.

All these five points are combined together under the jet momentum criteria to come up with an MV system that has uniformity in air distribution, optimal jet performance without over ventilation, minimal drafts, and optimal occupant comfort.

2.2.2 Major Zones in Mixing Ventilation

Much literature classifies a Mixing Ventilation -equipped space into four distinct zones to explain the air jet behaviour in the space.

i. Zone 1:

This is the zone in the ventilation space that comes just after the diffuser outlet. The velocity of air is thus the same as the velocity at the outlet of the diffuser. Here, the flow is axial with no change in the air jet velocity.

ii. Transition zone:

The transition zone is the zone in the ventilation space where the inlet air velocity starts decreasing and starts spreading all over the ventilation space. Thus, this zone is the zone from which the actual mixing process tends to initiate.

iii. Turbulent mixing zone:

This is the most important zone in the ventilation space. In this zone, the air jet goes through fully developed turbulence, which causes efficient air mixing within the zone. The zone spans about 25 to 100 outlet diameters.

iv. Terminal zone:

This is the zone in the ventilation space where the occupants are located. In this zone, the air velocity decreases significantly, and it goes through a uniform distribution all over the space.

This jet momentum theory is also useful for adjusting the throw to these four zones for optimal thermal comfort within the space.

2.3 Ventilation rate (Q)

Ventilation rate is the volume of air supplied or removed from the given space in one second. It quantifies the effectiveness of the building space ventilation system towards maintaining a good indoor air quality(Franco & Schito, 2020). It is normally expressed in terms of m^3/s or L/s. The basic idea of ventilation is based on the relation that exists between the pollutant concentration and the ventilation rate within the space. Thus, the ventilation rate is dependent on factors like occupancy, pollution level, building type, activity level, etc. The basic ventilation rate Q required in a simplified space to create a steady oxygen concentration is given as

$$\text{Ventilation rate (Q)} = \frac{V}{C - Co} \qquad (2)$$

Where V is the volume of pollution, with C and C_o being the concentration of pollutants at indoor and Outdoor. Ventilation rate also determines the Air Change per Hour (ACH) for a given space, which is a relative measure of the frequency of complete replacement of room air with fresh air within one hour(Pan et al., 2024). The relation between the ventilation rate, volume of pollutant, and Air Change per Hour (ACH) is given as

$$\text{ACH} = \frac{Q \times 360}{V} \qquad (3)$$

2.4 Thermal Comfort

According to ASHRAE Standard 55, thermal comfort can be defined as " that condition of mind which expresses satisfaction with the thermal environment". Thus, thermal comfort is a measurable variable, though it may sometimes be seen as an abstract concept. The standard ASHRAE-based quantification of thermal comfort is based on two interrelated indices called Predicted Percentage of Dissatisfaction(PPD) and Predicted Mean Vote (PMV). The standard definition of thermal comfort is based on six primary parameters and other additional local parameters so that a global comfort could be attained, avoiding localized discomfort. It includes parameters like air temperature, mean radiant temperature, metabolic rate, air speed, clothing insulation, and relative humidity(Almesri et al., 2013a).

2.4.1 Predicted Mean Vote (PMV)

Predicted Mean Vote, or simply PMV, is an index used for the quantification of a group of people regarding the thermal environment. It is based on a scale that ranges from -3 to 3, with the negative three denoting cold and the positive three denoting hot, while zero indicates neutral. There is a systematic formula for the computation of this value. The indicator balances six major factors related to the ventilation system, which are given as follows:

1. Air temperature
2. Humidity
3. Air speed
4. Metabolic rate (Activity)
5. Clothing Insulation
6. Mean Radiant Temperature

$$\text{Predicted Mean Vote (PMV)} = (0.303 \cdot e^{-0.036M+0.028}) \cdot L \qquad (4)$$

Where,

M = Metabolic rate (W/m^2)

L = Thermal Load (W/m^2)

The idea is focused on adjusting the thermal condition in such a state that it is acceptable to the majority of the people in the group. This value can be computed using various tools like CBE, Pythermalcomfort, etc.

2.4.2 Predicted Percentage Of Dissatisfaction (PPD)

The Predicted Percentage OF Dissatisfied or simply PPD is a variable that is used for quantifying the percentage of individuals who are likely to feel uncomfortable under the provided thermal environment using the PMV(Dos Reis et al., 2022). Thus, the value is simply related to PMV based on the empirical formula proposed by Fanger.

$$PPD = 100 - 95 \times e^{-0.03353PMV^4 - 0.2179PMV^2} \qquad (5)$$

The formula basically provides an estimation for the percentage of occupants that are expected to be dissatisfied with the thermal conditions. It has a non-linear deviation, where even a slight PMV deviation from the neutral value, 0, could lead to substantial discomfort. In normal practice, a ventilation design is aimed at keeping the PPD value below 10%, where the PMV value ranges from -0.5 to 0.5, to make the system comfortable for the maximum number of occupants.

2.4.3 Age Of Air

In HVAC, the age of air is a parameter that signifies the average time for a freshly supplied air to reach a ventilated space's specific location, normally the breathing zone. For instance, air coming from the ceiling diffuser might take 50 seconds to reach the occupant's level(Ning et al., 2016). The metric is very important as it is a strong basis for signifying the efficiency of the system in displacing stale air with fresh air. During CFD analysis, this can be determined assuming air as a tracer and integrating its residence time, which helps identify the location where there is any sort of air stagnation or poor ventilation. In normal practice, the mean age of air is maintained in such a way that a minimum of 95% of the occupied zone is kept below a desired threshold, thus helping maintain optimum indoor air quality.

2.4.4 Draft/ Draught

In HVAC, draft is defined as the unwanted and uncomfortable local cooling effect on the human body resulting from airflow. In some instances, air at a certain speed, if

allowed to flow around certain parts of the human body, may give a chilly sensation, though the room's air temperature might be fine(Ribeiro et al., 2015). ASHRAE guidelines recommend an upper limit for the draft rates in normal office conditions of less than 10 % of occupants feeling discomfort. Many CFD-based approaches use the computation of d localized zir speeds and weigh them against the comfort criteria to ensure the system against any draft zones. Draft is mainly affected by the throw of the diffuser; thus, a precise design of the diffuser can help eliminate the draft.

2.4.5 Effective Draft Temperature (EDT)

Effective draft temperature, or simply draft temperature, is a thermal comfort metric that integrates the temperature and airspeed difference to analyze the degree of local discomfort resulting from cool airflow. The value is computed for various points under the given ventilated space to ensure both the temperature difference and airflow are kept under the allowable limit, thus minimizing the discomfort that might result from cold air movement or breezes.

2.4.6 Vertical Temperature Difference

Vertical temperature difference, or simply thermal gradient, quantifies the vertical temperature difference between the ankle level and head level of the occupant within the ventilated space. The accepted value for thermal gradient is based on ASHRAE Standard 55, which is less than 3 ^{o}C for seated occupants to prevent cold feet and warm head. The value of thermal gradient could be very high for tall spaces like warehouses, atria, due to strong stratification, sometimes over 10 °C, reducing the energy efficiency and thermal comfort. The effects can be mitigated using techniques such as destratification fans. CFD-based vertical temperature layers can also be used to limit the thermal gradient within the comfort limit.

2.4.7 Envelope Height

Envelope height is the total height of the enclosed space that separates the indoor and outdoor spaces. It is thus the distance from the lowest reference level to the top of the conditioned space boundary. Envelope height is often an important parameter when analyzing the ventilation space. For a stratification-based ventilation system like DV, it is very important to relate the envelope height and the ventilation system, as it is the

envelope height that decides how well the ventilation system is affected by the space geometry. In many studies, they may often perform dimensionless scaling of the envelope space using its height so that a dimensionless correlation can be built for scaling.

2.4.8 Air Distribution Index(ADI)

Air Distribution Index (ADI) is a combined parameter used in quantifying the effectiveness of the given ventilation system. ADI basically measures the ventilation system's effectiveness in maintaining thermal comfort and desired indoor air quality. Thus, ADI is often expressed as the sum of the Thermal Comfort Number ($N_{T.C}$) and Air Quality Number ($N_{A.Q}$). These two values in combine gives a number that quantifies how well the ventilation system is at maintaining thermal comfort and indoor air quality.

$$ADI = [(1\frac{|S|}{3})\times\mathcal{E}_t](N_{T.C})+[(\frac{\tau_n}{\bar{\tau_p}})\times\mathcal{E}_c](N_{A.Q}) \quad (6)$$

Where,

|S|= Overall Thermal Sensation

$\mathcal{E}_t$= Ventilation Effectiveness (Heat Removal)

$\mathcal{E}_c$= Ventilation Effectiveness (Contaminant Removal)

τ_n=Room time constant (1/ACH)

$\bar{\tau_p}$= Local Mean Age Of Air

Ventilation effectiveness ($\mathcal{E}_c$) is the measure of the ventilation system's ability of removing contaminant from the envelope space as given below

$$\text{Ventilation Effectiveness } (\mathcal{E}_c) = \frac{C_o - C_i}{C_m - C_i} \quad (7)$$

Where

C_o= Contaminant Concentration at Outlet

C_i= Contaminant Concentration at Inlet

C_m= Mean Contaminant Concentration at Occupied Zone

The other way to look at the effectiveness of an air distribution system is the effectiveness of the system in allowing the thermal exchange between the supply and room air. This type of effectiveness is known as ventilation effectiveness for heat removal (ε_t), as shown below.

$$\text{Ventilation Effectiveness } (\varepsilon_t) = \frac{T_o - T_i}{T_m - T_i} \qquad (8)$$

Where

T_o= Temperature at Outlet

T_i= Temperature at Inlet

T_m= Mean Temperature at Occupied Zone

2.4.9 Richardson Number

The Richardson number (Ri) is a crucial dimensionless parameter used to evaluate the stability of indoor airflow and determine whether thermal stratification will persist. It represents the ratio of buoyancy forces to inertial (momentum) forces. In the context of your thesis research, it serves as a mathematical indicator of the "strength" of the displacement effect. In a ventilation context, Ri determines the dominant heat transfer mechanism. When Ri is greater than, buoyancy forces dominate, allowing for the stable stratification necessary for successful Displacement Ventilation (DV). Conversely, when Ri is less than 1, forced convection (momentum) dominates, leading to the uniform mixing characteristic of Mixing Ventilation (MV). Mathematically, it is defined as given below:

$$\text{Richardson Number (Ri)} = \frac{g \times \beta \times \Delta T \times H}{U^2} \qquad (9)$$

Where,

g = Acceleration due to gravity (m/s^2)

β = Thermal expansion coefficient ($0.0033k^{-1}$ for air)

ΔT= Temperature difference (K)

H= Characterisitics length (Height of the room)

U = Velocity of air at inlet (m/s)

2.5 Related Past Works

2.5.1 Mixing ventilation found with high airborne contaminant dispersion risk.

(Ribeiro et al., 2015) investigated air ventilation system to analyze the dispersion of contaminants in a human-occupied space. Two ventilation systems, namely Mixing Ventilation and displacement ventilation, were studied following a numerical simulation. The room model used for the simulation was dimensioned in a way that it could represent a common purpose room found around shopping malls and in apparel stores. The simulation considered one occupant to be sick with releasing contaminant gas from the mount. The case of contaminant dispersion from the sick occupant to the room was studied individually under both mixing and displacement ventilation, one after another. The simulation results showed that Mixing Ventilation with a higher risk of contaminants dispersion, which adds risk of spreading to the airborne environment.

2.5.2 Displacement ventilation is found with better air change efficiency

(Qiu-Wang & Zhen, 2006) performed a numerical and experimental study of indoor climate in a classroom using Mixing Ventilation and displacement ventilation. Thus, the paper presented the indoor climate for both summer and winter under different occupant densities. It initially measured the thermal comfort in a half-sized classroom with four air suppliers. Later, the measured data were taken for CFD validation for the entire classroom. Comparison was then made between the indoor climate parameters using CFD simulations under different air diffusers, for both summer and winter. The study showed that Displacement Ventilation had the best performance for the occupied zone with an air change efficiency of 1.4 compared to 1 for the others. Also, the perforated duct diffusers were found to be unstable, causing a high local draft of around 20% at the occupied zone.

2.5.3 Local mean age of air as an indicator of indoor air quality in a ventilation system.

(An et al., 2024) comparison of the local mean age of air between displacement and Mixing Ventilation for office heating conditions during winter. Here, Displacement

Ventilation and Mixing Ventilation systems were briefly compared against each other with the local mean age of air as the comparative index for specifying the indoor air quality under the two ventilation strategies. A CFD-based simulation was done for the room under both simulations, one after another, and all the major thermal comfort metrics, temperature distribution, and mean age of air were recorded. The simulation study found the Displacement Ventilation system to be more effective at improving the indoor air quality in winter when compared to the Mixing Ventilation system. The implementation of a Displacement Ventilation system was seen with the additional benefit of more uniform air temperature variation for the office space. Thus, the application of Displacement Ventilation with a ceiling fan coil unit and Aps on the floor was regarded as a reliable means for the enhancement of indoor air quality.

2.5.4 Airborne transmission in low-ceiling rooms under displacement ventilation.

The danger of COVID-19 airborne transmission in low-ceiling spaces, like lift cabins, with mechanical Displacement Ventilation was assessed in this study using computational fluid dynamics (CFD) models(Wang & Hong, 2023). The models considered the impact of respiratory jet dynamics and the thermal environment of the human body on infection transmission. In order to lower the danger of airborne transmission in those kinds of confined indoor environments, a potential mitigation method based on ventilation thermal management was suggested using the study's findings. The results showed that the effectiveness of removing airborne particles (Ep) grows quickly at first, hits a plateau (Ep,c) at a critical ventilation rate (Qc), and then increases more slowly after Qc as the ventilation rate (Qv) rises. Because of the greater interaction between the ventilation and the thermal plume produced by the inhabitants or infectors, the Qc for low-ceiling rooms was lower than that of high-ceiling rooms. Ep was strongly associated with the thermal stratification fields, which are defined by the temperature gradient, thermal interface height, and temperature iso-surface height, according to additional examination of the flow and temperature fields. The simulations also showed that Qc and Ep,c are impacted by the infector's location relative to the ventilation inlet or outlet. Higher Qc and lower Ep,c are seen when the infector is in a corner because there may be a local hot spot of high infection risk there. Finally, based on the simulations, it suggested a ventilation thermal management technique to lower the danger of airborne transmission in low-ceiling rooms by raising the ventilation

temperature. The results suggested that the transmission of airborne illnesses in restricted places is significantly influenced by the heat environment.

2.5.5 Displacement ventilation and mixing ventilation systems regarding ventilation effectiveness in offices.

(Makris et al., 2025) investigated the effect of supply and exhaust position on contaminant distribution for an office with a ceiling cooling system using a CFD tool. It included a detailed comparison between the Mixing Ventilation and Displacement Ventilation with either wall or floor-mounted diffusers. The exhaust vent in Mixing Ventilation was located directly under the opposite wall or supply, whereas the Displacement Ventilation had an outlet at the ceiling or upper sidewalls. In addition to the success of pollutant removal and the percentage of unsatisfied PD [%], a discomfort index for the entire office was created and computed. Furthermore, it was discovered that Displacement Ventilation does not always provide higher-quality air than Mixing Ventilation, and that its effectiveness was very susceptible to the location of exhaust grilles in the scenario under consideration.

2.5.6 Airborne particle exposure in an office with mixing and displacement ventilation.

(Liu et al., 2022) studied the various thermal comfort parameters like particle number concentration, air velocity, and temperature for an office under two types of ventilation systems, Displacement Ventilation and Mixing Ventilation, under different rates of ventilation. The study found that Displacement Ventilation, with better indoor air quality, when weighed against Mixing Ventilation, was due to a substantial stratification effect in displacement ventilation. An increment in ventilation rate was found with a reduction in particle contamination under both ventilation systems, though the relation between the two parameters was not proportional. As the ventilation rate increased from 2 ACH to 4 ACH and 6 ACH, the mixing ventilation system was seen with a reduction in particle concentration by 20 % and 60 %. However, the same rate of increment in ventilation for Displacement Ventilation only reduced the concentration by 10 % and 40%. Thus, the Mixing Ventilation was seen with a ventilation effectiveness of 1, while the number was much higher for the displacement ventilation.

The computational outcomes were found to be in good agreement with the experimental data.

2.5.7 Numerical study on the influence of a ceiling height

(Li et al., 2025)found that thermal stratification in a given room's displacement ventilation is highly affected by its ceiling height. This stratified airflow was enhancing indoor air quality and thermal comfort by ensuring that the cooler, fresher air remains in the occupied zone, while warmer, contaminated air is efficiently removed. This phenomenon can also be related to the fact that it is the ceiling height in the displacement ventilation that often becomes decisive for how much od stratification or separation is between the lower clean breathing zone and above the contaminated stratified zone. Thus, a case with much lower ceiling height may often lead to mixing between the upper contaminated air layer and the lower zone as there may not be enough vertical space above the occupant zone for the hot air to accumulate.

2.5.8 Computational fluid dynamics for comparison of mixing and displacement ventilation

(Khan, Mboreha, et al., 2022) concentrated around a comparative analysis of Mixing Ventilation (MV) and Displacement Ventilation (DV) for an indoor space, resembling an office room with a total of four occupants. The work was based on a 3D Computational Fluid Dynamics (CFD) simulation, using FLUENT. Metrics like temperature distribution, airflow pattern, velocity distribution, etc., served as the major basis for comparing the two ventilation strategies for the given office room. The work found the Displacement Ventilation (DV), with better overall thermal compared under identical rate of supply when compared against its mixing counterpart.

2.5.9 Application of Computational Fluid Dynamics (CFD) in thermal comfort analysis.

Mixing and displacement ventilation systems incorporated into a fitting room were investigated using Computational Fluid Dynamics (CFD)(Khan, Bennia, et al., 2022). The main findings showed very satisfactory results that agreed well with those available in the literature. When compared against each other, the Displacement Ventilation (DV) was seen with a higher draft rate around the floor level. The finding could even be

correlated with the fact that displacement ventilation takes in cool air at the floor level, which may often cause a draft around ankles due to direct exposure to incoming cool air velocity, if it isn't designed properly. However, it was also the displacement ventilation, on the other hand, that showed a very uniform temperature profile within the cubicles.

2.5.10 Higher flow rates in displacement ventilation does not guarantees better indoor air quality

(Yang et al., 2022) employed a Direct Numerical Simulation (DNS) to study mechanical ventilation under a wide range of ventilation rate, Q (0.01-0.1 m^3/s/person). A cooler lower zone beneath an upper warmer zone having height h, which also depends on the ventilation rate. The study found the scaling relation $h \sim Q^{3/5}$, as suggested in previous works for weaker ventilation. For the value of Q within this regime, the CO_2 concentration was seen to decrease. But, for too strong ventilation, the value h was seen to be insensitive to ventilation rate, with the decrease in CO_2 concentration towards the ambient range. Under these Q values, pollutant concentrations were very low, with further dilution having no significant effect. The phenomenon was seen as a case where vertical kinetic energy for the ventilation flow was significant compared to the potential energy of thermal stratification.

2.5.11 Numerical and experimental study on the indoor climate in a classroom with mixing and displacement air distribution methods.

(Zhao et al., 2022) assessed indoor air quality and thermal conditions for a classroom under half-occupied winter and fully occupied summer scenarios under three variations of mixing and displacement air distribution strategies. The work was all based on CFD simulation, with a later stage focused on comparison of simulation outcomes with a full-scale test, for some validation. A summarized finding of the work concluded the indoor air quality to be best under the displacement ventilation. This was presented by the fact that displacement ventilation was the one found with minimal age or air and the highest air change efficiency in the occupied zone. On the other side, the ceiling diffuser-based air distribution strategy was seen as effective in maintaining good indoor thermal conditions in the occupied zone.

2.5.12 An air distribution index for assessing the thermal comfort and air quality in uniform and nonuniform thermal environments.

A New Air Distribution Index (ADI) was developed for the performance analysis, including both thermal comfort and indoor air quality(Almesri et al., 2013a). This performance index can be used for analyzing the performance of both uniform and non-uniform thermal environments. It was basically the sum of thermal comfort number($N_{T.C}$) and air quality number ($N_{A.Q}$). Thus, this performance index will be very helpful for comparing the performance of Displacement Ventilation (DV) and Mixing Ventilation (MV) under different heat loads and ceiling heights.

2.5.13 CFD Models for the prediction of temperature difference and ventilation effectiveness with displacement ventilation.

The performance of an air distribution system was looked at in two different scenarios(Jiang & Haghighat, 1993). This was because air distribution systems are normally expected to deliver in two different ways: the first being the ventilation effectiveness, which basically signifies the effectiveness of the air distribution system in removing contaminants from the space. The ventilation effectiveness (ε_c) is generally determined using the formula

Chapter 3: METHODOLOGY

3.1 Conceptual Framework

A CFD-based numerical approach was used to study the effect of internal heat gains on the effectiveness of MV and DV, about thermal comfort and IAQ parameters. Thus, the work included a detailed sequential methodology allowing clarity, consistency, and clarity of result.

Theoretical computations were first done for the ventilation space, in this case, the room, to determine the incoming air flow rate and temperature. Since the study was done for two different types of ventilation methods, namely DV and MV, it required two separate calculations. A Cooling Load Temperature Difference (CLTD) method was used for determining the cooling load for the room, and thus the Cubic Feet Minute (CFM), and the incoming air temperature for the room. This was the value later used in the CFD simulation for the room under Mixing Ventilation (MV). The CLTD method was based on the ASHRAE Handbook.

DV had a slightly different method for cooling load calculations, as it can be done in various ways based on thermal comfort, IAQ requirements(Lastovets et al., 2020).The most common one in the method given by the Air Infiltration and Ventilation Center (AIVC). This method allowed computation based on the important simulation parameters required for the displacement ventilation, such as the supply air velocity, supply air temperature, etc.

Once all the theoretical computations were finished, a detailed CAD model was developed for the given room, including detailed room dimensions, supply diffuser, outlet, and occupants. The sensible and latent heat gain inside the room space were represented through the cell zone conditions. The developed model, when taken to simulation under the boundary condition determined through the theoretical computation, will give the realistic operation condition for the given space under the determined cooling load.

The CFD framework solved the governing equations of mass, momentum, and energy conservation under steady-state conditions. A turbulence model was employed to account for turbulent transport within the indoor airflow field. In addition to that, scalar transport equations were also used to simulate water vapor, carbon dioxide dispersion,

and to compute the Local Mean Age of Air (LMAA), which serves as a key ventilation effectiveness metric. The simulations were done using consistent solver settings and boundary conditions across all scenarios to ensure that performance differences arise solely from configuration changes or occupancy variation.

The detailed conceptual flowchart for the project is given in Figure 8 which will all start with a detailed literature review.

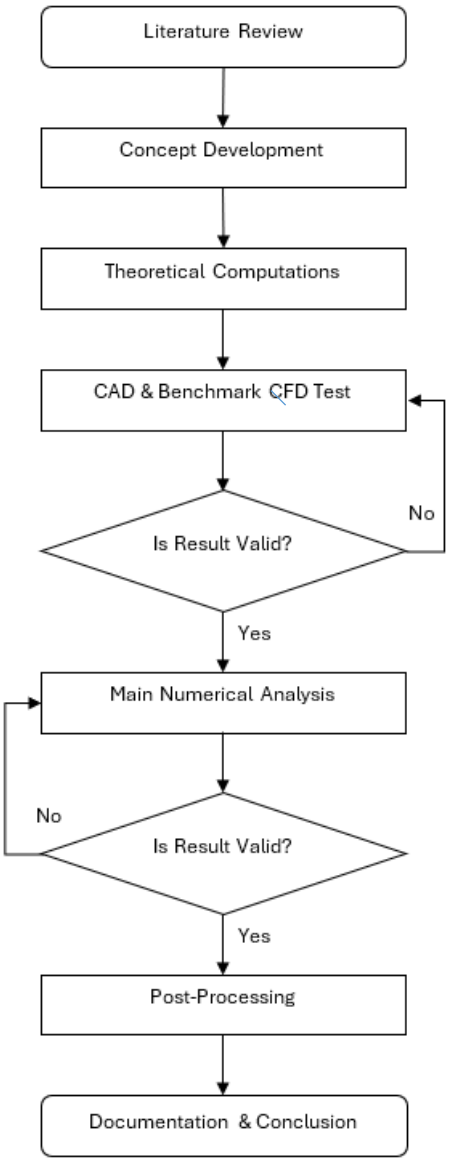

Figure 8: Conceptual flowchart

3.2 Theoretical Computations

The total cooling load of the space was defined as the summation of all sensible and latent heat gains entering the conditioned space at the design hour.

$$Q_{\text{total}} = Q_{\text{sensible}} + Q_{\text{latent}} \tag{9}$$

The sensible component accounts for the temperature change of air and surfaces, while the latent component accounts for moisture removal due to humidity differences.

3.2.1 Envelope Heat Transfer

Heat transfer through opaque building elements was calculated using steady-state conduction theory. The total thermal resistance of a multilayer wall is:

$$R_{\text{total}} = R_{si} + \left(\frac{L_1}{k_1} + \frac{L_2}{k_2} + \cdots + \frac{L_n}{k_n}\right) + R_{so} \tag{10}$$

Where R_{si} and R_{so} represent internal and external surface resistances respectively, L is layer thickness (m), and k is thermal conductivity (W/m·K).

$$U = \frac{1}{R_{\text{total}}} \tag{11}$$

The sensible heat gain through opaque surfaces is then computed as:

$$Q_{\text{wall}} = U_{\text{wall}} \times A_{\text{wall}} \times (T_{\text{out}} - T_{\text{in}}) \tag{12}$$

Where U_{wall} is the overall heat transfer coefficient (W/m²·K), A_{wall} is exposed wall area (m²), T_{out} is outdoor dry-bulb temperature (°C), and T_{in} is indoor setpoint temperature (°C).

For glazing systems, conductive heat gain was similarly determined:

$$Q_{\text{window,cond}} = U_{\text{glass}} \times A_{\text{window}} \times (T_{\text{out}} - T_{\text{in}}) \tag{13}$$

Solar heat gain through glazing was computed using the Solar Heat Gain Coefficient (SHGC) method:

$$Q_{\text{window,solar}} = A_{\text{window}} \times SHGC \times E_{\text{vertical}} \times IAC \quad (14)$$

Where $SHGC$ represents the fraction of incident solar radiation transmitted as heat, Vertical is solar irradiance on a vertical surface (W/m²), and IAC is the interior attenuation coefficient due to shading devices.

3.2.2 Internal Heat Gains from Occupants

Occupant heat gain is divided into sensible and latent components based on metabolic activity.

$$Q_{\text{people,sensible}} = \sum \left(N_i \times q_{\text{sensible},i}\right) \quad (15)$$

$$Q_{\text{people,latt}} = \sum \left(N_i \times q_{\text{latent},i}\right) \quad (16)$$

Where N_i represents the number of occupants of type i, q_{sensible} and q_{latent} represent per-person heat emission rates (W/person).Table 3-1shows the details of the space, including its basic dimensions and geographical location, which was used for cooling load calculation using CLTD.

Table 3-1: Details for the room

Parameters	Value
Length(m)	7
Breadth(m)	3.8
Height(m)	3
Latitude	28.20° N
Longitude	83.98° E

The computed room loads can basically be categorized into sensible heat load and latent heat load. CLTD was based on peak design conditions, considering the peak outdoor temperature and solar gain, which remain for a very short period of the day, as values like temperature, solar gain, and humidity change throughout the day. Considering such factors and thermal lag, a steady external heat gain value was taken for the CFD

simulation, 30% of the external heat gain determined using the CLTD realistic ACH value. The internal heat gain, on the other hand, was kept the same as calculated manually. The details for the sensible and latent heat load from the space are given in the. The space has a sensible heat load of around 70 w/m^2, which is a typical value for operation of both DV and MV, thus allowing a good comparison. The space also had a latent load of 409 W resulting from nine occupants. The desired room temperature and humidity were 297K and 50% RH. With the given sensible and latent load value, the supply air RH and temperature were found to be 291 K and 55%, as determined from the psychometric chart. The CFM value was 350 CFM, which gave an ACH value of around 7, which is normal for a classroom or conference space like this, as per ASHRAE 62 and 55. The details for the supply conditions and cooling loads are given in Table 3-2.

Table 3-2: Supply details

S.No	Parameter	Values
1.	Sensible Load(W)	1862
2.	Latent Load(W)	409
3.	Inlet Supply Temperature	291
4.	Inlet Supply Humidity	55%
5.	CFM	350

3.3 CAD and Benchmark CFD Test

3.3.1 Geometry Definition and Modeling of Space

A detailed CAD model was developed for the chosen space to represent the real room conditions. The classroom was modeled as a rectangular enclosure with internal dimensions of 7 m (length) × 3.8 m (width) × 3 m (height). The dimensions were based on the dimensions of the actual space for which the cooling loads were previously calculated, with some simplifications in the geometry to ensure meshing and numerical stability.

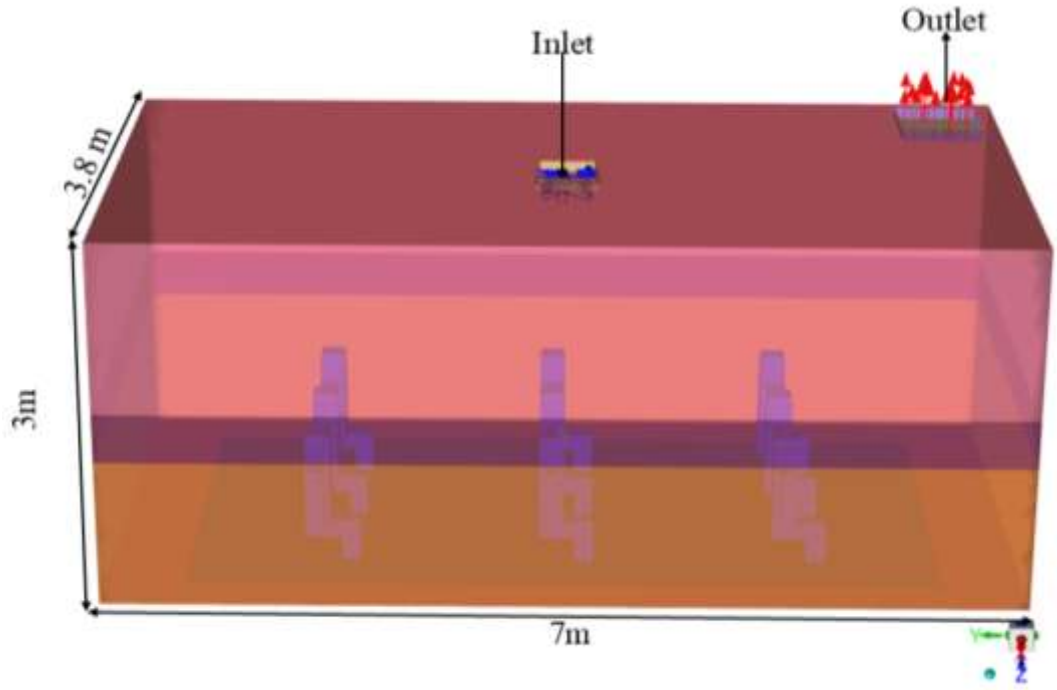

Figure 9: CAD model for mixing ventilation with ceiling outlet

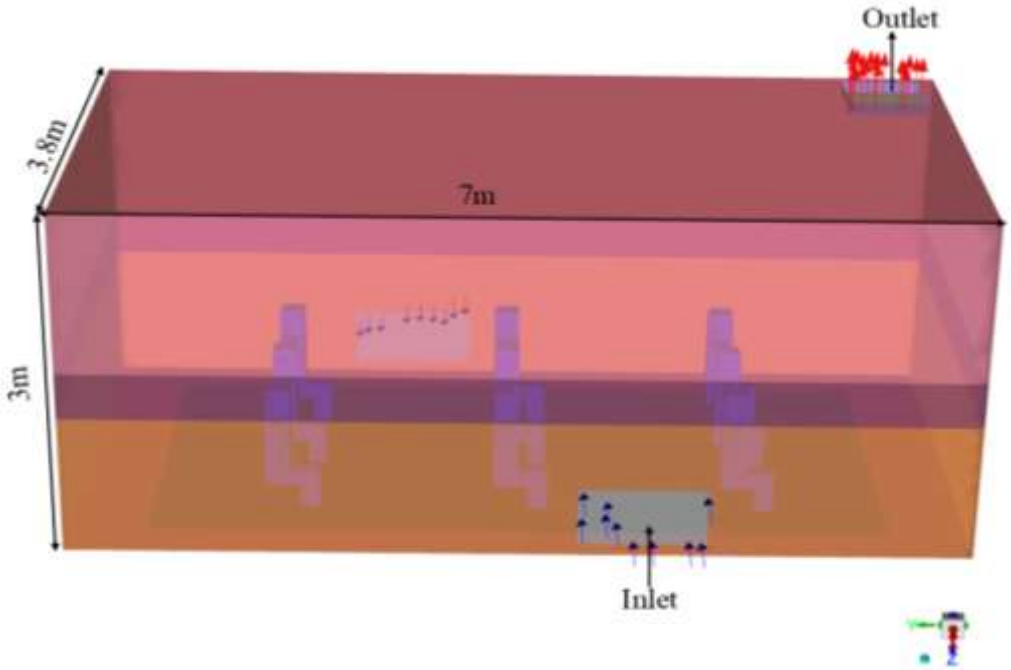

Figure 10:CAD model for displacement ventilation

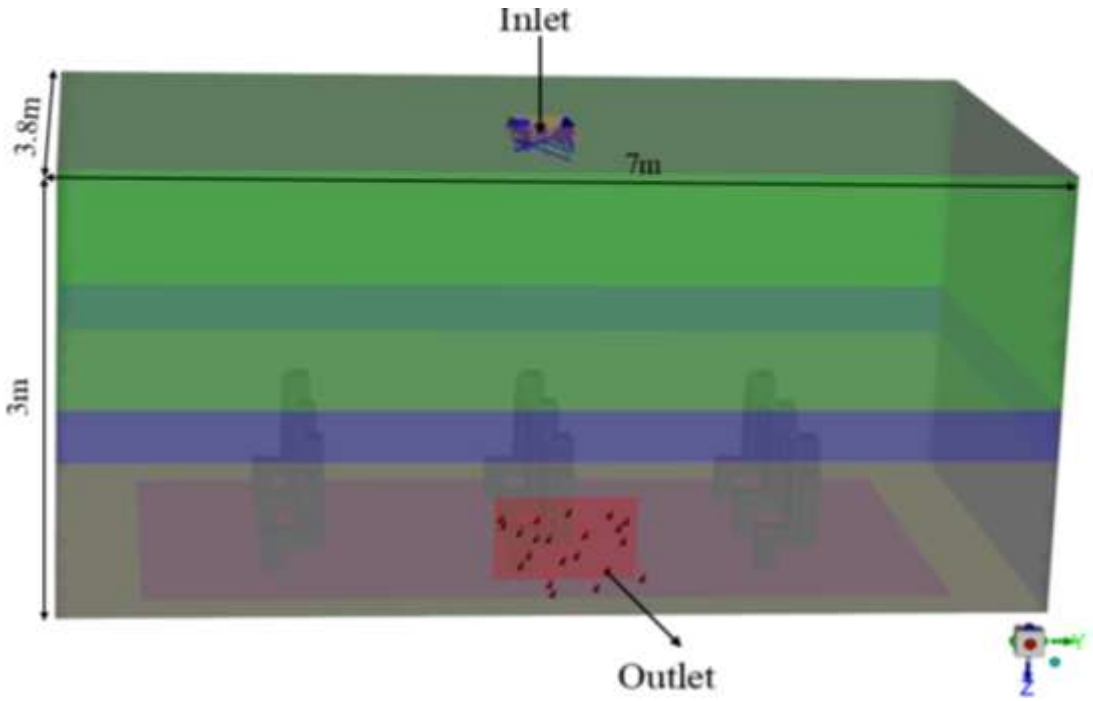

Figure 11: CAD model for mixing ventilation with a floor outlet

The CAD includes the modeling for the room space, inlet, outlet, and simplified human geometry. Meanwhile, room equipment, furniture, etc, were not included in the model to simplify the room geometry, which works well with the meshing and CFD study. A total of three types of ventilation system arrangements were modeled: MV, DV, and MV with floor outlet.

3.3.2 Definition of Space

The room was divided into two zones along the vertical height, namely, the occupant space and the other space. The occupant space was the space within the room that corresponds from floor level up to 1.2 m height. This definition for the occupant space was chosen based on similar previous works and the definition of the occupant zone in the case of a sedentary occupant across different previous works. Likewise, the space in the room that extends from 1.2 m height to above was taken as other space. The division in the vertical direction was made to make it convenient to study the effects of uneven heat gain in the space on the perfromance of the ventilation system. The occupant space generally contributes to heat gain from occupants, floor equipments etc as per the type of activity. Whereas the space above the occupant space mainly accounts

for heat gain from the roof, wall, lights, etc. Thus, the heat gain in this space varies depending on the day, night, or purpose the space is used.

Thus, this type of definition made for the space will allow study how the two types of ventilation systems behave in space with different types of heat gain distribution. The classification of space into occupant space and other space is thus based on the characterization of the space as per the distribution of total heat gain among occupant space and other space(Dominguez Espinosa & Glicksman, 2017).These divisions of the room space will later allow us to study the effect of localized heat gain on the thermal comfort and IAQ parameters.

Likewise, the concept of adjacent space was followed while developing the CAD model for the room. Thus, the minimum distance of 0.6 m is maintained between the occupant and the walls so that the occupant's proximity to the wall doesn't affect the thermal comfort felt by the occupant. This was to avoid drafts, thermal discomfort, and recirculation zones near the occupant, which are often seen near the wall in both DV and MV. Many standards, like REHVA, have defined this spacing between wall and occupant to exclude the space near the wall where the boundary layer effect dominates.

3.3.3 Diffuser Modeling

A four-way square diffuser of 500mm by 500mm was chosen for the simulation, that was having blade angle of 65° and a lip angle of 10°. Modelling for the actual diffuser, along with all the same blades and lip, makes it challenging, as the blade thickness is 10 mm, and such a small lip angle produces regions requiring very fine meshing, thus increasing the overall meshing and computational demand. Thus, for CFD-based ventilation system studies where the main focus is on thermal comfort and IAQ analysis are often based on simplified numerical models for diffuser models like the box method, momentum method, etc(Srebric & Chen, 2002). The modelling of the diffuser was thus based on the momentum method, where the four-way diffuser was represented with a simpler numerical equivalent using the momentum method. The momentum method is based on distributing the inlet velocity at the diffuser inlet into x,y, and z components based on the blade and lip angle so that the simplified diffuser mimics the behaviour of the actual diffuser with a much simpler geometry. Talking about the displacement

ventilation, a rectangular linear diffuser was chosen, and a similar momentum method was used for velocity distribution.

3.3.4 Modeling Human Geometry

The sedentary occupants in the space were represented in a simplified modelling model, a common technique used in many CFD-based thermal comfort and IAQ studies(Foda & Sirén, 2012). The CAD model representation of a sedentary occupant was thus done using simplified cubical sections interconnected to one another, in a way that it represents a thermal manikin having the same surface area as that of an adult sedentary occupant. A basic view of the human mainikin modelling is given in Figure 12.

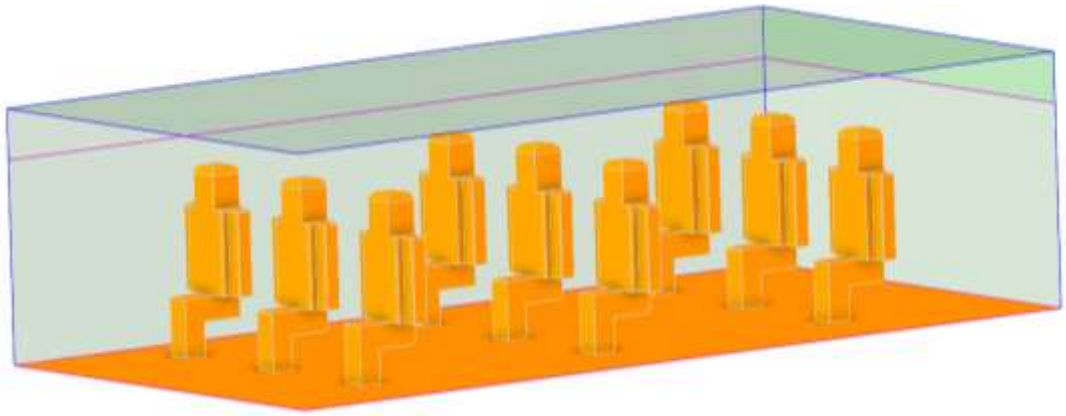

Figure 12: Simplified CAD geometry for occupant

3.3.5 Meshing

Meshing is often regarded as the most important step in a CFD simulation. All the simulations were done using poly-hexacore meshing. This type of meshing combines the features of both polyhedrax mesh, suitable for meshing complex geometry, and hexacore mesh, suitable for bulk flow meshing, like in indoor environments(Chen et al., 2022). These meshes also come with higher faces per cell, fewer cells, lesser convergence time, and numerical stability for HAVC applications. That way, the mesh was capable of precisely containing the complex geometries around the diffuser, human body, wall, and the bulk region inside the room. The other two parameters were also looked for during the meshing process, namely, skewness and orthogonal quality. The local mesh sizing around the inlet, outlet, and human, along with minimum and maximum surface mesh sizing, was adjusted to a maximum skewness of less than 0.4. Likewise, the orthogonal quality of the volumetric meshing was assured by keeping the

minimum orthogonal quality above 0.5. These two parameter values thus allowed generating a mesh that was compatible with CFD for thermal comfort and IAQ study(Liu et al., 2022).

3.3.6 Governing Equations

In the given simulation, air is assumed to behave as an incompressible fluid. This assumption was mathematically represented by the continuity equation for incompressible flow:

$$\nabla \cdot v = 0 \tag{17}$$

where v is the velocity vector of the airflow. Equation (2) represents the balance of pressure forces, viscous force, and body forces within the control volume. The momentum conservation equation is defined by several physical variables and transport properties.

$$\nabla\cdot(\rho vv)=-\nabla p+\nabla\cdot[\mu_{eff}(\nabla v+(\nabla v)\ T)]+\rho g \tag{18}$$

The momentum transport was described using fluid density (ρ), velocity (v), and static pressure (p), with gravity (g) acting as the body force. The equation incorporated convective transport and a viscous diffusion term that utilized effective viscosity (μ_{eff}) and the strain rate tensor. Additionally, a scalar transport equation was employed to determine the local mean age of air within the simulation.

$$\nabla\cdot(\rho v\tau)-\nabla\cdot(\rho\xi_i\nabla\tau)=\rho \tag{19}$$

The local mean age of air, τ, was governed by a steady-state scalar transport equation where the source term ρ represented a residence-time increase of one second per second. The equation accounted for advection via the velocity field v and mixing through effective diffusivity ξ_i, which combined molecular and turbulent transport.

$$\xi_i = (2.88 \times 10^{-5})\rho + \frac{\mu_{eff}}{Sc_t} \tag{20}$$

Equation (15) defines the effective diffusion coefficient (ξ_i) used in scalar transport modeling. The first term $(2.88 \times 10^{-5})\rho$ represents molecular diffusion scaled with fluid density. The second term, $\mu_{eff}/\ Sc_t$, accounts for turbulent diffusion, where μ_{eff} is the effective viscosity (sum of molecular and turbulent viscosity) and Sc_t is the turbulent Schmidt number. This formulation allows both molecular and turbulence-induced mixing to be considered in scalar transport.

Additionally, Equation (4) utilized a species transport equation to simulate the working fluid as a mixture of air, water vapor, and carbon dioxide.

$$\nabla\cdot(\rho v Y_i)-\nabla\cdot(\rho D_{i,eff}\nabla Y_i) = S_i \quad (21)$$

The conservation of mass for the i_{th} species was utilized to govern chemical species distribution, where Y_i represented the local mass fraction. The transport equation incorporated fluid density (ρ), velocity (v), and an effective diffusion coefficient ($D_{i,eff}$) that accounted for both molecular and turbulent diffusivity. Any additions or subtractions of the species, such as occupant-generated CO_2 and H_2O, were handled by the source term S_i.

$$\Gamma_i = -D_i\nabla Y_i \quad (22)$$

The diffusive mass flux of species i is defined by Fick's Law, where Γ_i ($kg/m^2\cdot s$) represents the mass flux vector. The diffusion coefficient for the species is denoted by D_i (m^2/s), and ∇Y_i (m^{-1}) is the gradient of the mass fraction. The negative sign signifies that the species transport occurs in the direction of decreasing concentration, moving from higher to lower mass fraction regions. In turbulent CFD simulations, D_i is typically replaced by an effective diffusion coefficient that includes the effects of turbulent eddies.

Equation (24) defines the diffusive mass flux (Γ_i) based on Fick's law, where D_i is the diffusion coefficient and ∇Y_i is the concentration gradient of species i. Indoor airflow was modeled as a momentum-driven turbulent flow. Because pressure variations and air velocities were small, the flow was assumed incompressible, and air properties were considered constant. Indoor airflow turbulence was simulated using the standard k–ω turbulence model. This method enables accurate prediction of near-wall behavior by smoothly bridging the viscous sublayer, buffer region, and fully turbulent zone, depending on the local y^+value. Likewise, for the simulation of the DV RNG-K-ε model, a standard wall treatment was used.

3.3.7 CFD Setup

The CFD setup was run with all care for the boundary and initial conditions. The simulation included two extra models in addition to the basic momentum equation and energy equation. Surface to Surface (S_2S) radiation model was used for the simulation as a thermal comfort study required Mean Radiant Temperature (MRT). Likewise, the species transport model used with the operating fluid was defined as a mixture of air,

Carbon dioxide(CO_2), and water vapor (H_2O). The boundary condition included a mass flow inlet at a mass flow rate of 0.20 kg/s (350CFM at 291K). This mass flow rate at the inlet was resolved into different components using the momentum method, so that the inlet mimics the Coanda effect of the selected four-way diffuser with a 65° blade angle and 10° lip angle.

Talking about the wall boundary conditions, all the walls of the room and the ceiling are taken as adiabatic walls. The floor was taken as a constant temperature wall at 295 K. The human body surface was represented as a constant heat flux wall of 56 $W/m^{2,}$ which is equivalent to the sensible heat generated by a sedentary occupant.

The cooling load for the space, other than that contributed by the occupant, was represented as a volumetric heat gain. For that, the space was divided into two cell zones as given in Figure 13. It had an occupant zone that extended from the floor to 1.2 m and another cell zone extending from 1.2 m to above. To account for the latent heat in the space, a constant humidity generation (H_2O) of $6.56 \times 10^{-6} m^3/kg.s$ is given at the inner occupant cell zone. Likewise, the occupant cell zone was also given a CO_2 volumetric generation rate of $2.92 \times 10^{-6} m^3/kg.s$, which results from the total of nine occupants in the space. The H_2O and CO_2 volumetric generation rate was given only for the occupant zone to represent a real scenario.

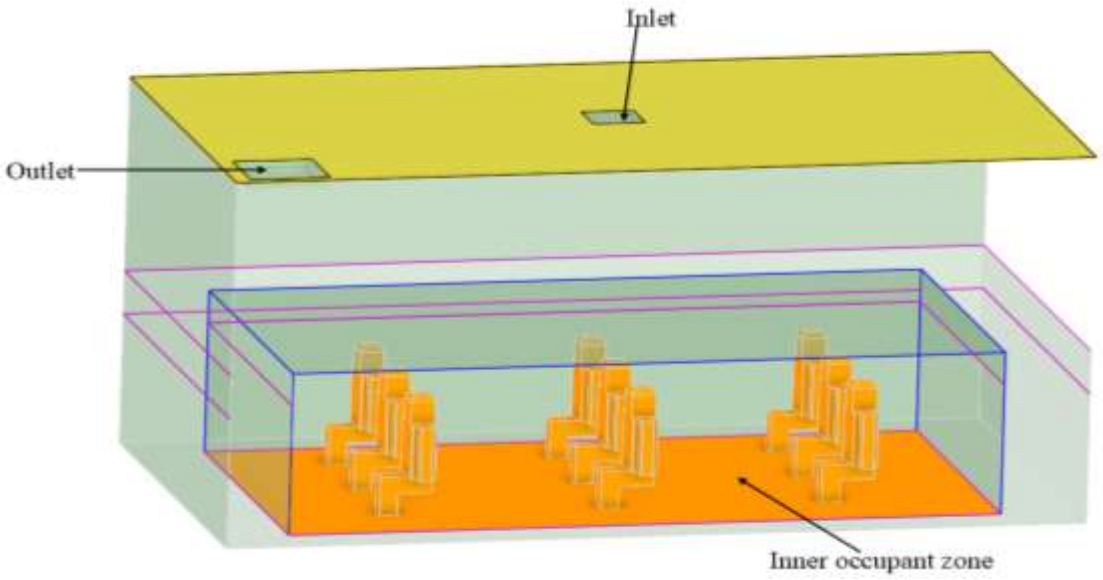

Figure 13: Inner box with occupant where CO_2 and Humidity generation is defined

For the User Defined Scalar (UDS), which in this case was the local mean age of air, a compiler was loaded for the mean age of air. The value of the scalar was kept zero at the inlet, whereas its value at the outlet was specified by a zero flux. The variation of the scalar within the cell zones was specified as per the UDS code.

Once all the boundary conditions were defined, a pressure-based solver with second-order upwind discretization, and pressure–velocity coupling was handled through the SIMPLE (Semi-Implicit Method for Pressure-Linked Equation) algorithm. Convergence monitoring was done using residual histories, with under-relaxation applied to stabilize momentum and turbulence equations. Report definitions were also made for basic parameters like velocity, temperature, etc., around the occupant space to look at the convergence. Convergence criteria were set to 10^{-3} for momentum, 10^{-6} for energy, and 10^{-6} for user-defined scalars. Finally, the heat flux balance across domain boundaries was checked to ensure the overall error remained below 1%.

3.4 Numerical Analysis

The numerical analysis included a detailed Fluent-based simulation for the selected room and number of occupants under the determined cooling load values. The numerical analysis done under this simulation study can basically be categorized into two different groups, namely thermal comfort parameters and IAQ parameters. The ventilation systems simulated included MV, a uniform thermal environment-based ventilation system, and DV, a ventilation system based on a non-uniform thermal environment(Almesri et al., 2013a). Thus, while studying thermal comfort, a volume-based average may not be suitable to represent thermal comfort. MV has almost a uniform thermal environment throughout the room, as it is based on turbulent mixing. On the contrary, DV has significant stratification that creates a non-uniform temperature and velocity field within the room along the vertical height. Thus, three constant mesh iso-surfaces were taken along vertical height: 0.1m, 0.5 m, and 1m from the floor, as given in Figure 14. These iso surfaces correspond to the feel, often prone to cold draft, the main body(torso), and the human head height (breathing plane).

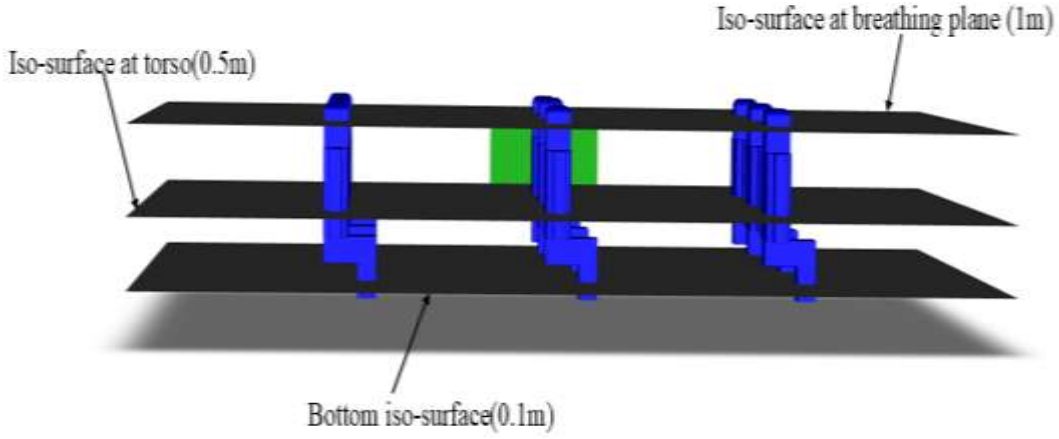

Figure 14: Iso planes used for averaging the CFD results for thermal comfort and IAQ parameters

The numerical analysis basically starts with the extraction of raw data for the fundamental parameters related to thermal comfort, mainly temperature, velocity, Relative Humidity (RH), and Mean Radiant Temperature (MRT). For each of these fundamental indices, the area-weighted average value will be taken in the three iso-surfaces as previously defined. And then the average of the indices at the three iso surfaces located at feet, torso, and head level is again averaged to get the final average value for basic parameters like velocity, temperature, and RH. This type of method can be seen used in previous works related to the comparison of uniform and non-uniform thermal environments (Almesri et al., 2013a).

The numerical analysis for the value related to IAQ, namely local mean age of air, CO_2 ppm, follows a slightly different approach. Thus, the local mean age of air and CO_2 ppm value are taken from just a point near the human head, as the IAQ parameters were mostly studied in the breathing plane, where it is most important (Almesri et al., 2013a).

3.4.1 Thermal Comfort Parameters

These parameters basically quantify the thermal comfort within the given space. It is related to variables, namely, velocity, temperature, Mean Radiant Temperature (MRT), and Relative Humidity (RH), which can be attained from the simulation. Likewise, there are two other variables related to thermal comfort, metabolic activity, and

clothing, which will be assumed for the given case of a sedentary occupant. The current numerical analysis for thermal comfort will try to quantify the overall thermal comfort for the given ventilation in terms of thermal comfort number ($N_{T.C}$). The number combines the thermal effectiveness of the ventilation (ε_t) and thermal sensation, S, which is the absolute value of PMV.

$$\text{Thermal Comfort Number } (N_{T.C}) = [(1 - \frac{|S|}{3}) \times \varepsilon_t] \quad (23)$$

The procedure for determining the thermal comfort number, $N_{T.C,}$ started by first determining the average value of basic thermal comfort parameters using the values attained at the three iso-surfaces previously mentioned. After that, the values were fed to the Center for Built Environment (CBE) thermal comfort tool to get the PMV value, whose absolute value gives the thermal sensation value, S. After that, the thermal effectiveness of the ventilation system was determined using the temperature values at inlet, exhaust, and the average temperature value determined using the three iso-surface values. Lastly, the determined thermal sensation value and thermal effectiveness (ε_t) were put together in an equation to get the thermal comfort number.

3.4.2 IAQ Parameters

The Indoor Air Quality (IAQ) parameters basically quantify the performance of the given ventilation system in providing the desired indoor air quality. The given simulation will use a variable called the air quality number, which is the combination of three basic variables related to air quality: Contaminant Removal Effectiveness (CRE), Mean Age of Air, and Room Time constant, which is the inverse of the Cubic Feet Per Minute (CFM)

$$\text{Air Quality Number } (N_{A.Q}) = [(\frac{\tau_n}{\bar{\tau_p}}) \times \varepsilon_c] \quad (24)$$

Where,

ε_c= Ventilation Effectiveness (Contaminant Removal)

τ_n=Room time constant (1/ACH)

$\bar{\tau_p}$= Local Mean Age Of Air

That way, the air quality number will be used as an overall parameter that quantifies the performance of the given ventilation system in facilitating a good indoor air quality. The procedure for determining the Air Quality Number ($N_{A.Q}$) using the CFD simulation starts by first determining the local mean age of air at the breathing plane. After that, the average CO_2 ppm concentration was determined at the inlet, outlet, and just near the breathing plane. These three CO_2 ppm values were used to determine Contaminant Removal Effectiveness (ε_c). Then, finally, the Contaminant Removal Effectiveness (ε_c) value was used together with the local mean age of air and room time constant to get the Air Quality Number.

3.4.3 Mesh Independence Test

Mesh independence served as an important method to determine the level of refinement needed for the mesh sizing to perform the simulation, ensuring the outcomes are independent of the size of mesh cells. Thus, the simulation for the room was first started with around 0.78 million cells at first, and the average temperature value at the occupant space was taken as the resulting parameter. In successive simulations, the mesh sizing was further refined, thus generating simulations with 1.46 million cells that further increased to 2.68 million, 3.92 million, and finally 4.97 million cells. When the resulting average temperature value was plotted against the total number of cells, an initially sharply declining plot was attained. The plot was steeper as the mesh number increased from 0.78 million to 2.68 million, indicating the initial mesh sensitivity of the simulation. However, as the mesh number increased from 2.68 million to 3.92 million, the slope of the plot decreased drastically, with very small changes seen for the temperature value despite an increase in the number of cells. Further increasing the cell from 3.92 million to 4.97 million, the plot went nearly asymptotic with the x-axis, thus confirming the mesh independence of the result, as shown in Figure 15. Thus, this mesh sizing was targeted in all the simulations done.

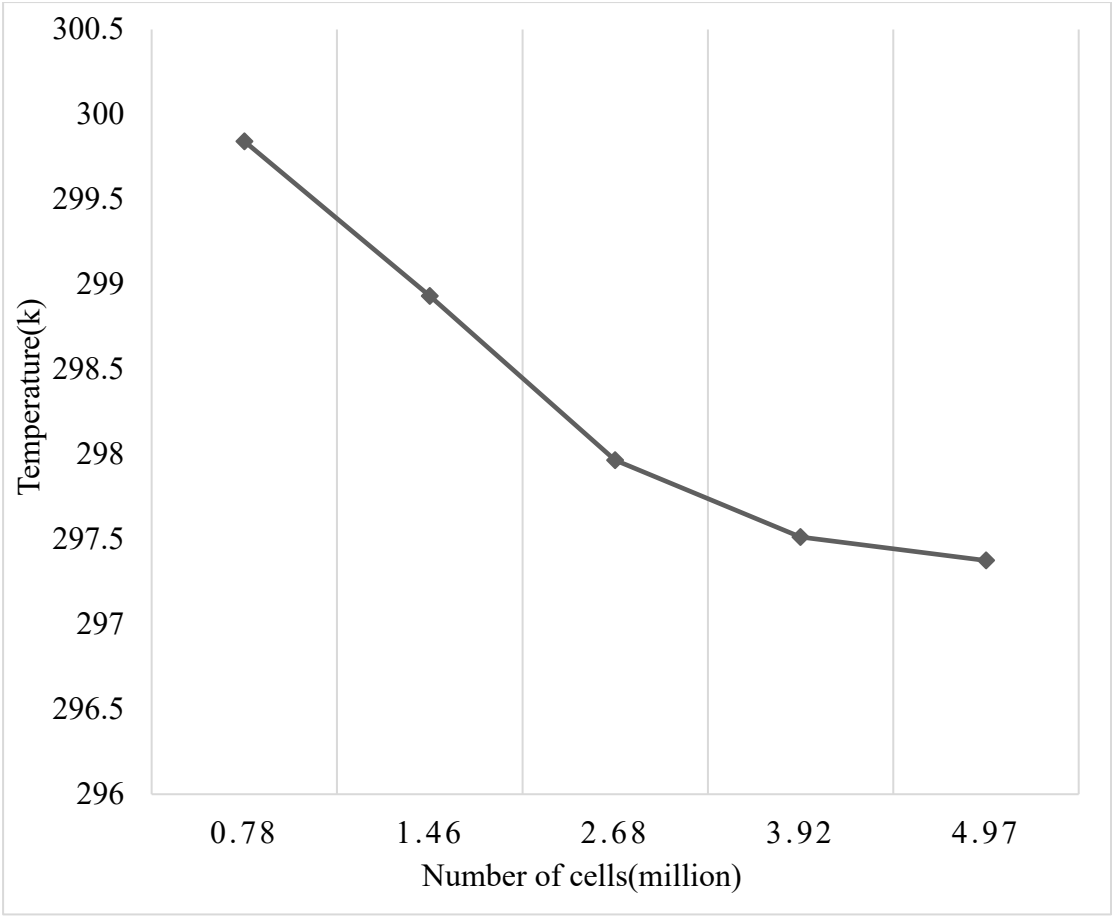

Figure 15: Plot for mesh independence test

3.4.4 Setup For Different Cases

There are three types of ventilation systems being simulated in the study. It includes a basic MV with a ceiling-mounted inlet and ceiling-mounted outlet, a MV with a ceiling-mounted inlet and outlet grille at floor level, and lastly a displacement ventilation. The arrangements are given in Figure 16

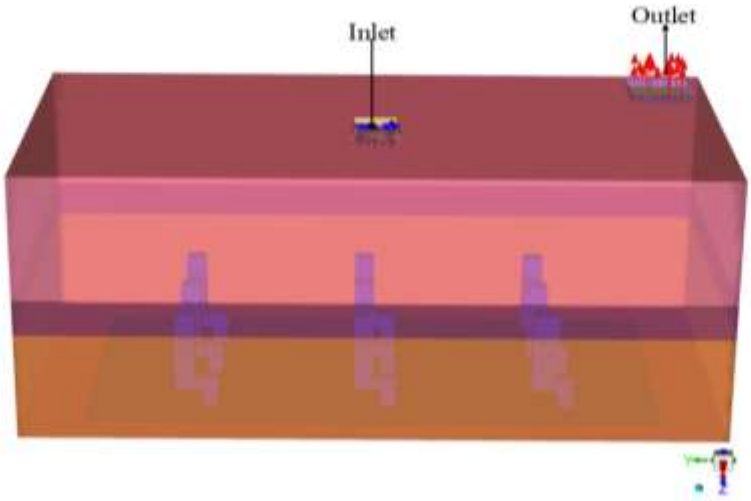

a. Mixing ventilation with a ceiling outlet

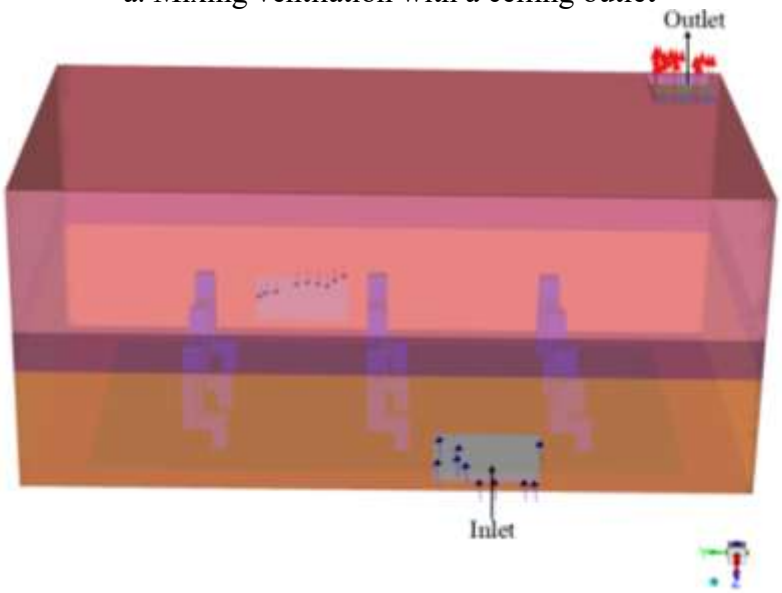

b. Displacement ventilation

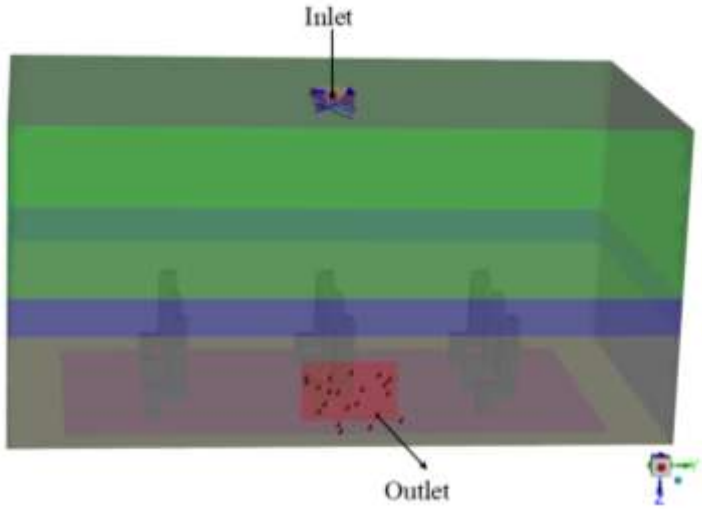

c. Mixing ventilation with floor outlet

Figure 16: CAD model for the three ventilation systems studied

Each of the three ventilation systems will have its three cases, as shown in Figure 16.

A total of nine simulations were performed. The human heat gain will be represented as a wall flux of 56 W/m^2, whereas the other sensible heat gain throughout the room will be taken as volumetric heat gain. These cases were used to quantify how the thermal comfort and IAQ parameters of a given ventilation system are affected by the vertical distribution of the heat gain within the space.

The three cases represented were typically relevant to the fact that a space has different vertical heat distribution depending on the purpose it is used for or operating condition.(Menchaca-Brandan et al., 2017). Case 1 was relevant to uniform heat gain distribution, like in an office or a similar type of space. Case 2 was relevant to spaces like lecture halls or classrooms. Case 3 was the extreme case, which can be seen in spaces like workstation clusters, data entry centers, or even workshops. The three cases differentiated by heat gain distribution are given in Table 3-3

Table 3-3: Cases of Different Heat Gains

Percentage of Total Heat	Occupant Space(0-1.2m)	Other Space (above 1.2m)
Case 1	68%	32%
Case 2	75%	25%
Case 3	80%	20%

Likewise, there were three other cases based on the vertical height of the space as given in Table 3-4. These cases were about analyzing how the ventilation system MV and DV perform when the vertical envelope height is different, despite all the heat gain values being the same. The cases were simulated because stratification-based ventilation systems like DV are often seen performing well in spaces with higher envelope height(Khan, Bennia, et al., 2022). On the contrary, MV was regarded as performing better under lower vertical height. Thus, three cases were simulated where the internal heat gain was the same but with a different envelope height. These cases were performed both MV and DV, and MV with a floor outlet, as done in previous cases related to heat gain distributions.

Table 3-4: Cases of different envelope height

S.N	Case	Envelope Height(m)
1.	Case 1	2.6
2.	Case 2	3
3.	Case 3	3.4

The heat gain under different envelope heights was kept constant for the ease of comparison. Though in practical increase in envelope height may be associated with an increase in envelope area, which itself increases the cooling load, a slightly dissimilar approach has been followed. With the adiabatic wall boundary condition used, the study was done to determine the sensitivity of the ventilation system with a given internal heat gain and envelope height.

Thus, successful simulation of all the cases allowed a detailed study on how MV, DV, and MV with floor outlet perform under different cases of heat gain distribution and vertical envelope height.

Chapter 4: RESULTS AND DISCUSSION

4.1 Result for MV with ceiling inlet and ceiling outlet

4.1.1 Result for Thermal Comfort

The thermal comfort for different cases of mixing ventilation with both the inlet diffuser and the outlet located at the ceiling was briefly studied using three key thermal comfort parameters: thermal sensation (S), thermal effectiveness (ε_t), and thermal comfort number ($N_{T.C}$). Both the value for thermal sensation and thermal effectiveness decreased as we went from the first case to the third case. As more heat was localized at the occupant floor level in the latter two cases, there was a slight decrease in thermal sensation, thermal effectiveness, and finally thermal comfort. The detailed values for the thermal comfort parameters are given in Table 4-1.

Table 4-1: Thermal comfort results for MV with ceiling inlet and outlet

Case	Thermal Sensation (S)	Thermal Effectiveness(ε_t)	Thermal Comfort Number ($N_{T.C}$)
1	0.50	1.10	0.92
2	0.49	1.09	0.92
3	0.48	1.05	0.88

The value thermal sensation is the absolute value of PMV, which is obtained by feeding the CFD attained results for velocity, humidity, temperature, and mean radiant temperature to the CBE thermal comfort tool. These values are area-weighted average values taken from three iso-surfaces, 0.1m from the floor(ankle level), 0.5m from the floor(torso level), and 1 m from the floor (breathing level). The plot for velocity and temperature variation along the vertical slicing plane taken at the center of the room can be seen in Figure 17 and Figure 18.

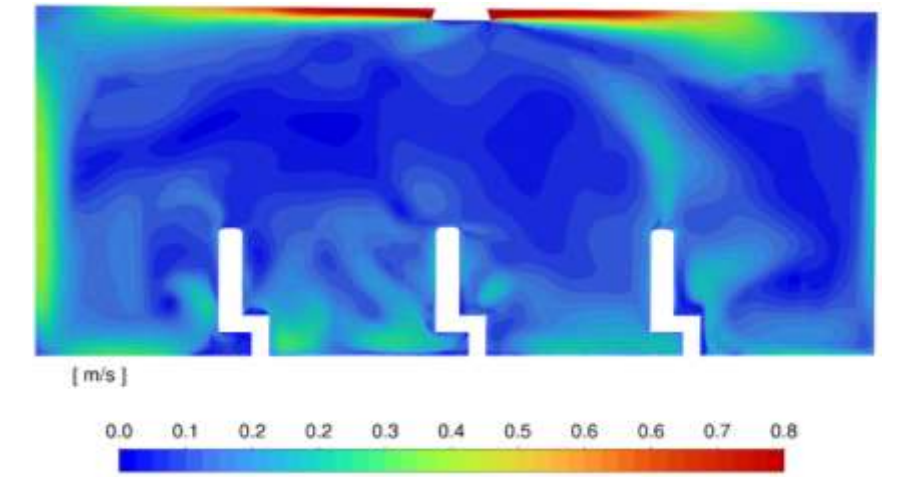

Case 1

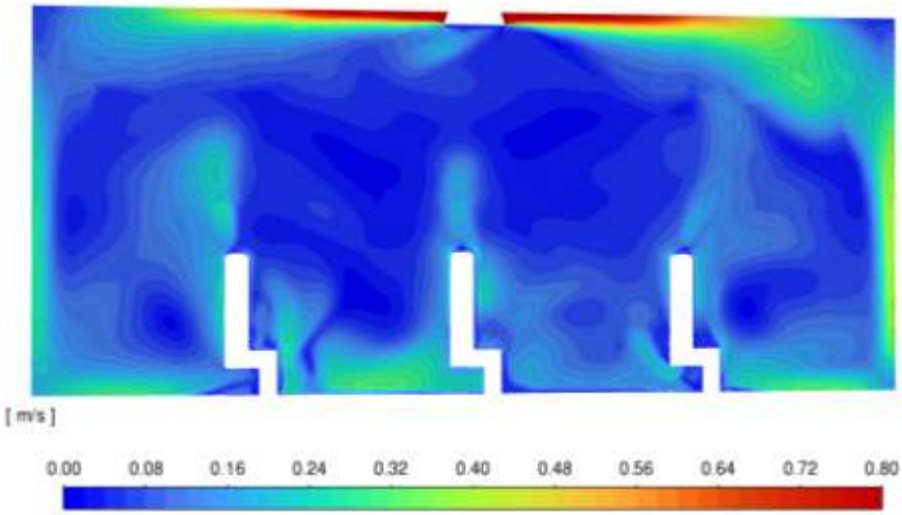

Case 2

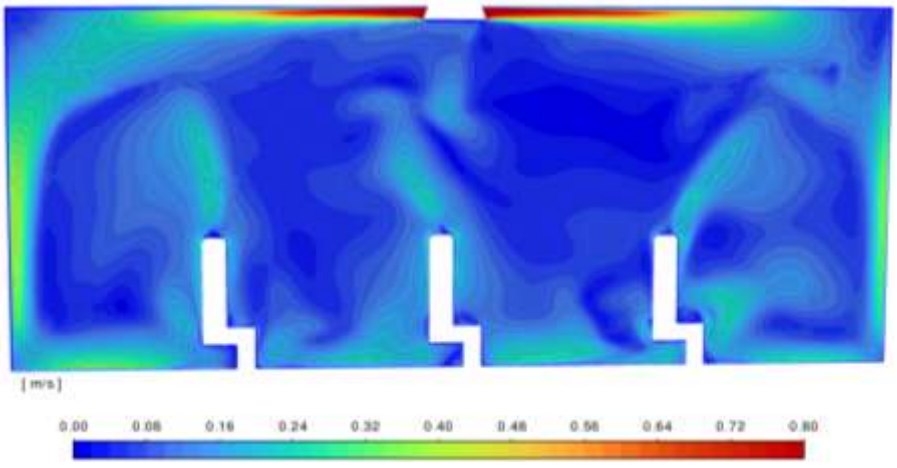

Case 3

Figure 17: Contour for Velocity for the MV with ceiling outlet under the different cases

When looking at the contour for velocity under the three cases of heat gain distribution, the average velocity around the occupant was 0.14 m/s, 0.13 m/s, and 0.11 m/s for case 1, case 2, and Case 3. The velocity values were under the ASHRAE Standard 55 specified limit of 0.3 m/s.When looking at the velocity contour plot, the one with uniform heat gain is seen with a much more uniform velocity field compared to the other two. This was attributed to the turbulent mixing MV relies on, which works best for a uniform heat gain environment. In cases of uneven heat gain concentration, MV tends to short-circuit where the supply air reaches the outlet before it even mixes with the dead spots or area of heat concentration. (Yuan et al., 2013).

The average temperature around the occupant in cases 1, 2, and 3 was found to be 297.2 K, 297.3 K, and 297.5 K, respectively. Though the temperature values were within the ASHRAE Standard 55 thermal comfort limit, the increase in temperature around the occupant space in the latter two cases suggests a decline in thermal effectiveness of MV as the heat gain was localized around the occupant space. This corresponds to the change pattern previously seen in the velocity contour plot.

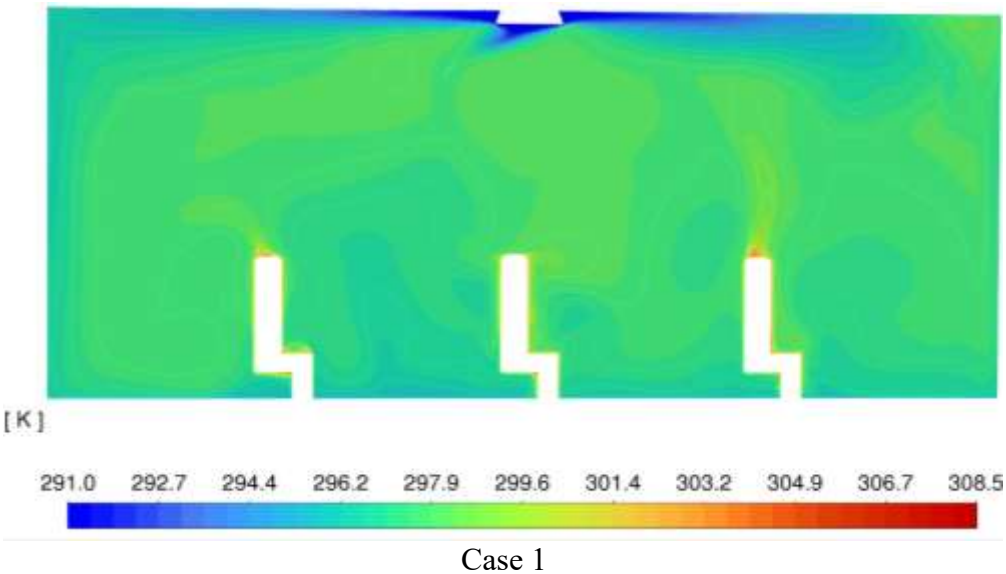

Case 1

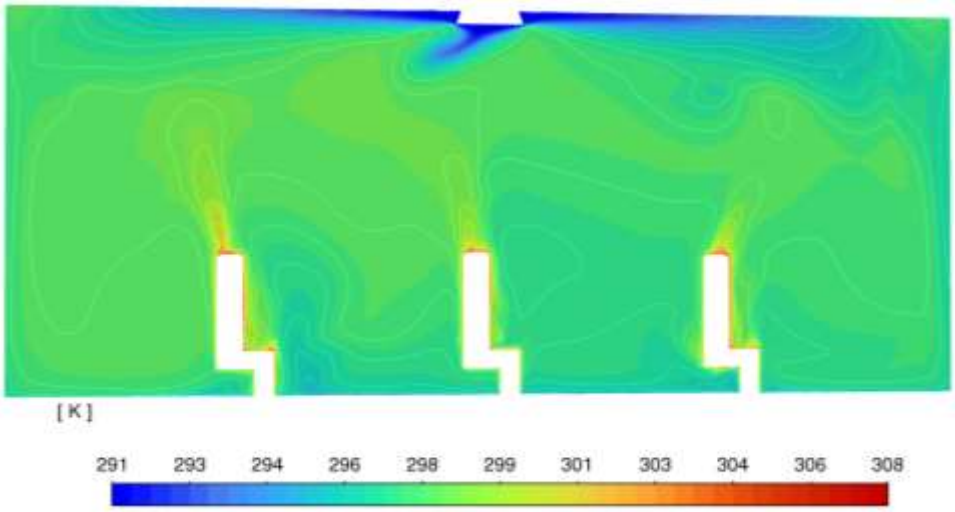

Case 2

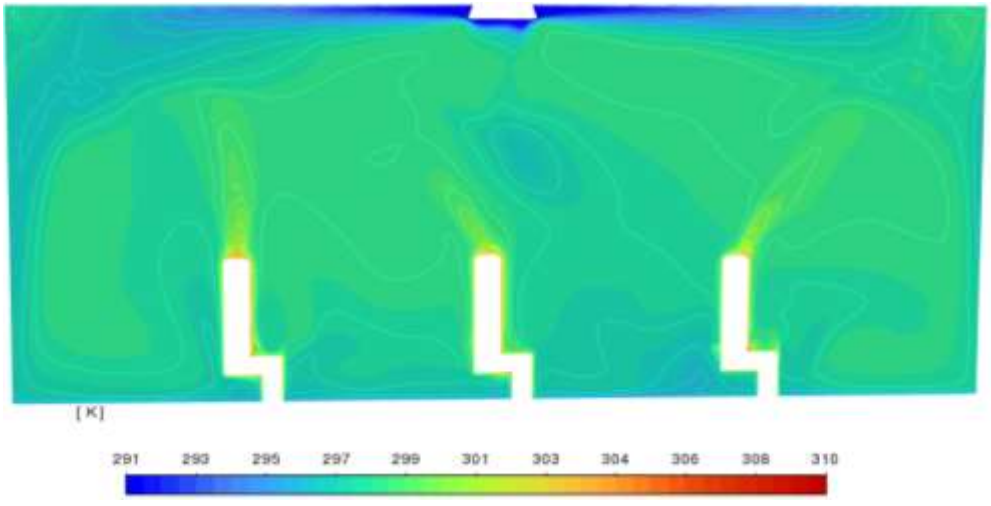

Case 3

Figure 18: Temperature Contour for the MV with ceiling outlet under the different cases

4.1.2 Result for IAQ parameters

The result for the different IAQ-related parameters for the MV with ceiling outlet is given in Table 4-2. The value for the age of air at the breathing zone was seen increasing as the occupant zone heat became highest, while the contaminant removal effectiveness and the air quality number were seen decreasing as the occupant zone heat increased.

Table 4-2: IAQ parameters for the MV with Ceiling Outlet

Case	Room time Constant (τ_n)	Age of Air (τ_p^-)	Contaminant Removal Effectiveness (CRE)	Air Quality Number ($N_{A.Q)}$
1	0.133	0.122	0.97	1.06
2	0.133	0.123	0.96	1.04
3	0.133	0.125	0.92	0.98

The contour plot for the mean age of air and CO_2 PPM concentration is given in Figure 19 and Figure 20.The CO_2 ppm concentration breathing height for the first case was found to be 539, which was the lowest among the three. The values for the other two cases were found to be 541 and 554, respectively. In general, the CO_2 ppm concentration was seen to increase as more heat was concentrated in the occupant zone. This was attributed to the poor performance of mixed ventilation as the localized heat gain increased, which led to a stagnant zone near the breathing height, thus increasing the CO_2 ppm concentration. In all three cases, the local mean age of air near the breathing height was less than the ASHRAE allowable limit of 1000, which suggested a contaminant removal within the space.

The local mean age of air near the breathing height for the first case was found to be 0.122 hr, which was the lowest among the three. The values for the other two cases were found to be 0.123 hours and 0.125 hours, respectively. In general, the local mean age of air was seen to increase as more heat was concentrated in the occupant zone. This was attributed to the poor performance of mixed ventilation as the localized heat gain increased, which led to a stagnant zone near the breathing height, thus increasing the local mean age of air. In all three cases, the local mean age of air near the breathing height was less than the room time constant of 0.133, which suggested a good air exchange within the space

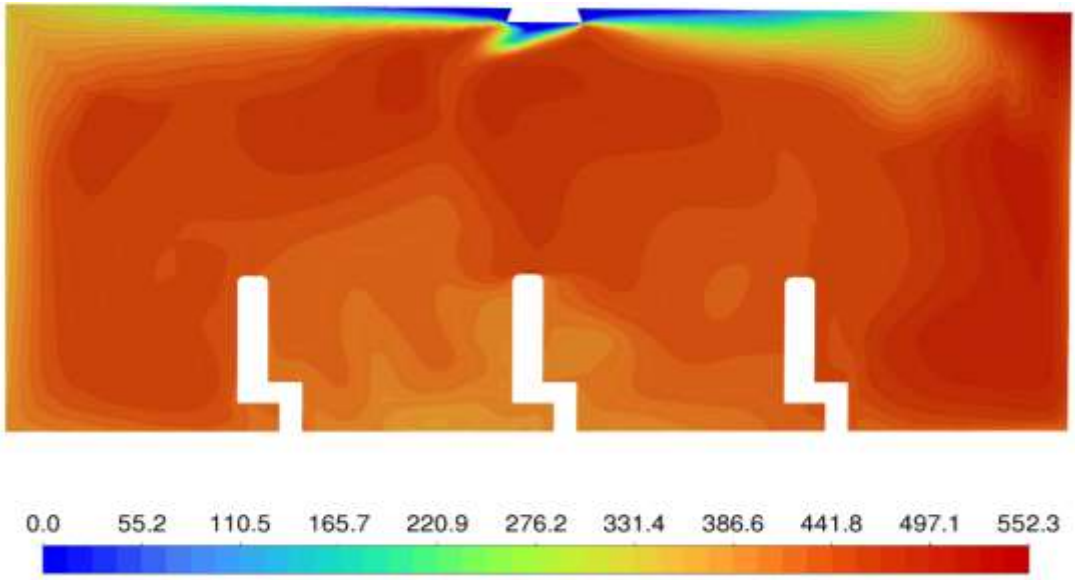

Case 1

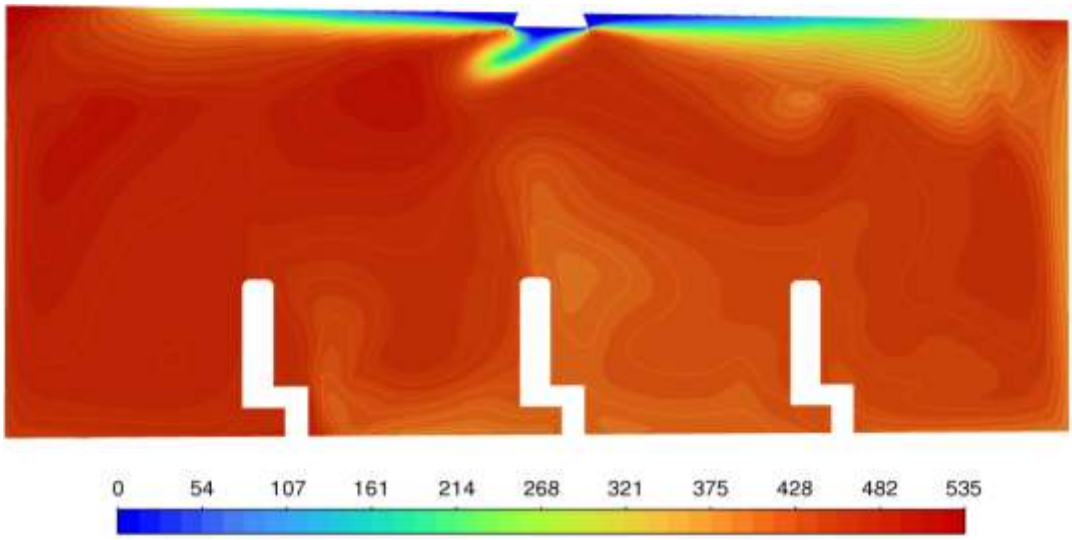

Case 2

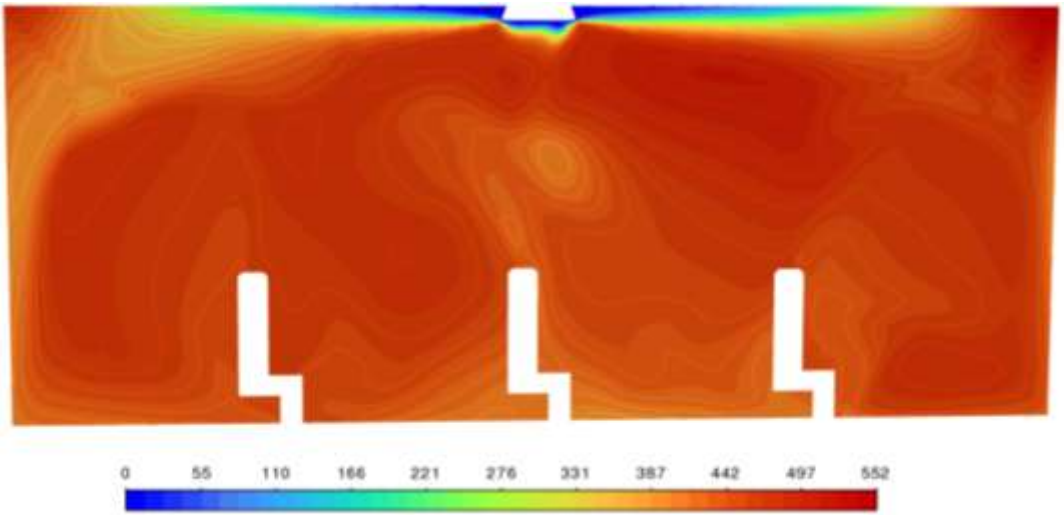

Case 3

Figure 19: Contour for Mean Age of Air for MV with ceiling outlet

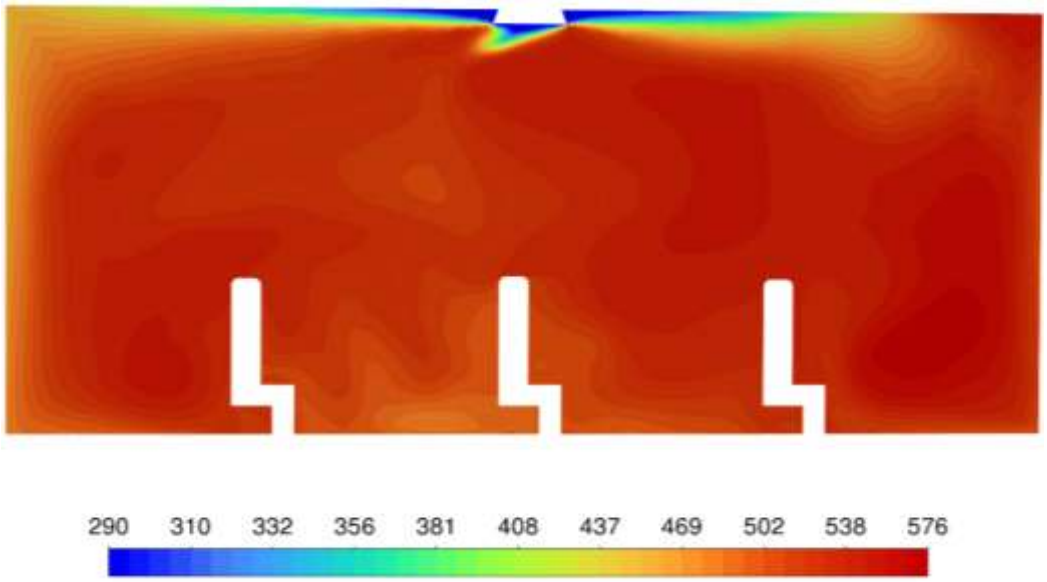

Case 1

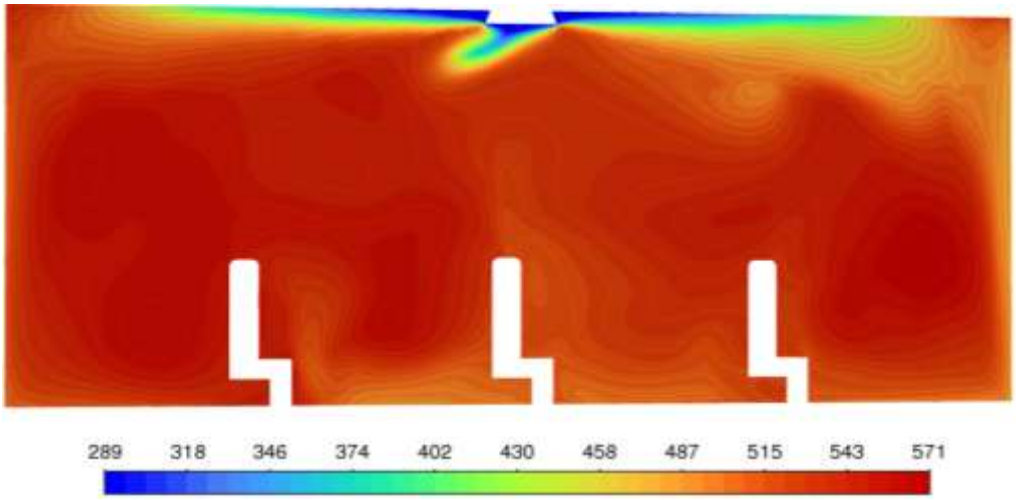

Case 2

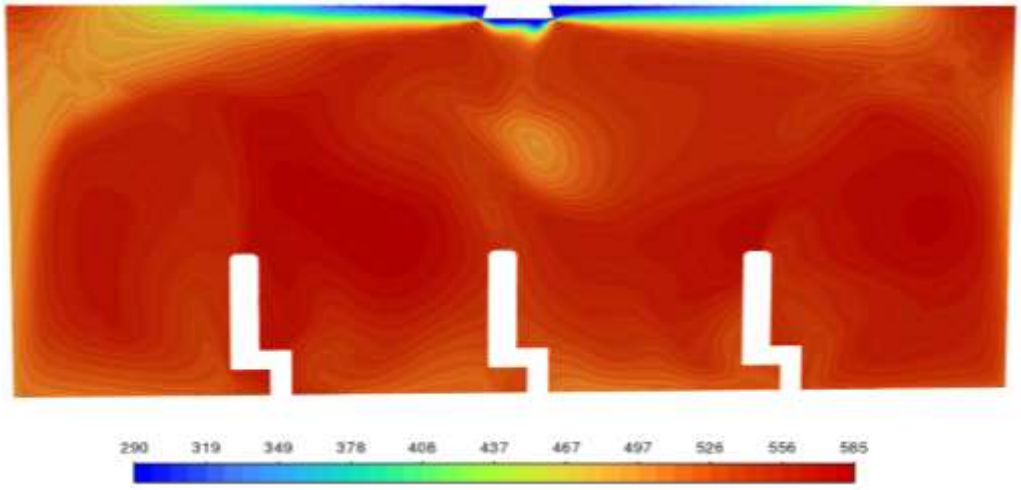

Case 3

Figure 20: CO_2 ppm concentration for MV with ceiling outlet

4.1.3 Result For Air Distribution Index(ADI)

The result for the Air Distribution Index (ADI) for the MV with ceiling outlet is given in Figure 21. The ADPI value can be seen decreasing as the occupant zone of the room contributed a higher amount of total cooling load. Out of three cases, the first case with uniform heat gain distribution was seen with the highest ADI value of 1.98. The ADI value then followed a declining path as more heat gain was contributed from the lower occupant zone with 1.96 in case 2, which eventually declined to 1.86 in case 3. The air quality number and thermal comfort number also followed a similar type of trend, where they were optimal for the case of uniform heat gain and lowest for the case with high occupant zone heat. The values attained for ADI, thermal comfort number, and air quality number were in a good range compared to those attained in previous similar work (Almesri et al., 2013a). The declining perfromance of MV was attributed to the inability of the jet to destroy the stagnant zones when a high amount of heat is concentrated at some space, as MV is mostly suitable for working with a uniform heat gain distribution.

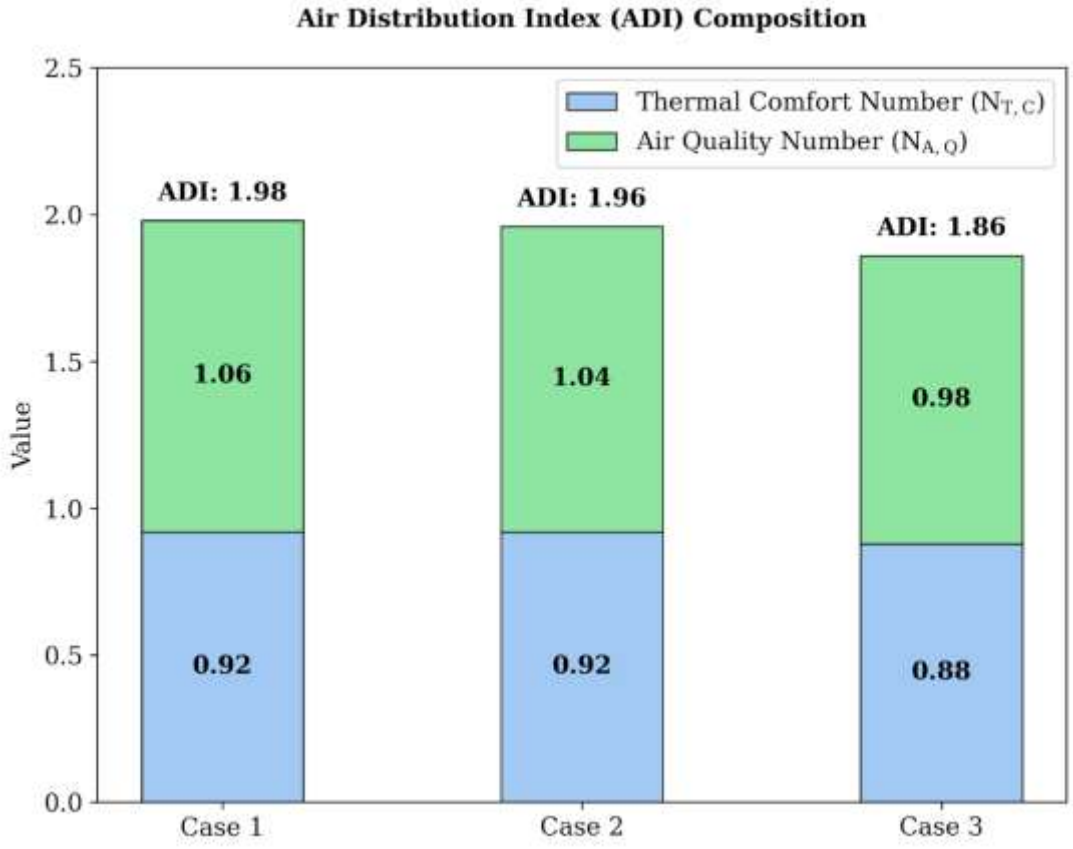

Figure 21: Chart for ADI under the MV with ceiling outlet

4.2 Result for MV with ceiling inlet and Floor Outlet

4.2.1 Result for Thermal Comfort

The thermal comfort for different cases of mixing ventilation with both the inlet diffuser and the outlet located at floor level was briefly studied using three key thermal comfort parameters: thermal sensation (S), thermal effectiveness (ε_t), and thermal comfort number ($N_{T.C}$). The value for thermal sensation is seen slightly decreasing as the occupant level heat increases as given in Table 4-3. Whereas the thermal effectiveness can be seen as slightly incremental as we go from the first case to the third case, as more heat is localized at the occupant floor level in the latter two cases, thus giving a slight increase in thermal effectiveness and finally thermal comfort. The increase in thermal effectiveness and thermal comfort number can be attributed to the proximity of heat sources to the floor outlet, which allows a short path for air to exit the outlet, as it is only mixed when heat is concentrated at the occupant or floor zone.

Table 4-3: Thermal comfort results for MV with ceiling inlet and outlet

Case	Thermal Sensation (S)	Thermal Effectiveness(ε_t)	Thermal Comfort Number($N_{T.C}$)
1	0.52	0.92	0.76
2	0.46	0.93	0.79
3	0.45	0.95	0.80

The value thermal sensation is the absolute value of PMV, which is obtained by feeding the CFD attained results for velocity, humidity, temperature, and mean radiant temperature to the CBE thermal comfort tool. These values are area-weighted average values taken from three iso-surfaces, 0.1m from the floor(ankle level), 0.5m from the floor(torso level), and 1 m from the floor (breathing level). The plot for velocity and temperature variation along the vertical slicing plane taken at the center of the room can be seen in Figure 22 and Figure 23.

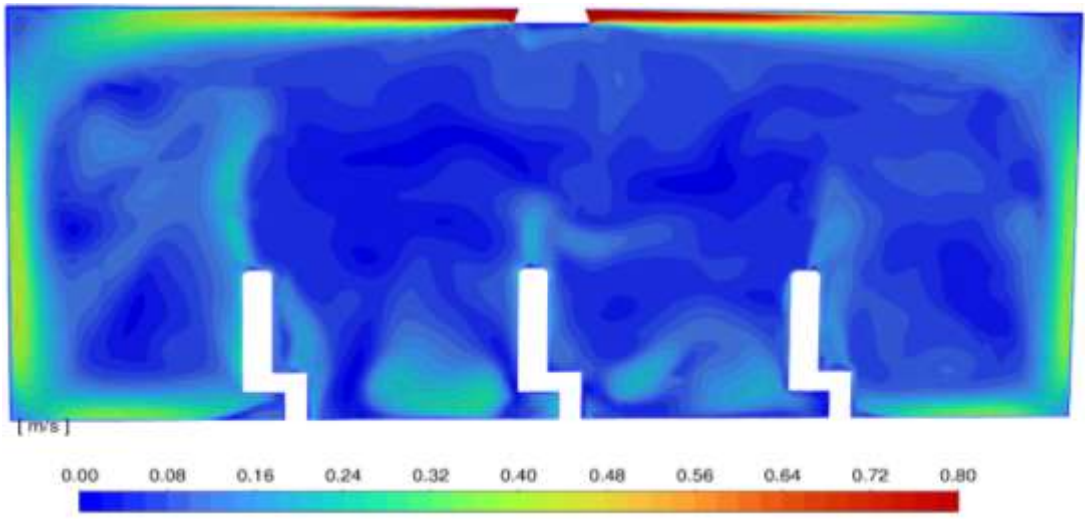

Case 1

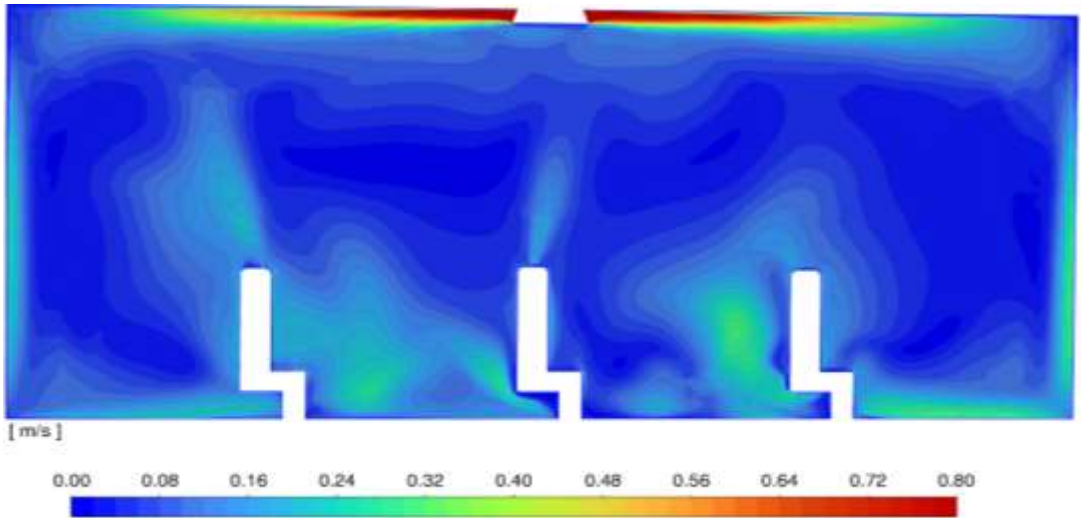

Case 2

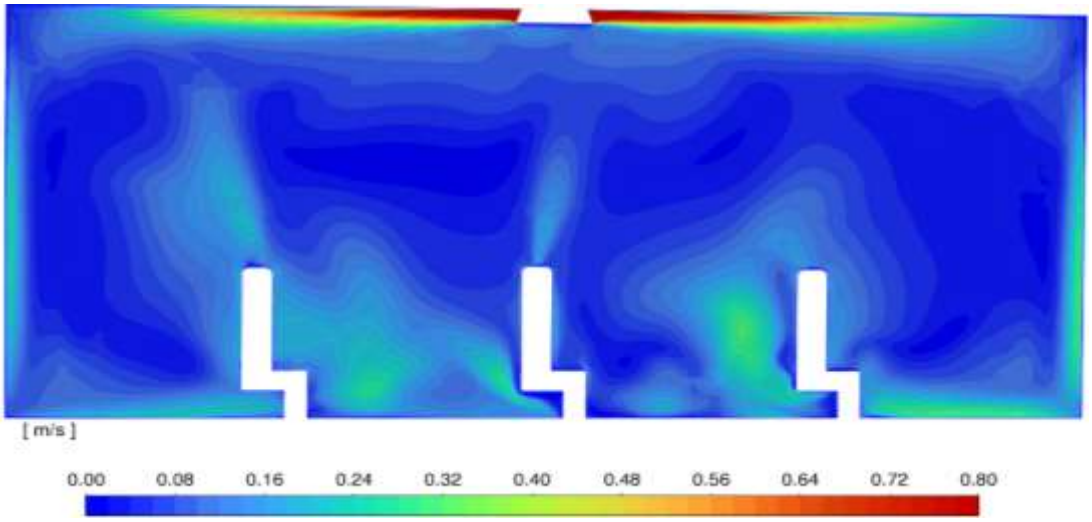

Case 3

Figure 22: Contour for Velocity for the MV with floor outlet under the different cases

When looking at the contour for velocity under the three cases of heat gain distribution, the average velocity around the occupant was 0.13 m/s, 0.13 m/s, and 0.14 m/s for case 1, case 2, and Case 3. The velocity values were under the ASHRAE Standard 55 specified limit of 0.3 m/s.When looking at the velocity contour plot, the one with uniform heat gain is seen with a much more uniform velocity field compared to the other two. This was attributed to the turbulent mixing MV relies on, which works best for a uniform heat gain environment.

The average temperature around the occupant in cases 1, 2, and 3 was found to be 297.79 K, 297.73 K, and 297.70 K, respectively. The temperature values were within the ASHRAE Standard 55 thermal comfort limit; the decrease in temperature around the occupant space in the latter two cases suggests an increase in thermal effectiveness of the latter two cases. Compared to MV with a ceiling outlet, this type of MV can be seen with less velocity and a high temperature value, which suggests its lower performance compared to the normal ceiling outlet-based MV.

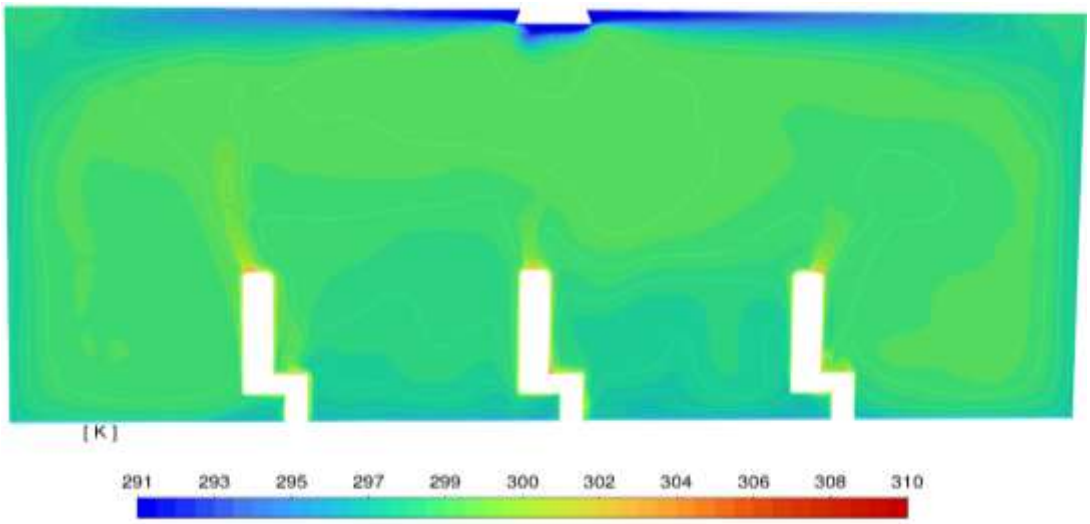
[K]
291 293 295 297 299 300 302 304 306 308 310

Case 1

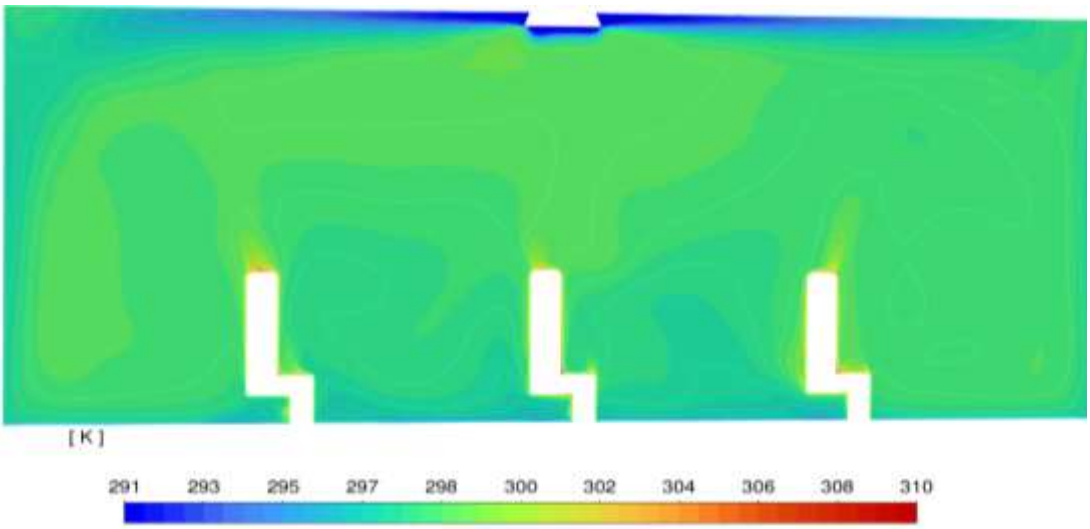
[K]
291 293 295 297 298 300 302 304 306 308 310

Case 2

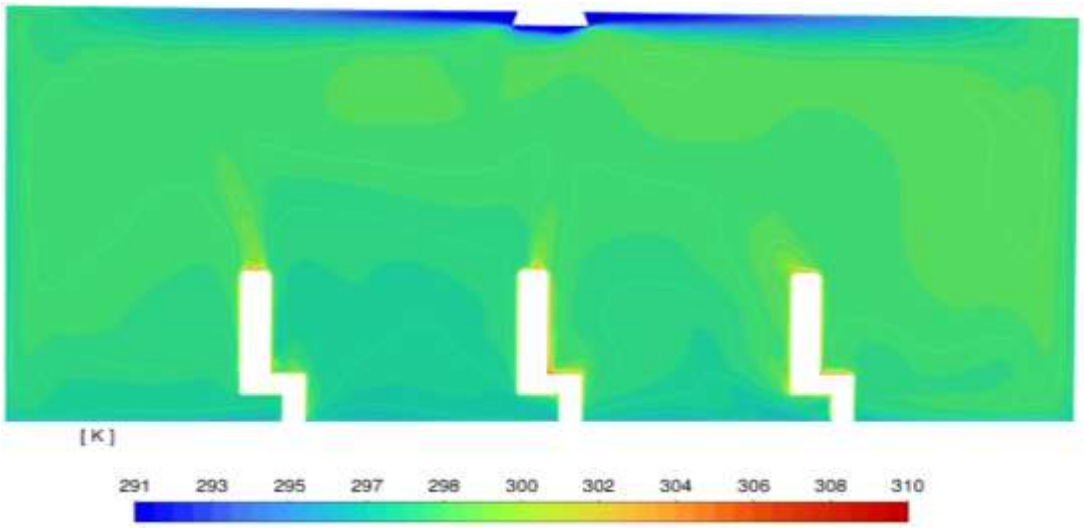
[K]
291 293 295 297 298 300 302 304 306 308 310

Case 3

Figure 23: Temperature Contour for the MV with floor outlet under the different cases

4.2.2 Result for IAQ parameters

The result for the different IAQ-related parameters for the MV with the floor outlet is given in Table 4-2. The MV with floor outlet is seen with the highest contaminant removal effectiveness, air quality number, and lowest age of air under the second case, where the occupant zone has 75% of heat, and the rest space has 25% of heat. The second-highest value for these parameters is seen in the third case, where 80% of the total heat is coming from the occupant zone. Thus, MV with a floor outlet is seen working with better IAQ parameters under cases with higher occupant zone heat gain.

Table 4-4: IAQ parameters for the MV with floor Outlet

Case	Room time Constant (τ_n)	Age of Air (τ_p^-)	Contaminant Removal Effectiveness (CRE)	Air Quality Number ($N_{A.Q}$)
1	0.133	0.150	0.78	0.69
2	0.133	0.142	0.89	0.83
3	0.133	0.146	0.83	0.76

The contour plot for the mean age of air and CO_2 PPM concentration is given in Figure 24 and Figure 25.

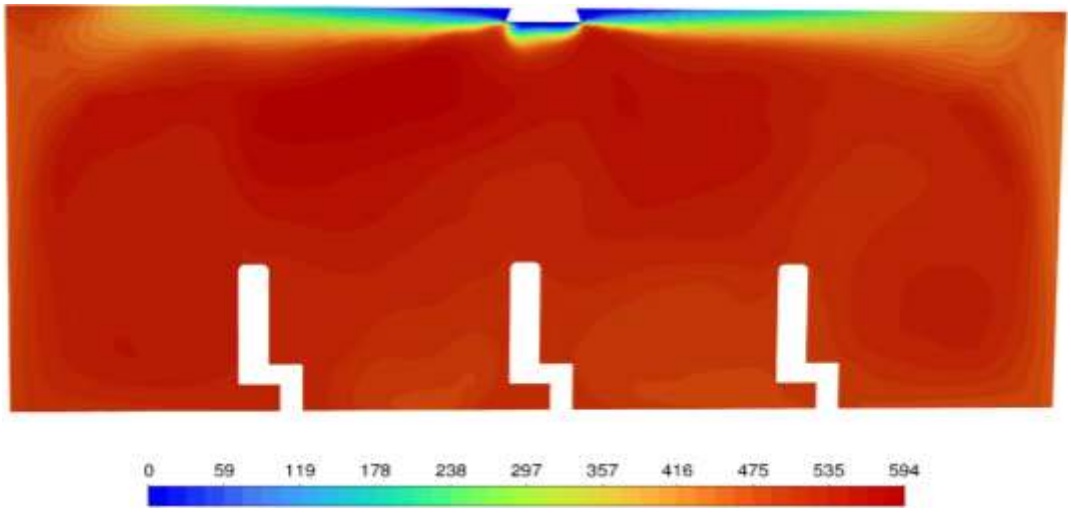

Case 1

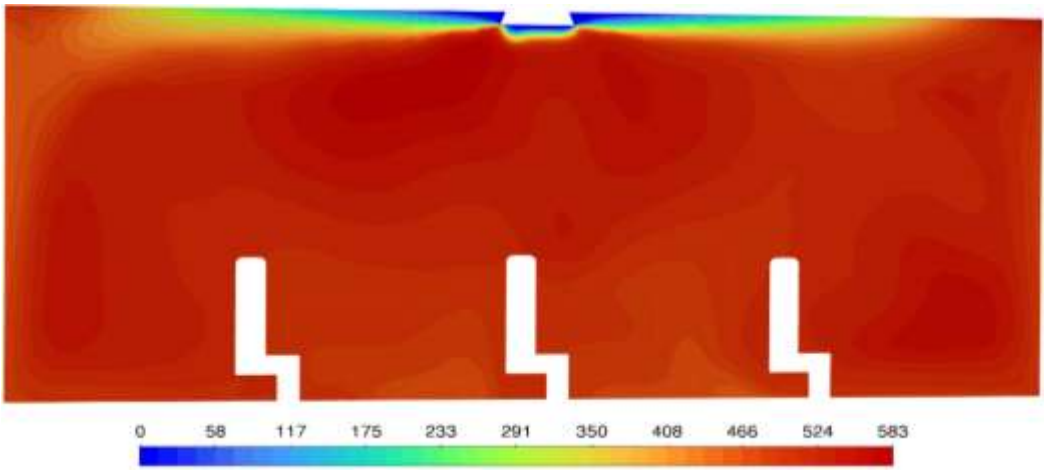

Case 2

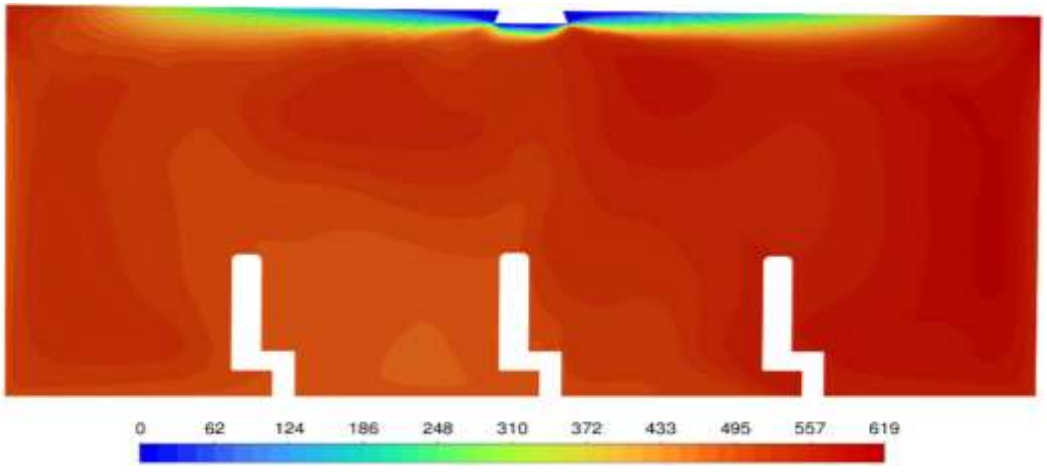

Case 3

Figure 24: Contour for Mean Age of Air for MV with floor outlet

The local mean age of air around breathing height was found to be maximum for the first case, with 0.15 hours, whereas the second case was seen with the minimal value of 0.142 hours. Similarly, the third case was seen with the highest local mean age of air

corresponding to 0.146 hours. In all cases, the local mean age of air at the breathing plane was higher than the room time constant of 0.133 hours, which suggests inadequate air exchange in the ventilation system.

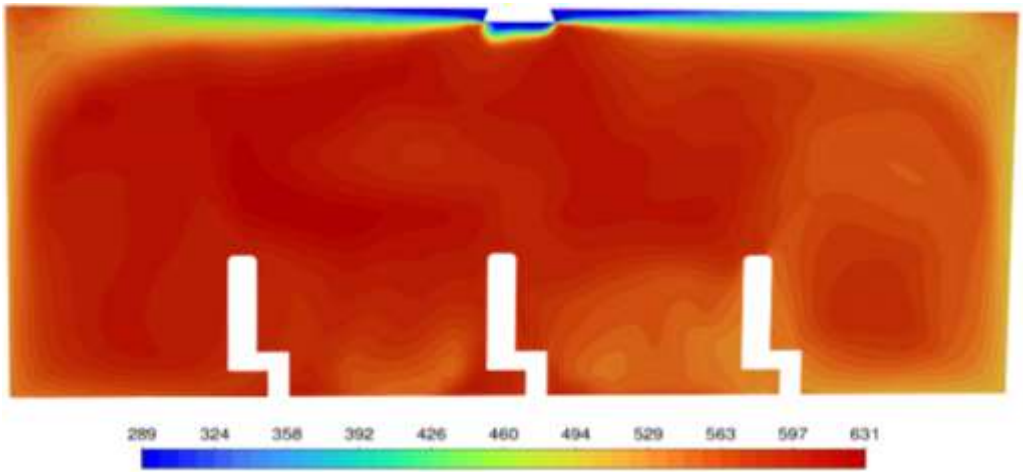

Case 1

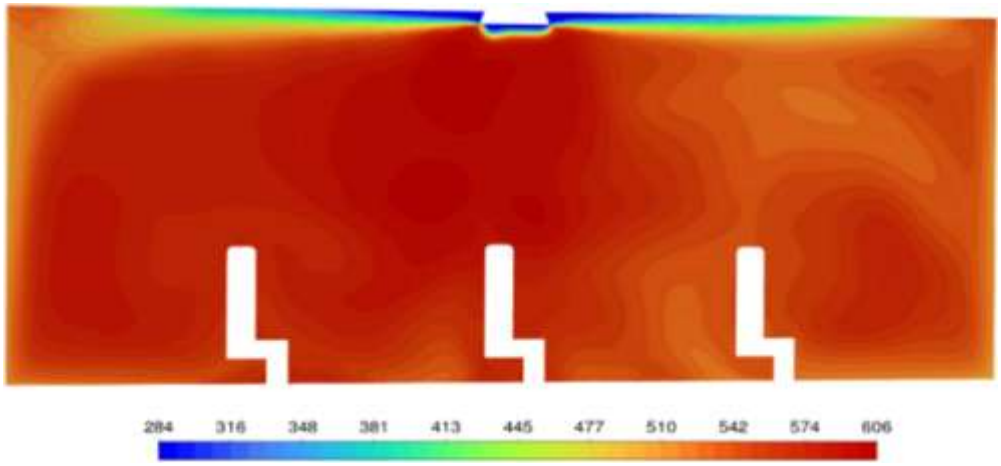

Case 2

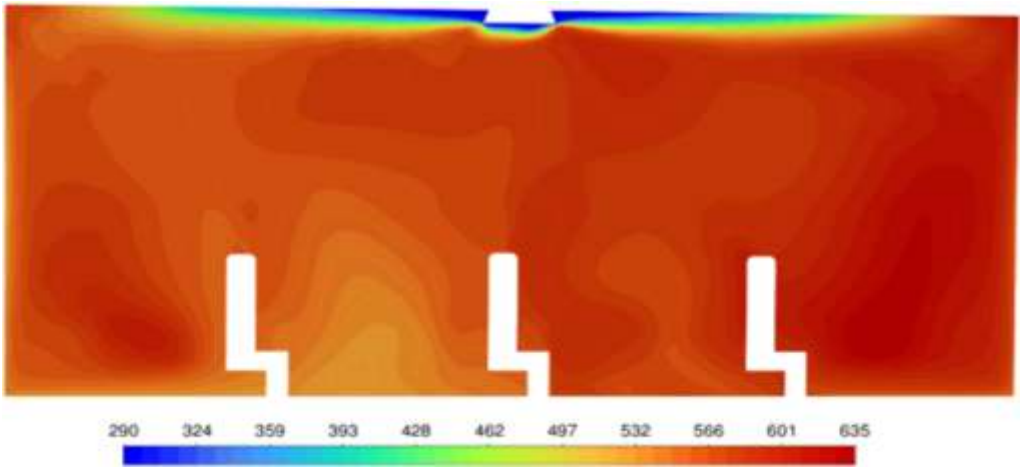

Case 3

Figure 25: CO_2 ppm concentration for MV with floor outlet

The CO_2 ppm concentration breathing height was found to be maximum for the first case, with 720, whereas the third case was seen with the minimal value of 714. Similarly, the second case was seen with the value corresponding to 717 . In all cases, the CO_2 ppm concentration at the breathing plane was less than the limit of 1000. However, the high value for CO_2 ppm compared to normal MV suggests the system inefficiency in contaminant removal.

4.2.3 Result For Air Distribution Index(ADI)

The result for the Air Distribution Index (ADI), for the MV with a floor outlet is given in

Figure 26: Chart for ADI under the MV with floor outlet. The ADI value can be seen as the highest for the second case. Overall, the MV with a floor outlet is seen performing better when there is a substantially large amount of heat in the occupant zone. However, the ADI values, thermal comfort number , air quality number are all lesses than its counterpart with ceiling outlet. Its enhanced perfromance for the case of lower heat gain concentration was attributed to its hybrdi flushing behavior and location of outlet near to the major heat gain zone. Its poor performance compared to MV with ceiling outlet was attributed to fact that a near floor outlet in a ceiling height of 3m is often not enough to dissipate momentum efficiently due to short circuit of air jet through outelt befire it evenly mixes out. The second case had highest ADI of 1.62 which was the highest followed by third case with 1.56 and first case with 1.46.m The air quality number and thermal comfort number also followe similar pattern. The ADI and other parameters value attained were found to be within the range as determined in previous works (Almesri et al., 2013a).

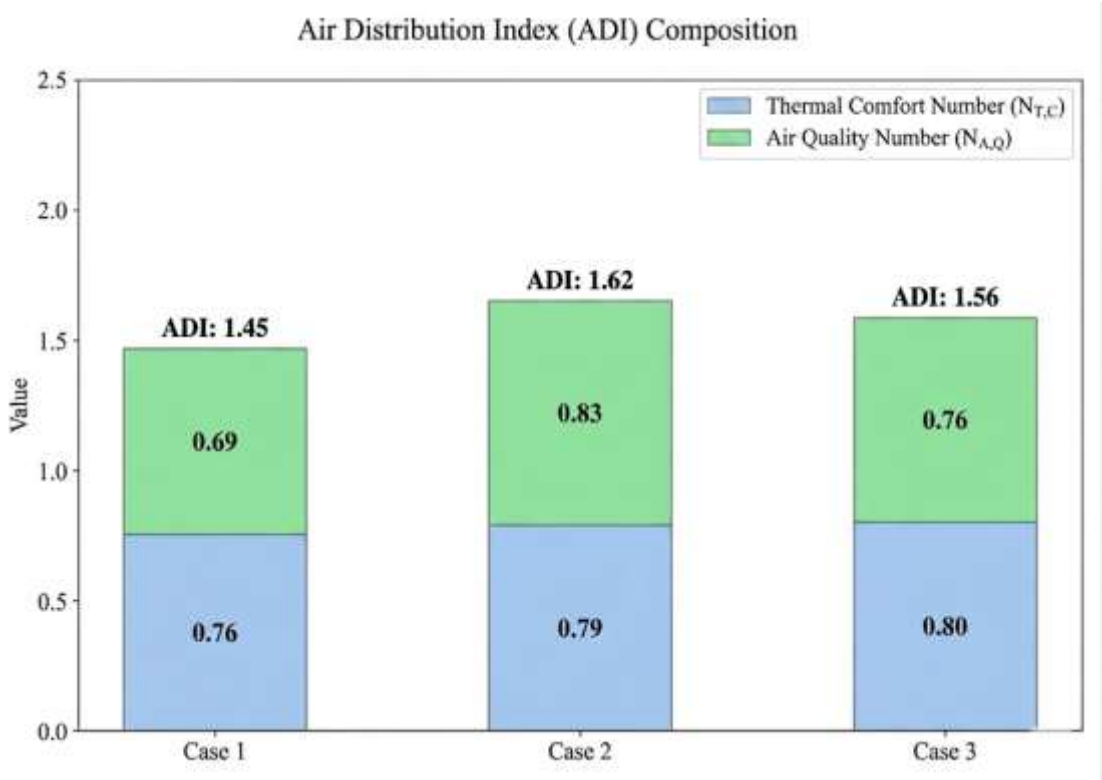

Figure 26: Chart for ADI under the MV with floor outlet

4.3 Result for DV

4.3.1 Result for Thermal Comfort

The thermal comfort for the different cases of dispalcement ventilation where inlet is located at floor level and outlet located at the ceiling are briefly studied. The study used three key parameters related to thermal comfort , namely, thermal sensation (S), thermal effectiveness (ε_t), and thermal comfort number ($N_{T.C}$). The thermal sensation value is seen increasing as more heat is coming from the occupant zone. Looking at the thermal effectiveness value, the second case is seen witht the highest value followed by the third case. The first case is seen with a slightly weaker thermal plume due to less heat at occupant zone whereas the other two cases has enough heat for plume stratification. However, a very strong plume coming from highly localized heat gain in the third case is seen to decrease the thermal effectiveness. This is often seen in DV as stronger thermal plume results in localized mixing within the occupant space instead of the air rising upward with the plume. The results are given in Table 4-5.

Table 4-5: Thermal Comfort Parameters for DV

Case	Thermal Sensation (S)	Thermal Effectiveness(ε_t)	Thermal Comfort Number ($N_{T.C}$)
1	0.21	1.228	1.142
2	0.33	1.609	1.432
3	0.39	1.519	1.322

The value thermal sensation is the absolute value of PMV, which is obtained by feeding the CFD attained results for velocity, humidity, temperature, and mean radiant temperature to the CBE thermal comfort tool. These values are area-weighted average values taken from three iso-surfaces, 0.1m from the floor (ankle level), 0.5m from the floor (torso level), and 1 m from the floor (breathing level). The plot for velocity and temperature variation along the vertical slicing plane taken at the center of the room can be seen in Figure 27 and Figure 28.

When looking at the contour for velocity under the three cases of heat gain distribution, the average velocity around the occupant was 0.061 m/s, 0.069 m/s, and 0.069 m/s for case 1, case 2, and Case 3. The velocity values were under the ASHRAE Standard 55 specified limit of 0.3 m/s. When looking at the velocity contour plot, the one with higher occupant level heat gain is seen with a much more uniform velocity. This was attributed to the thermal plume DV relies on, which works best for a case of high heat gain at floor level.

The average temperature around the occupant in cases 1, 2, and 3 was found to be 298.33 K, 298.46 K, and 298.90 K, respectively. The temperature values were within the ASHRAE Standard 55 thermal comfort limit. The vertical temperature gradient between head and feet was also under the limit.

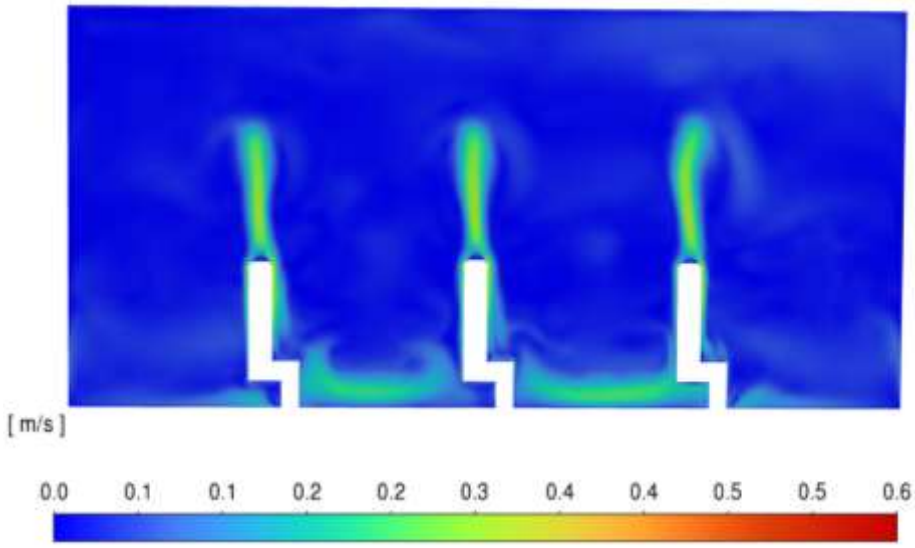

Case 1

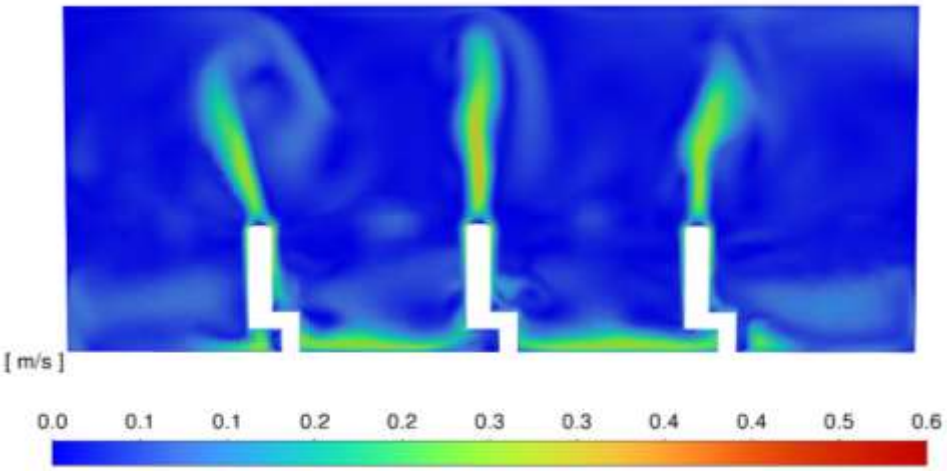

Case 2

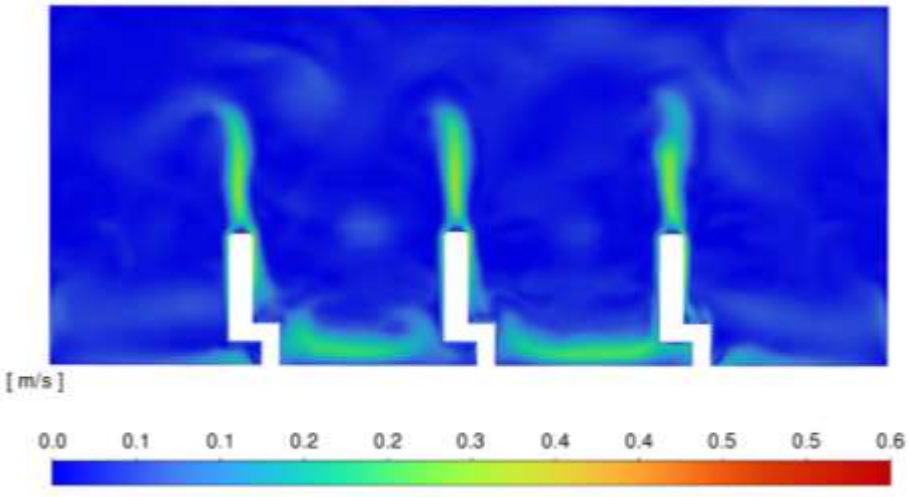

Case 3

Figure 27: Contour for Velocity for the DV with ceiling outlet under the different cases

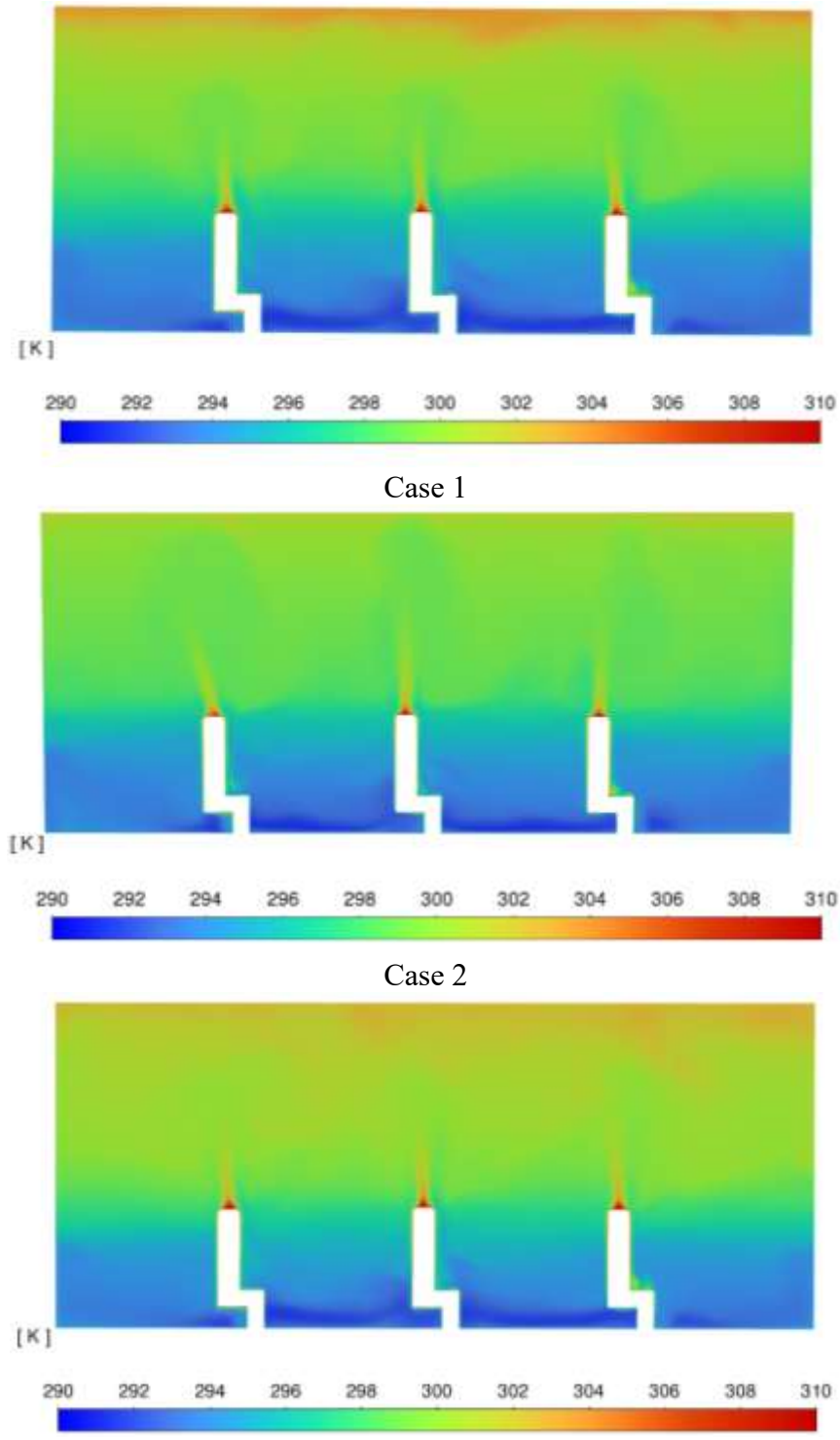

Figure 28: Temperature Contour for the DV with ceiling outlet under the different cases

4.3.2 Result for IAQ parameters

The result for the different IAQ-related parameters for the DV with the ceiling outlet is given in The minimum age of air value is seen for the second case, which has 75% of heat coming from the occupant zone. This is followed by the third case, which has around 80% of the heat contributed by the occupant zone. The pattern suggests DV performs better with IAQ parameters when occupant-zone heat is substantial; the relationship doesn't appear linear. This is because, to some extent, a higher amount of heat in the occupant zone widens the thermal plume and causes local mixing that may end up reducing the IAQ parameter, both the age of air and the contaminant removal effectiveness.

Table 4-6. The minimum age of air value is seen for the second case, which has 75% of heat coming from the occupant zone. This is followed by the third case, which has around 80% of the heat contributed by the occupant zone. The pattern suggests DV performs better with IAQ parameters when occupant-zone heat is substantial; the relationship doesn't appear linear. This is because, to some extent, a higher amount of heat in the occupant zone widens the thermal plume and causes local mixing that may end up reducing the IAQ parameter, both the age of air and the contaminant removal effectiveness.

Table 4-6: IAQ parameters for the DV with Ceiling Outlet

Case	Room time Constant (τ_n)	Age of Air (τ_p^-)	Contaminant Removal Effectiveness (CRE)	Air Quality Number ($N_{A.Q}$)
1	0.133	0.157	1.107	0.93
2	0.133	0.151	1.108	0.97
3	0.133	0.153	1.106	0.96

The contour plot for the mean age of air and CO_2 PPM concentration is given in Figure 29 and Figure 30.

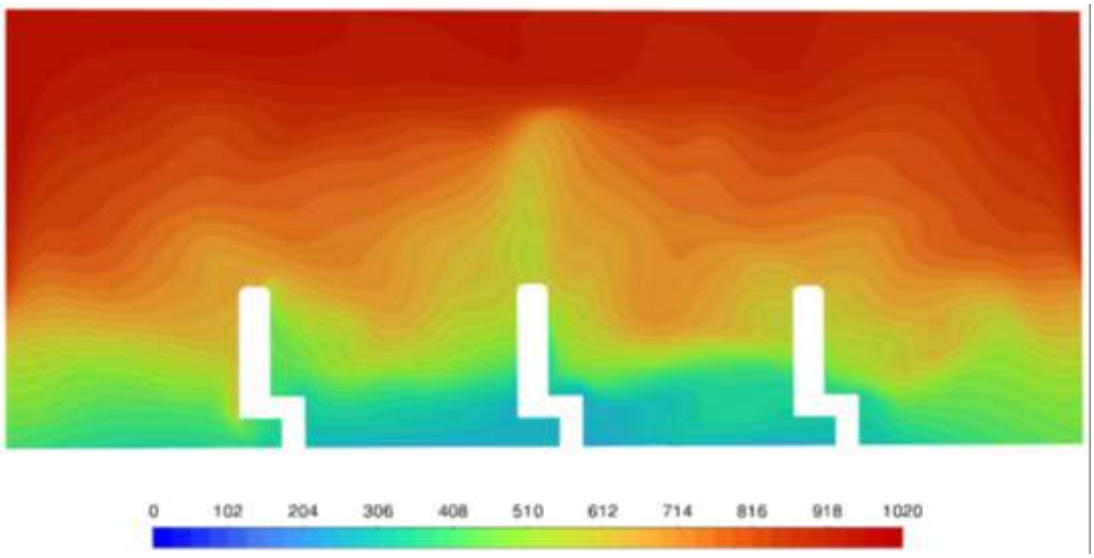

Case 1

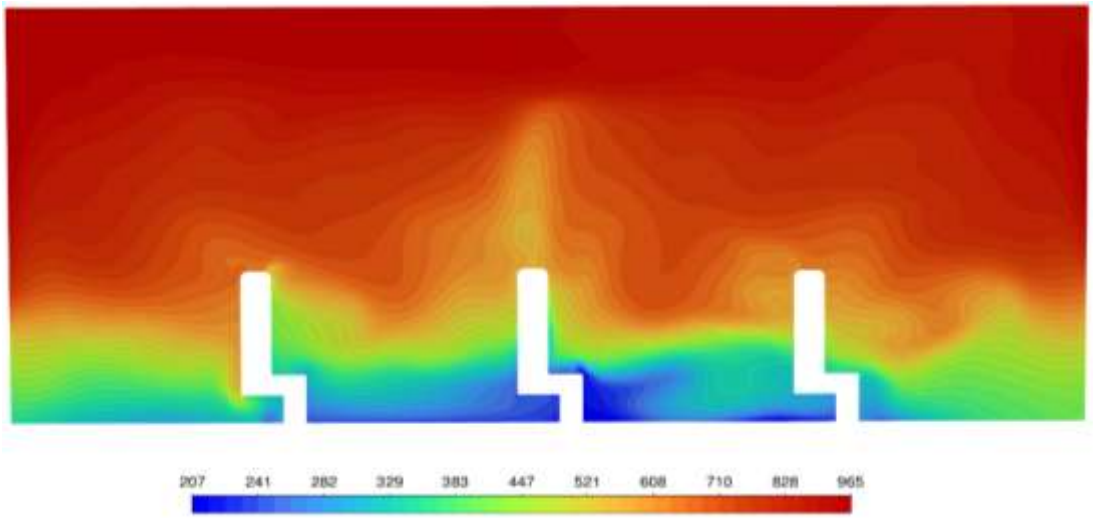

Case 2

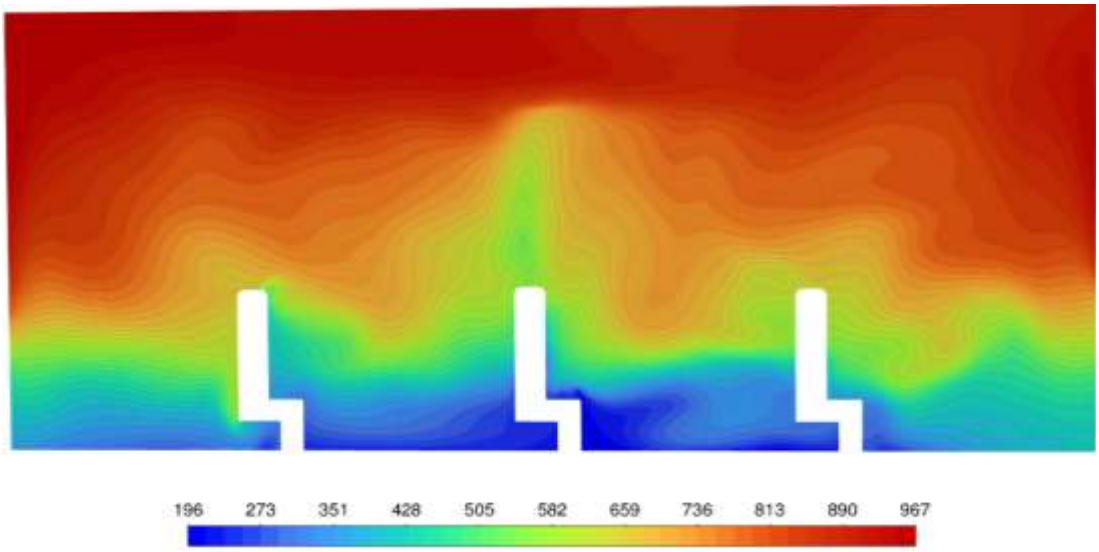

Case 3

Figure 29: Contour for Mean Age of Air for DV with ceiling outlet

The local mean age of air around breathing height was found to be maximum for the first case, with a value of 0.157 hours, whereas the second case was seen with the minimal value of 0.151 hours. Similarly, the third case was seen with the highest local mean age of air corresponding to 0.153 hours. In general, the DV was seen with a lower local mean age of air for cases with higher heat gain from the occupant zone. This was because higher heat gain at the occupant space gives a stronger thermal plume that makes strong stratification, thus causing faster dispersion of air from the breathing plane.

The CO_2 ppm concentration breathing height was found to be maximum for the first case, with 605, whereas the second case was seen with the minimal value of 564. Similarly, the second case was seen with the value corresponding to 584. In all cases, the CO_2 ppm concentration at the breathing plane was less than the limit of 1000. In general, the DV can be seen with less CO_2 ppm for the cases with high heat concentration at the floor level.

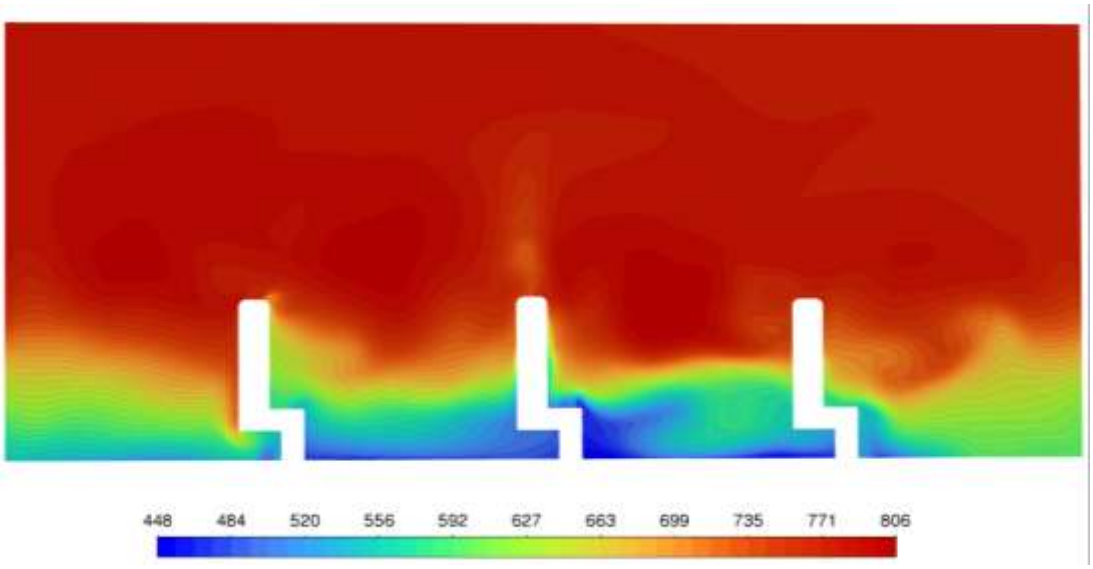

Case 1

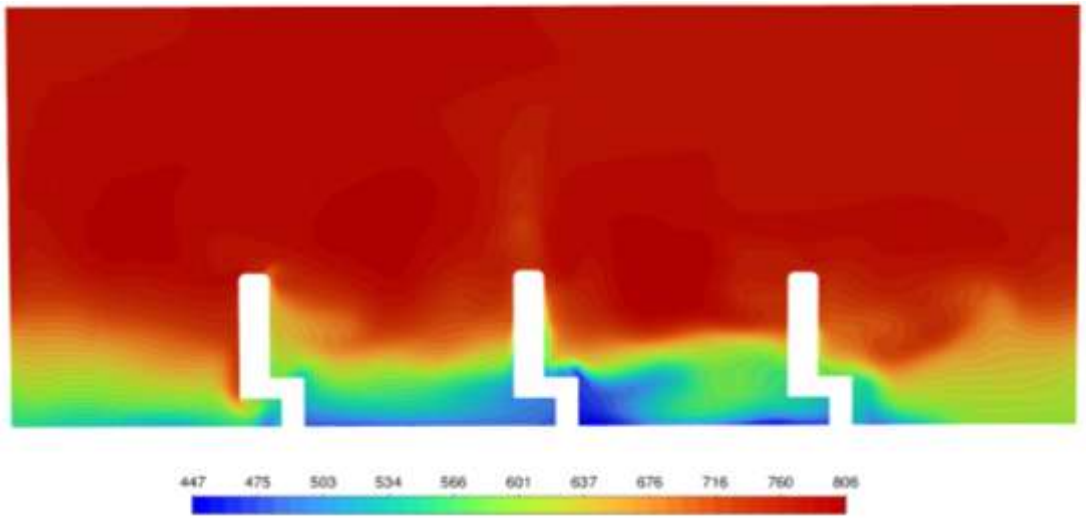

Case 2

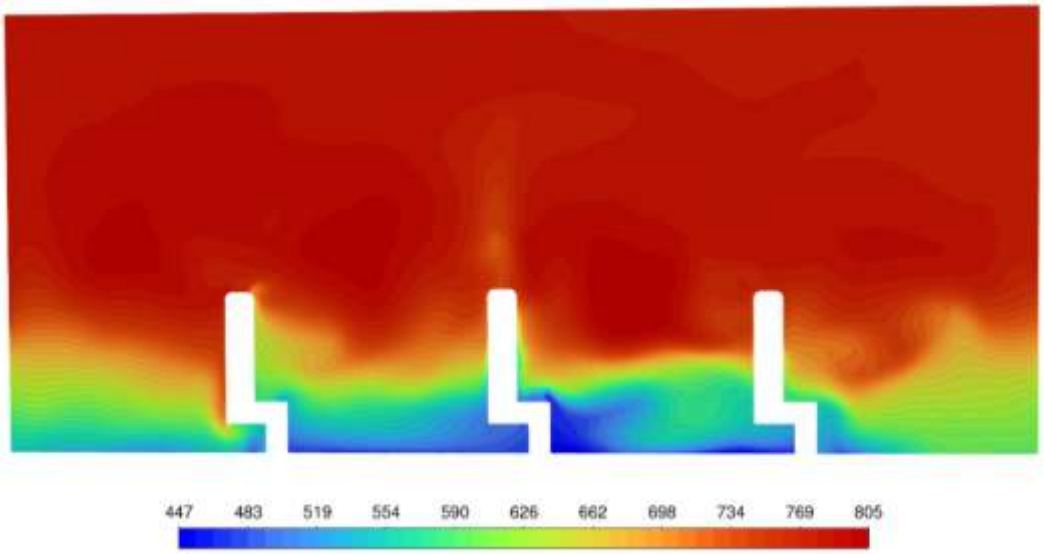

Case 3

Figure 30: CO_2 ppm concentration for DV with ceiling outlet

4.3.3 Result For Air Distribution Index(ADI)

The result for the Air Distribution Index (ADI) for the DV with a ceiling outlet is given in Figure 31. The ADI value can be seen as highest for the second case,2.41, which has 75% of the total cooling load contributed by the occupant zone. It was followed by the third case, 2.28, which has 80% of the total cooling load contributed by the occupant zone. Lastly, the first case was seen with an ADI value of 2.08. Similar patterns were also observed for the air quality number and the thermal comfort number. The overall ADI value attained in the case was in the range of once attained in previous works (Almesri et al., 2013b)Thus, DV performs better under a substantial amount of cooling load contributed by the occupant zone, as it is a ventilation system based on stratification and entrainment. However, the relationship is not always linear, which can be seen when going from the second to the third case. The non-linear relationship between the DV and occupant zone heat gain percentage can often be attributed to the concept of plume strength limit (Rees & Haves, 2013). The phenomenon helps understood how excessively high heat gain at the lower zone may lead to an unstable plume that causes uncontrolled stratification and eventually localized mixing instead of strong stratification.

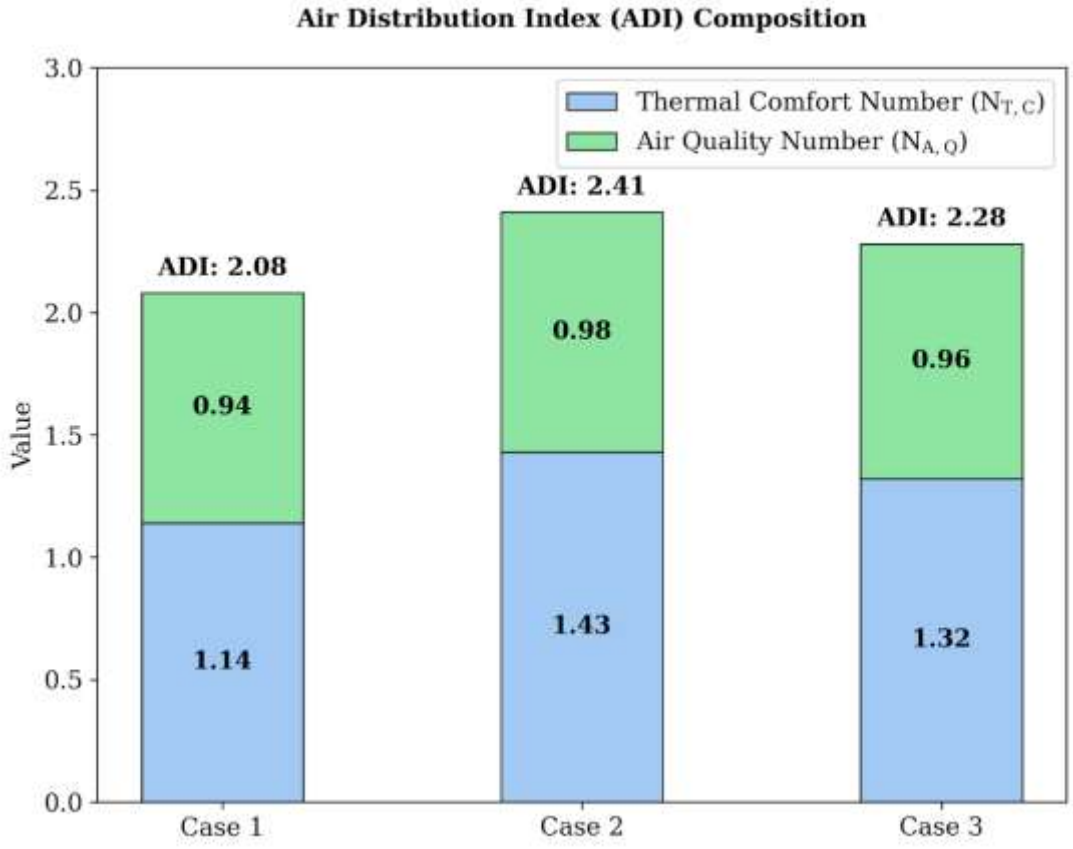

Figure 31: Chart for ADI under the DV with ceiling outlet

4.4 Effect of Vertical Height on Thermal Comfort Parameters and IAQ Parameters

The effect of vertical height on the thermal comfort and IAQ parameters was also studied. For each of the three types of ventilation arrangement, simulations were done under different vertical enclosure heights: 2.6 m, 3m, and 3.4 m. The three cases had the same amount of total heat gain, the same boundary condition, with only the vertical enclosure height being the major difference.

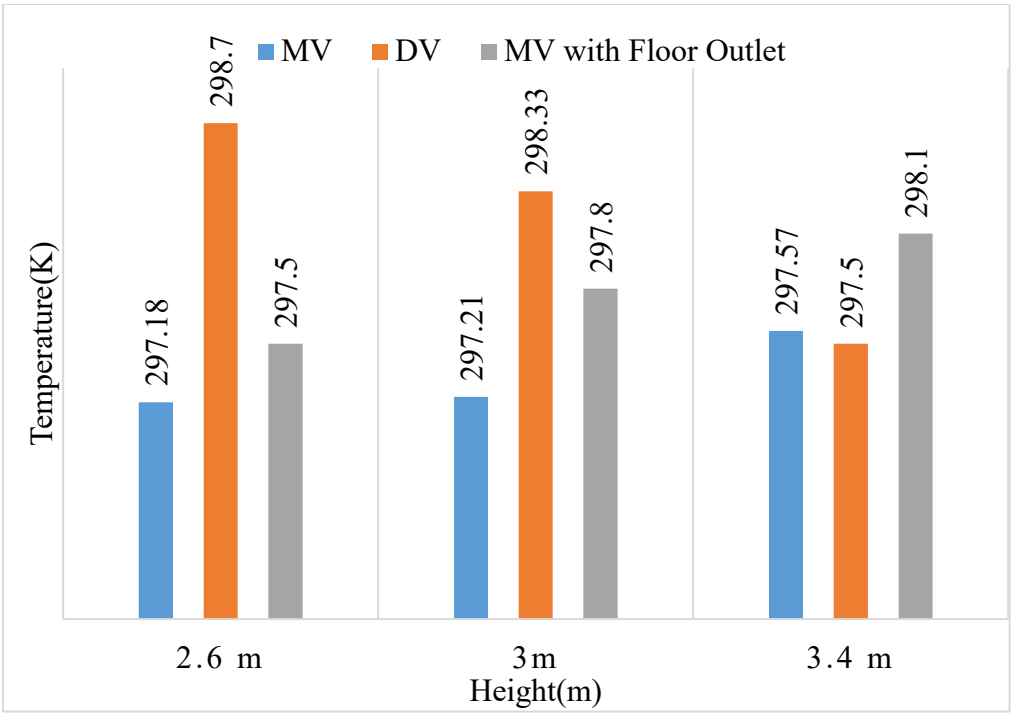

Figure 32: Average occupant zone temperature under different envelope heights

The results obtained from the CFD simulations indicate that the average temperature at the occupant space was maximum for the Displacement Ventilation (DV) case in the room with a 2.6 m height, reaching a value of 298.7 K. Conversely, the Mixing Ventilation (MV) case was seen with the minimal temperature value of 297.18 K within the same 2.6 m enclosure. As the simulation height was increased to 3.4 m, the MV with Floor Outlet case was seen with the highest average temperature corresponding to 298.1 K, as given in Figure 32.

In general, the DV system was seen with a higher local temperature for cases with lower enclosure heights. This was because a lower ceiling height restricts the vertical development of the thermal plume, causing the stratified warm layer to descend closer to the occupant zone. In the CFD model, as the room height increases to 3.4 m, the additional volume allows for better vertical separation of heat, resulting in a lower average temperature at the occupant level for the DV case compared to the more confined 2.6 m case.

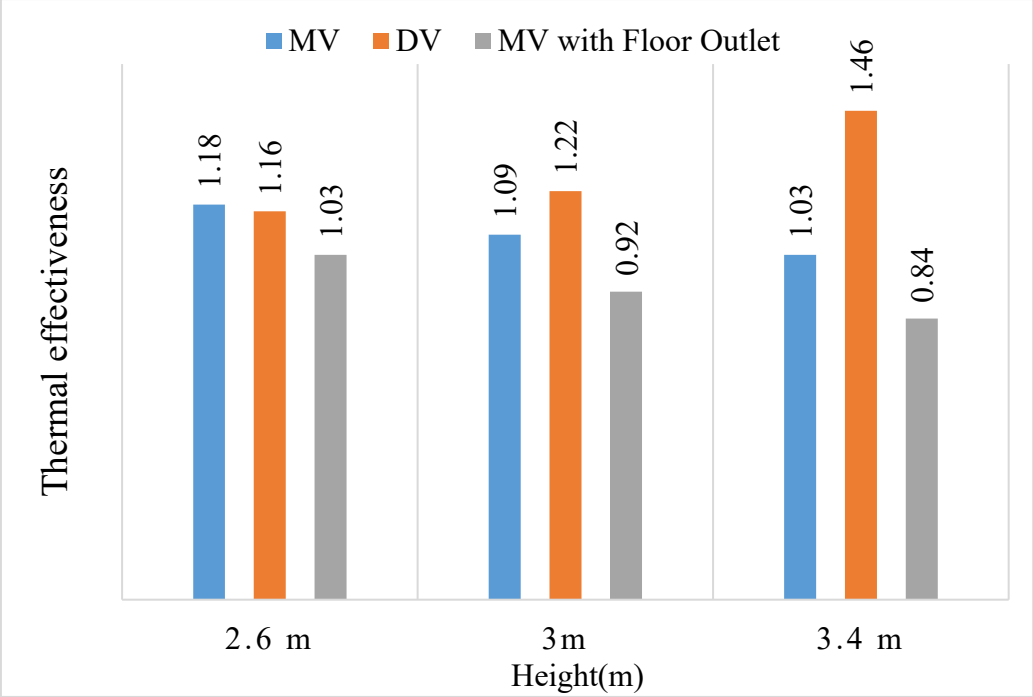

Figure 33: Thermal effectiveness under different envelope height

The results obtained from the CFD simulations indicate that the thermal effectiveness was found to be maximum for the Mixing Ventilation (MV) case in the room with a 2.6 m height, with a value of 1.18. Conversely, the MV with Floor Outlet case was seen with the minimal value of 1.03 within the same 2.6 m enclosure. As the simulation height was increased to 3.4 m, the Displacement Ventilation (DV) case was seen with the highest thermal effectiveness, corresponding to 1.46 as given in Figure 33.

In general, the DV was seen with a higher thermal effectiveness for cases with higher enclosure heights. This was because a greater vertical distance allows for a more established thermal stratification, where the buoyancy-driven flow effectively carries heat away from the occupant zone toward the upper exhaust. In the CFD model, as the room height increases, the efficiency of this heat removal process in the DV system improves significantly, whereas the effectiveness of the MV cases tends to decline as the larger volume makes it more difficult to maintain uniform temperature distribution throughout the increased space.

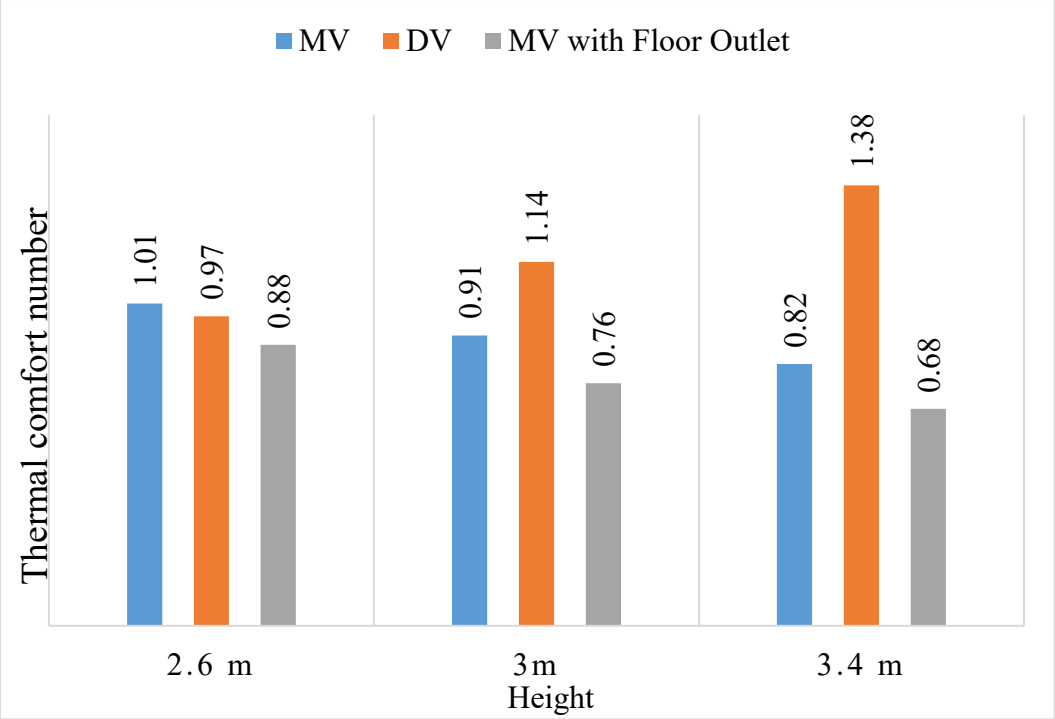

Figure 34: Thermal comfort number under different envelope heights

The results obtained from the CFD simulations indicate that the Thermal Comfort Number was found to be maximum for the Mixing Ventilation (MV) case in the room with a 2.6 m height, reaching a value of 1.01. Conversely, the MV with Floor Outlet case was seen with the minimal value of 0.88 within the same 2.6 m enclosure. As the simulation height was increased to 3.4 m, the Displacement Ventilation (DV) case was seen with the highest Thermal Comfort Number corresponding to 1.38, as given in Figure 34.

In general, the DV was seen with a higher Thermal Comfort Number for cases with higher enclosure heights. This was because a greater vertical height provided more space for the thermal plumes to develop, which allowed for a more efficient separation of the warm stratified layer from the occupied zone. In the CFD model, as the room height increased, the buoyancy-driven flow in the DV system became more effective at maintaining a favorable environment at the breathing level, whereas the performance of the MV cases was seen to decrease as the larger volume hindered the ability of the supply air to mix uniformly throughout the space.

4.5 Effect of Vertical Height on IAQ parameters

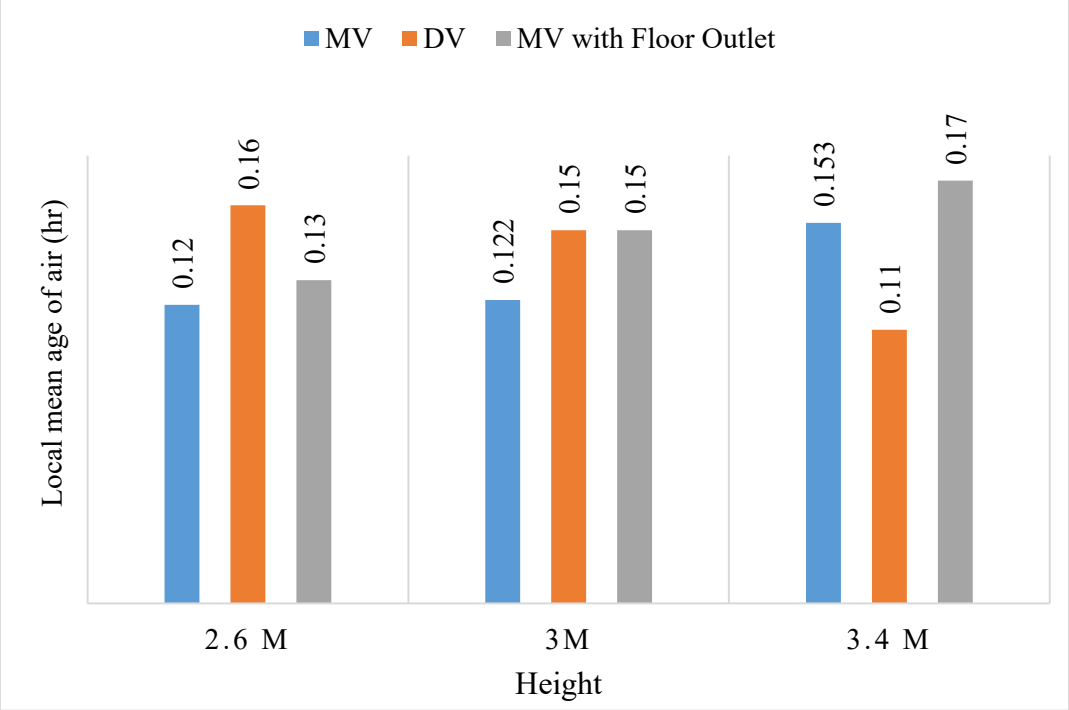

Figure 35: Local mean age of air at the breathing point under different envelope heights

The results obtained from the CFD simulations indicate that the local mean age of air at the breathing point was found to be maximum for the Displacement Ventilation (DV) case in the room with a 2.6 m height, with a value of 0.16 hours, whereas the Mixing Ventilation (MV) case was seen with the minimal value of 0.12 hours. Similarly, for the room with a 3.4 m height, the MV with Floor Outlet case was seen with the highest local mean age of air, corresponding to 0.17 hours, as given in Figure 35.

In general, the DV was seen with a lower local mean age of air for cases with higher enclosure heights. This was because a greater vertical height allowed for the development of a more robust thermal plume, which enhanced the buoyancy-driven flow and facilitated the rapid removal of stagnant air from the occupied zone. In the CFD model, as the enclosure height increased to 3.4 m, the air distribution in the DV system became more efficient at refreshing the breathing plane, while the MV cases exhibited an increase in the age of air as the larger room volume led to more extensive recirculation and slower air replacement.

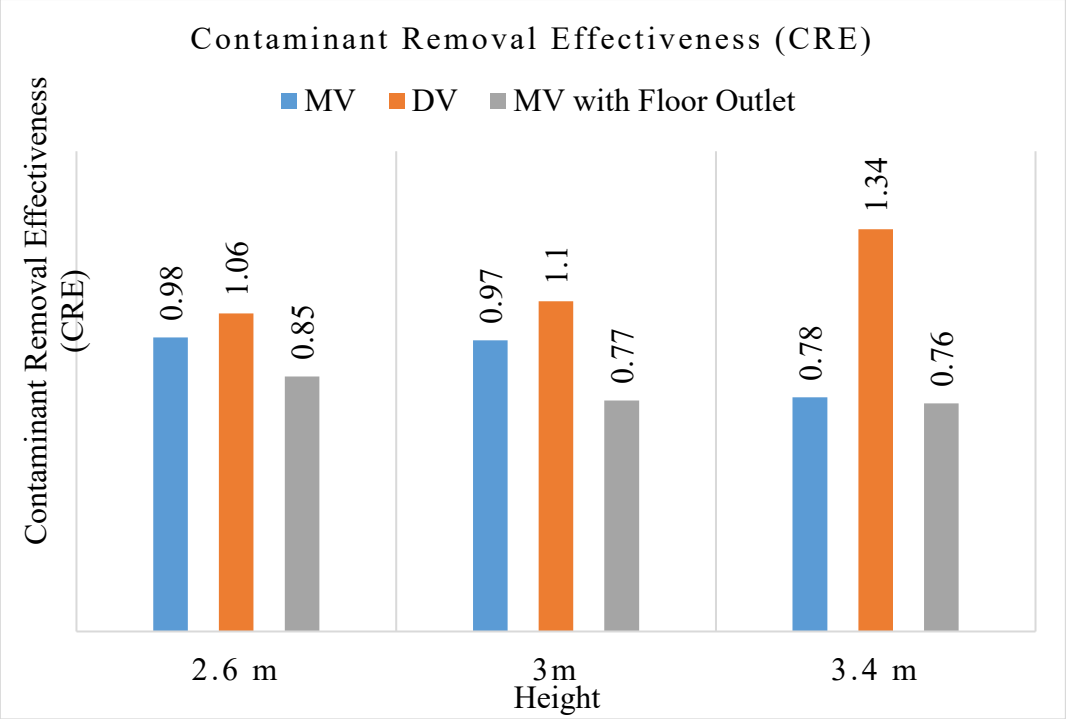

Figure 36: Contaminant Removal Effectiveness (CRE) under different envelope heights

The results obtained from the CFD simulations indicate that the Contaminant Removal Effectiveness (CRE) was found to be maximum for the Displacement Ventilation (DV) case in the room with a 2.6 m height, with a value of 1.06, whereas the MV with Floor Outlet case was seen with the minimal value of 0.85. Similarly, for the room with a 3.4 m height, the DV case was seen with the highest contaminant removal effectiveness, corresponding to 1.34, as given in Figure 36.

In general, the DV was seen with a higher CRE for cases with higher enclosure heights. This was because a greater vertical height allowed for a more distinct stratification of air layers, which enabled the buoyancy-driven plumes to carry contaminants more effectively toward the upper exhaust zone. In the CFD model, as the room height increased, the piston-like flow of the DV system became more efficient at purging pollutants from the breathing zone, while the effectiveness of the MV cases was seen to decline as the larger volume led to increased dilution and potential short-circuiting of the fresh air supply.

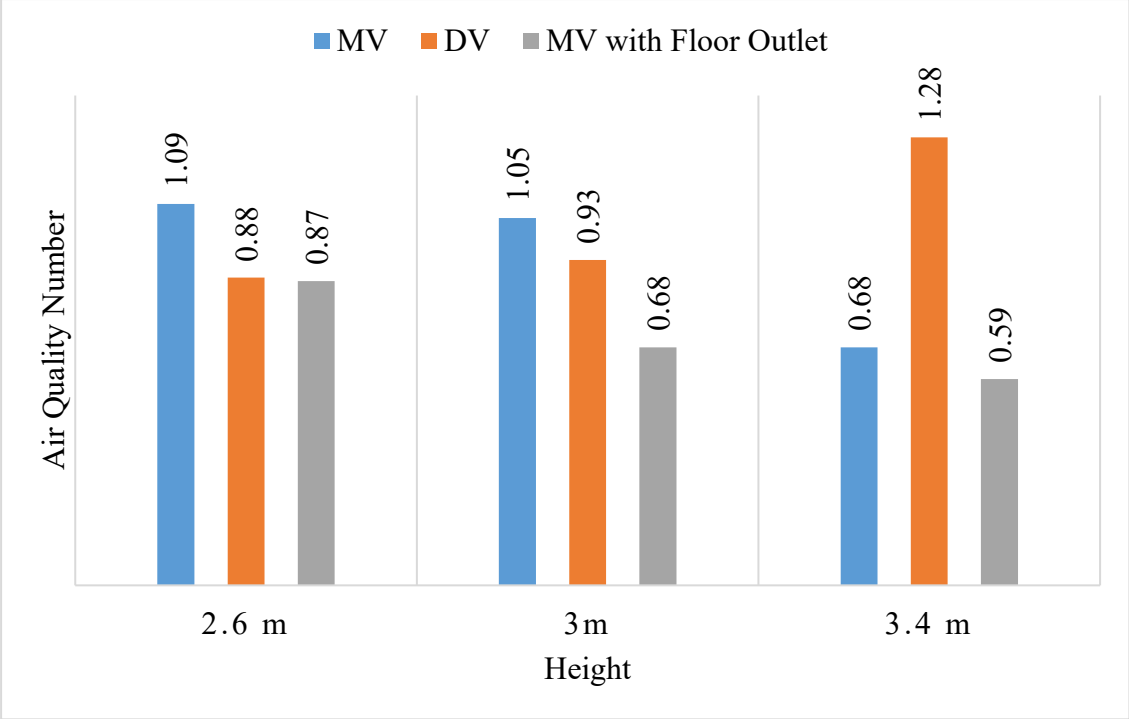

Figure 37: Air Quality Number under different envelope heights

The results obtained from the CFD simulations indicate that the Air Quality Number was found to be maximum for the Mixing Ventilation (MV) case in the room with a 2.6 m height, with a value of 1.09, whereas the MV with Floor Outlet case was seen with the minimal value of 0.87. Similarly, for the room with a 3.4 m height, the Displacement Ventilation (DV) case was seen with the highest Air Quality Number corresponding to 1.28, as given in Figure 37.

In general, the DV was seen with a higher Air Quality Number for cases with higher enclosure heights. This was because a greater vertical distance facilitated the formation of a more stable stratified environment, which allowed the buoyancy-driven flow to more effectively displace polluted air from the occupied zone. In the CFD model, as the room height increased, the performance of the DV system improved as it successfully localized fresh air at the breathing level, whereas the air quality in the MV cases was seen to deteriorate as the larger room volume promoted more extensive mixing of contaminants throughout the space.

This type of significant improvement in IAQ parameter for DV can be attributed to stronger stratification seen with an increase in envelope height. This can be quantified using a dimensionless number, Archimedes Number(Ar), which quantifies how strong

the buoyant forces are compared to inertial forces. The spaces with 2.6m, 3m, and 3.4 m were found with Ar numbers 2.2, 2.5, and 2.9, respectively. The increase in Ar number thus allows a faster displacement of air in an upward direction, which later deduces the mean local age of air in addition to reducing the concentration of CO_2 at the breathing plane. These two in combine increases the air quality number. The velocity vector diagram for DV under diffeent height is thus shown in Figure 38.

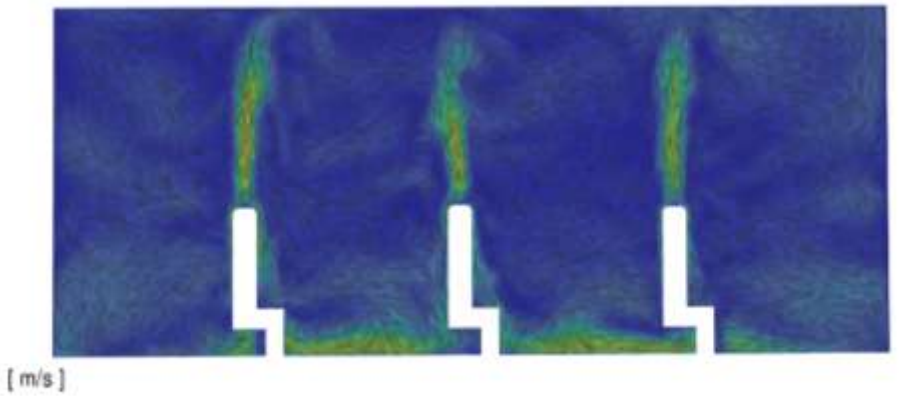

Velocity vector at vertical plane for 2.6 m envelope height

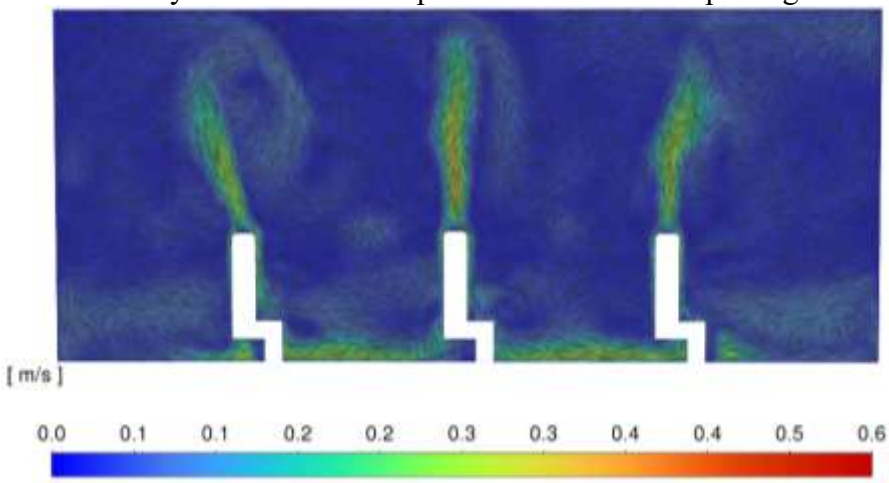

Velocity vector at vertical plane for 3 m envelope height

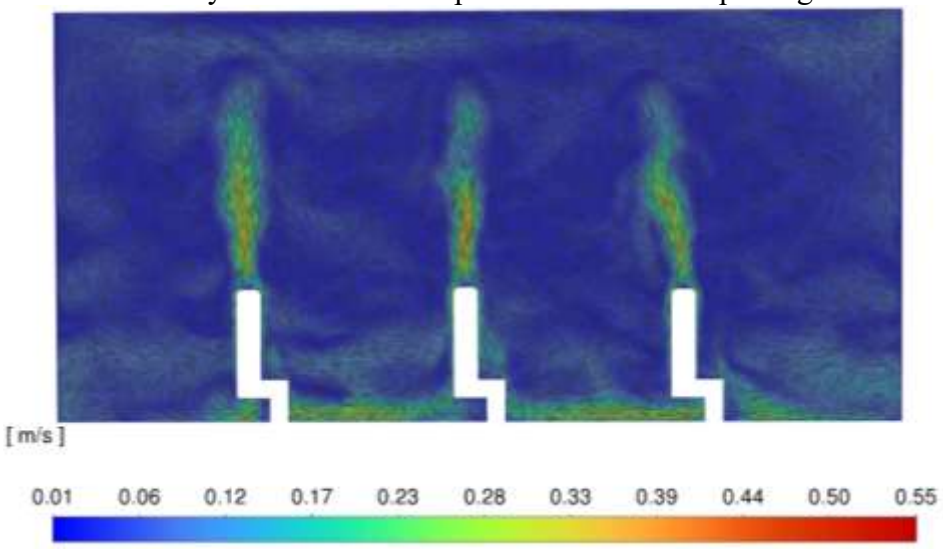

Velocity vector at vertical plane for 3.4 m envelope height

Figure 38: Velocity vector diagram for DV under different envelope heights

4.6 Effect of Vertical Height on Air Distribution Index (ADI)

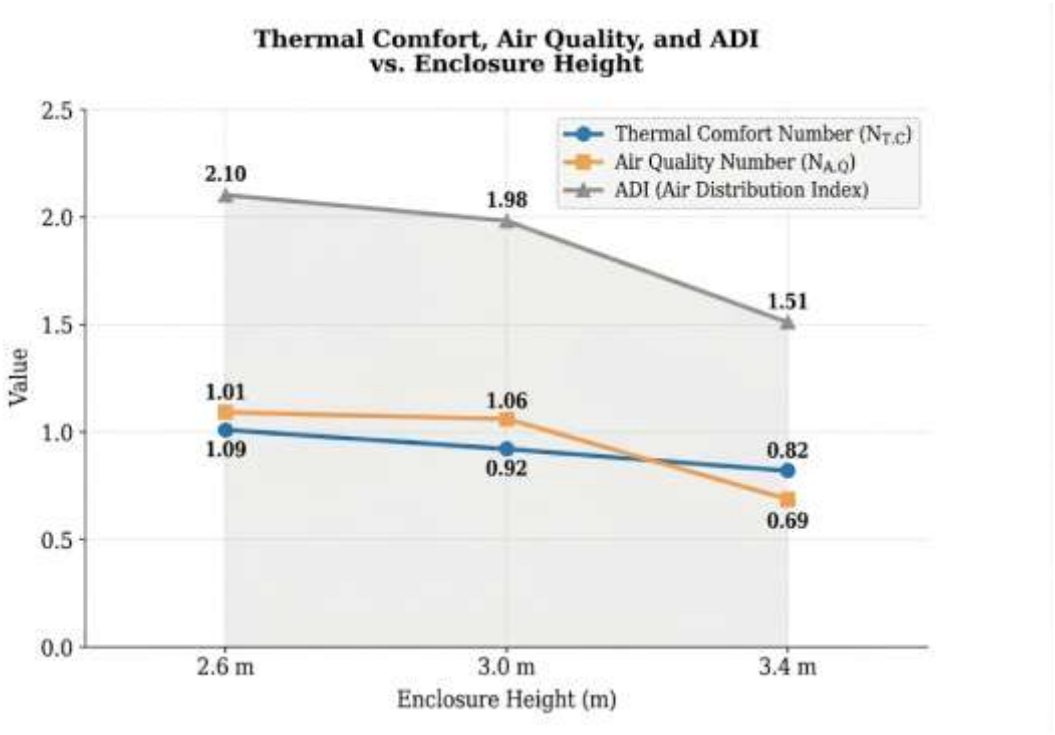

Figure 39: Air Distribution Index (ADI) under different envelope heights for MV

The results obtained from the CFD simulations indicate that the Air Distribution Index (ADI) was found to be maximum for the Mixing Ventilation (MV) case in the room with a 2.6 m height, reaching a value of approximately 2.1. Conversely, the MV case within the 3.4 m enclosure was seen with the minimal ADI value of 1.51. As the simulation height progressed from 2.6 m to 3.4 m, both the Thermal Comfort Number and the Air Quality Number showed a consistent decline, which was reflected in the decreasing trend of the overall ADI. The variables can be seen in Figure 39.

In general, the MV was seen with a lower ADI for cases with higher enclosure heights. This was because the increased vertical distance between the supply inlet and the occupant zone allowed for more extensive recirculation zones to form above the breathing plane, which trapped heat and contaminants rather than exhausting them efficiently(Aziz et al., 2012). In the CFD model, as the height increased to 3.4 m, the momentum of the supply air was insufficient to penetrate and effectively mix the entire vertical space, leading to stagnant air pockets and increased recirculation. Consequently, the ADI reached its lowest point in the tallest room, where these

recirculation effects most significantly hindered the delivery of fresh, conditioned air to the occupant space.

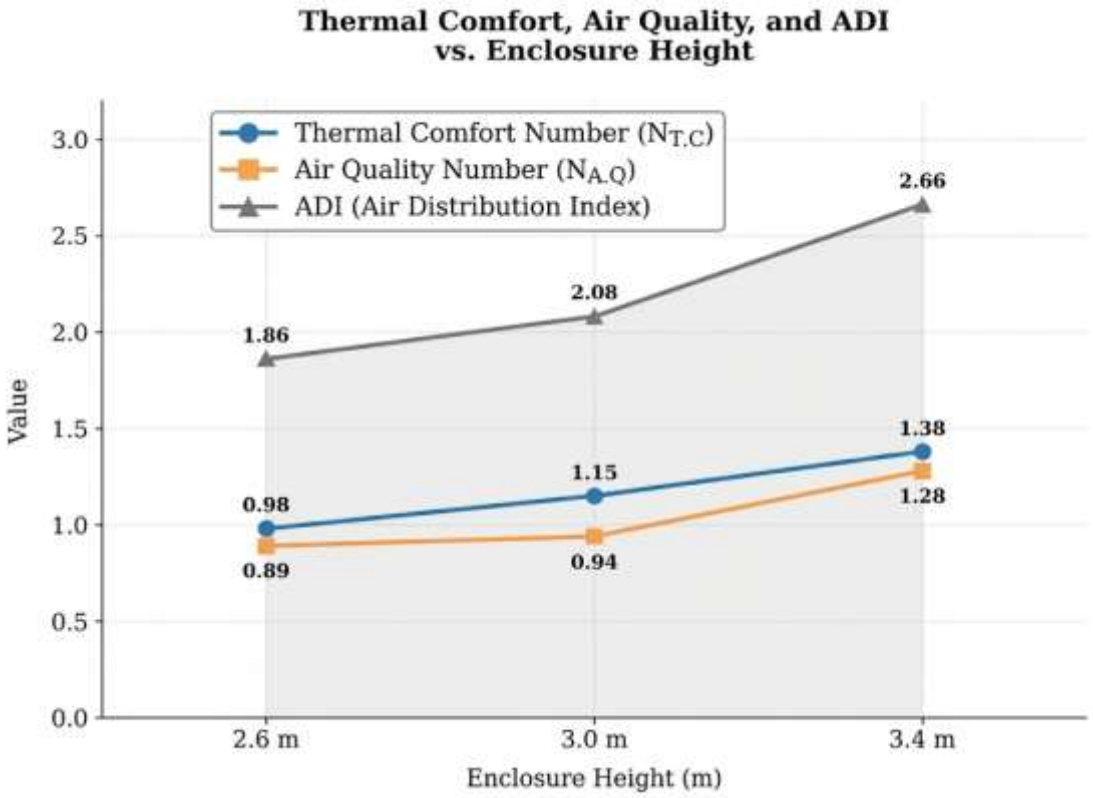

Figure 40: Air Distribution Index (ADI) under different envelope heights for DV

The results obtained from the CFD simulations indicate that the Air Distribution Index (ADI) was found to be maximum for the Displacement Ventilation (DV) case in the room with a 3.4 m height, reaching a value of approximately 2.67. Conversely, the DV case within the 2.6 m enclosure was seen with the minimal ADI value of 1.87. As the simulation height progressed from 2.6 m to 3.4 m, both the Thermal Comfort Number and the Air Quality Number showed a consistent increase, resulting in the upward trend observed in the overall ADI. The variation in the ADI value can be seen in Figure 40.

In general, the DV was seen with a higher ADI for cases with higher enclosure heights. This was because the increased vertical distance allowed for a more stable thermal stratification and reduced the impact of recirculation within the occupied zone (Lastovets et al., 2020). In the CFD model, as the height increased to 3.4 m, the buoyancy-driven flow became more effective at carrying heat and contaminants upward, away from the breathing level, without the interference of the mixing or

recirculation seen in shorter rooms. Consequently, the ADI reached its peak in the tallest room, where the separation between the fresh supply air at the floor and the polluted stratified air near the ceiling was most effectively maintained.

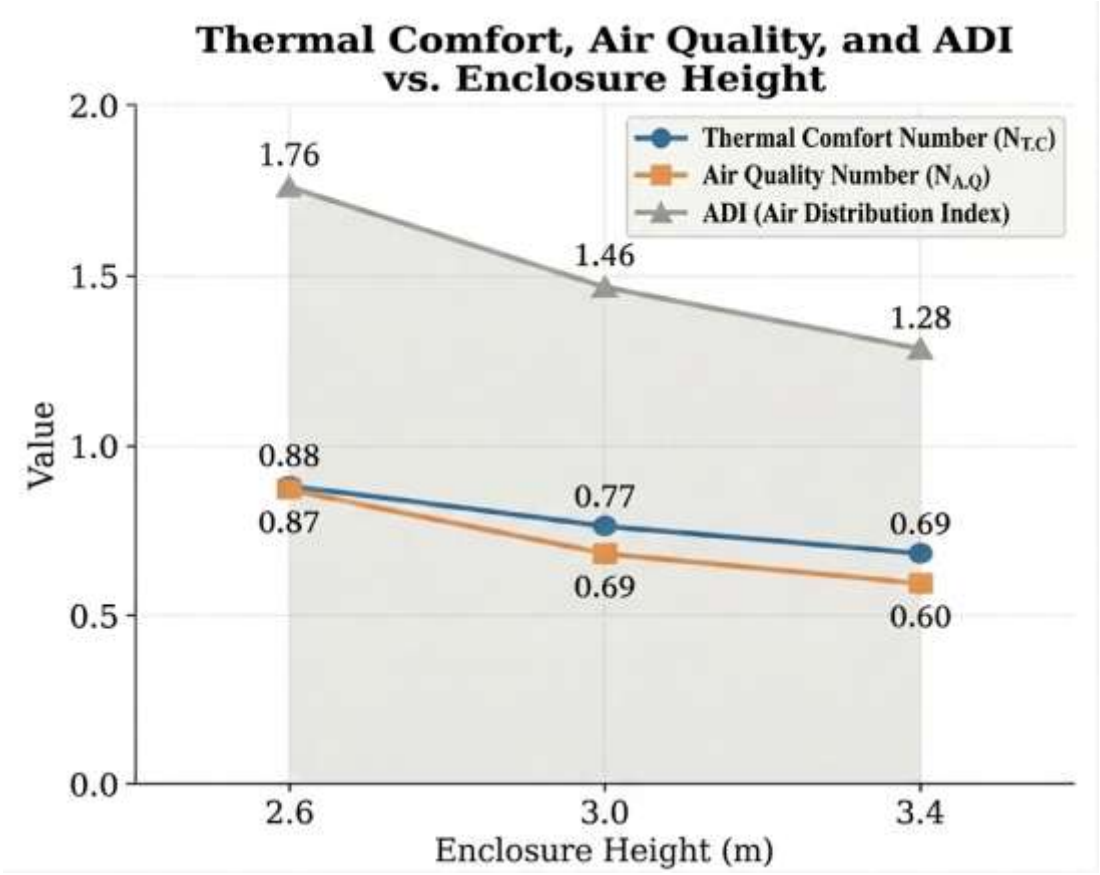

Figure 41: Air Distribution Index (ADI) under different envelope height for MV with floor outlet

The results, which were based on CFD simulation, demonstrated that increasing the enclosure height from 2.6m to 3.4m led to a consistent decline in the effectiveness of the mixing ventilation system. At the lowest height of 2.6m, the system achieved its highest performance with an ADI of approximately 1.78, suggesting that the momentum from the floor outlets was sufficient to maintain high thermal comfort and air quality levels within the smaller volume. However, as the height increased to 3m and 3.4m, the ADI followed a downward trajectory, eventually dropping to 1.28. This trend was mirrored by both the Thermal Comfort Number and the Air Quality Number, indicating that the mixing efficiency was compromised in taller enclosures where the

supply air struggled to maintain uniformity throughout the expanded space(Aziz et al., 2012). The variation is given in Figure 41.

4.7 Geometric and Heat Distribution Sensitivity of Displacement Ventilation

Comparison of the two ventilation strategies showed displacement ventilation to be highly sensitive to heat distribution and envelope height. While the sensitivity of MV to different cases of heat gain and envelope height was seen to be linear, the case was different with displacement ventilation. When looking at the three cases of heat gain distribution and envelope height, MV was seen underperforming as more heat was lumped around the occupant space. The relationship was linear, which can be compensated for with a few extra CFM than usual, which will be enough to increase the jet penetration enough to mix out the whole space. Similarly, the perfromance of MV under higher ceiling height could also be compensated by adding extra CFM that could generate jet penetration enough to recirculate through all of the stagnant zones in the space.

However, when looking at the DV's sensitivity to heat distribution, the relationship was quite non-linear.DV was seen performing well under cases that had higher heat contribution from the occupant zone. However, it performed best under the case where 75% of the heat was from the occupant zone rather than the third case where the occupant zone had 80% of the heat gain. The phenomena suggested the existence of a plume strength limit for DV between the two cases. The plume strength limit can be determined for the given space using a dimensionless number.

Richardson Number (Ri) is often used to understand the sensitivity of indoor stratifications(Rees & Haves, 2013). It is a dimensionless number that determines how strong the buoyancy force is compared to momentum forces. As shown in the table, the three cases had Ri values corresponding to 1.48, 1.60, and 1.58, which is a clear indication of stratification in the DV system. However, as Ri decreased from 1.60 in case 2 to 1.58 in case 3 suggests a point of inflection between 75% to 80% for the given case. It is the point after which the DV system won't have stable stratification due to excessive heat from the occupant zone. A second-order polynomial regression was utilized to model the non-linear relationship between internal heat loads and the Richardson Number in Figure 42. This approach allows for the identification of the

system's thermal tipping point through differentiation, providing a mathematical threshold for stable vertical stratification. It was determined using quadratic curve fitting, and the value for optimal occupant zone heat contribution for the case was found to be 76.36%.

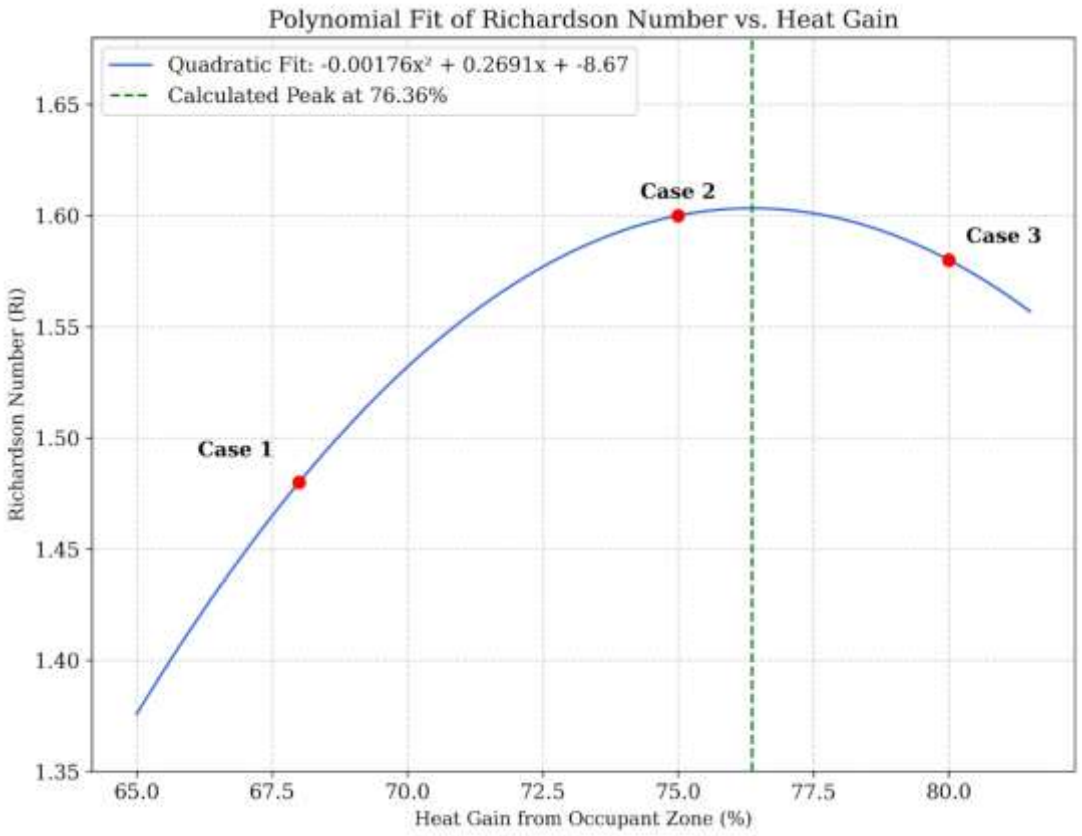

Figure 42: Richardson Number (Ri) versus heat gain intensity from the occupant zone

When looking at the sensitivity of the DV with the envelope height, a trend was seen which can be better visualized using the dimensionless number, Ri. The three cases of rooms with envelope heights of 2.6 m, 3m, and 3.4 m were found with Ri values corresponding to 1.37, 1.48, and 1.61, respectively. Despite all cases having the same volumetric heating-based Archimedes number (Ar), they were seen with different Ri numbers. This was because while Ar mostly signifies the behavior at the global level, Ri was determined based on the CFD results attained, which were based on how local stratification profiles were seen along the vertical plane of the room. The plot attained for the Ri versus the envelope height showed a quadratic curve. On approaching 2.6 m to 3m, the slope of the curve was about 0.275. However, as the curve approached from

3m to 3.4m, the slope of the curve was around 0.32, as given in Figure 43. The trend signified that for the given total heat gain, 3m envelope height was the critical point. The rapidly increasing slope of the curve after 3m indicated the stability in stratification with every meter of increase in envelope height after 3m.

Any envelope height less than 3m was found to be inefficient for DV for the space with the given heat gain and Ar number. Thus, for every envelope space with a given volumetric heat gain, there exists a minimal envelope height that is necessary for DV to meet the minimal stratification and ASHRAE-specified thermal gradient limit. The phenomenon can be attributed to the fact that DV works best when there is enough vertical space for stratification. In the case of a ceiling less than 3m, the momentum gained through the plume becomes too strong to be stratified within the given height, which can lead to disturbed stratification and poor effectiveness (Wang & Hong, 2023). Such phenomena at low ceiling often cause the contaminant and polluted air to recirculate back into the lower occupant zone instead of staying above under stratified layers. Such issues severely reduce the perfromance of DV, especially in terms of IAQ parameters.

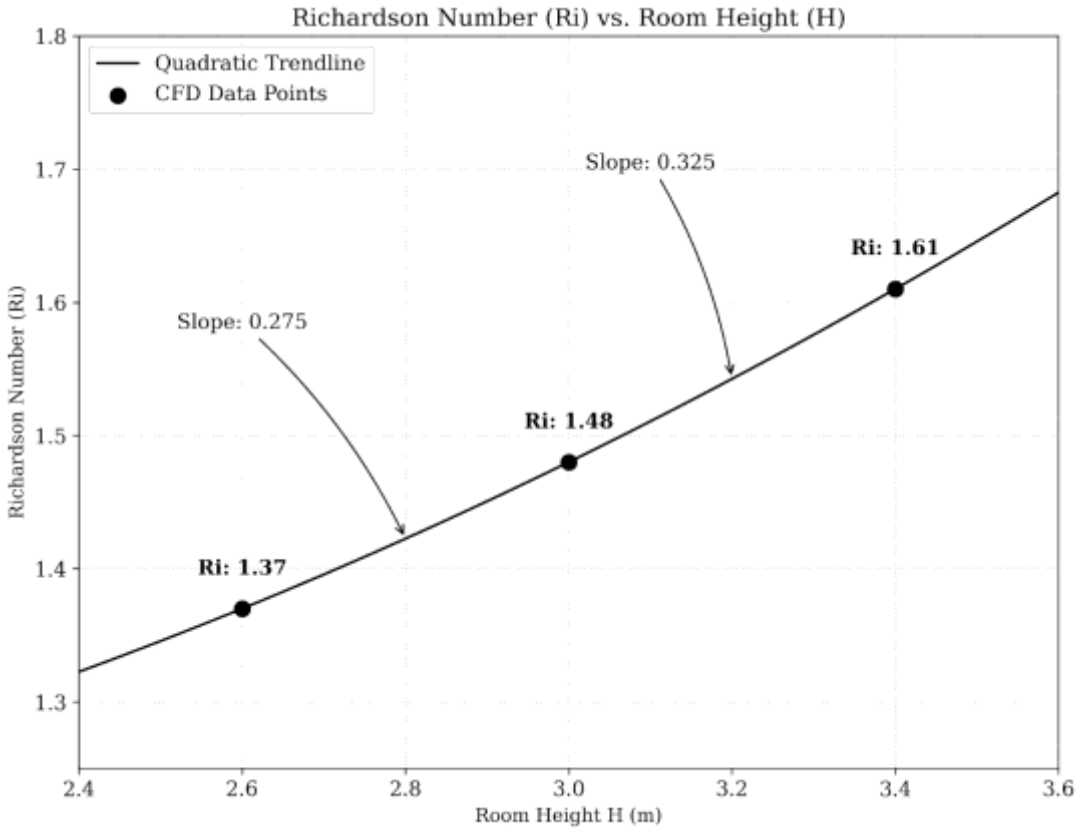

Figure 43: Richardson number versus ceiling height

The impact of ceiling height can also be seen on the overall thermal comfort in DV. In MV, a higher ceiling height just turned out to be a poor jet penetration limit in the room that leaves a stagnant zone. Such a drawback with increasing ceiling height was, however, compensable through some more momentum from the ceiling diffuser, which allows a higher jet throw to reach all spaces in the room. However, the sort of drawback a lower ceiling height brought to the case of DV was quite severe and hard to compensate for. In a stratification-based ventilation system like DV, the vertical temperature gradient between head and feet is often the most important parameter for thermal comfort, after ankle draft (Causone et al., 2010). When the head-to-feet temperature gradient was looked for in the cases of different ceiling heights, the case with a 2.6 m ceiling height was seen with a 4.5 K gradient. Likewise, the temperature gradient for a 3m ceiling was 3K, which eventually dropped down to 2.3K for the 3.4m ceiling height. The phenomenon described the existence of a minimal envelope height required for DV to meet the thermal gradient limit. For the three cases studied, 3m was the minimal height, as the case of 2.6m was seen with a head-foot temperature gradient

value exceeding the allowable ASHRAE limit. The detailed plot for the temperature gradient can be seen in Figure 44

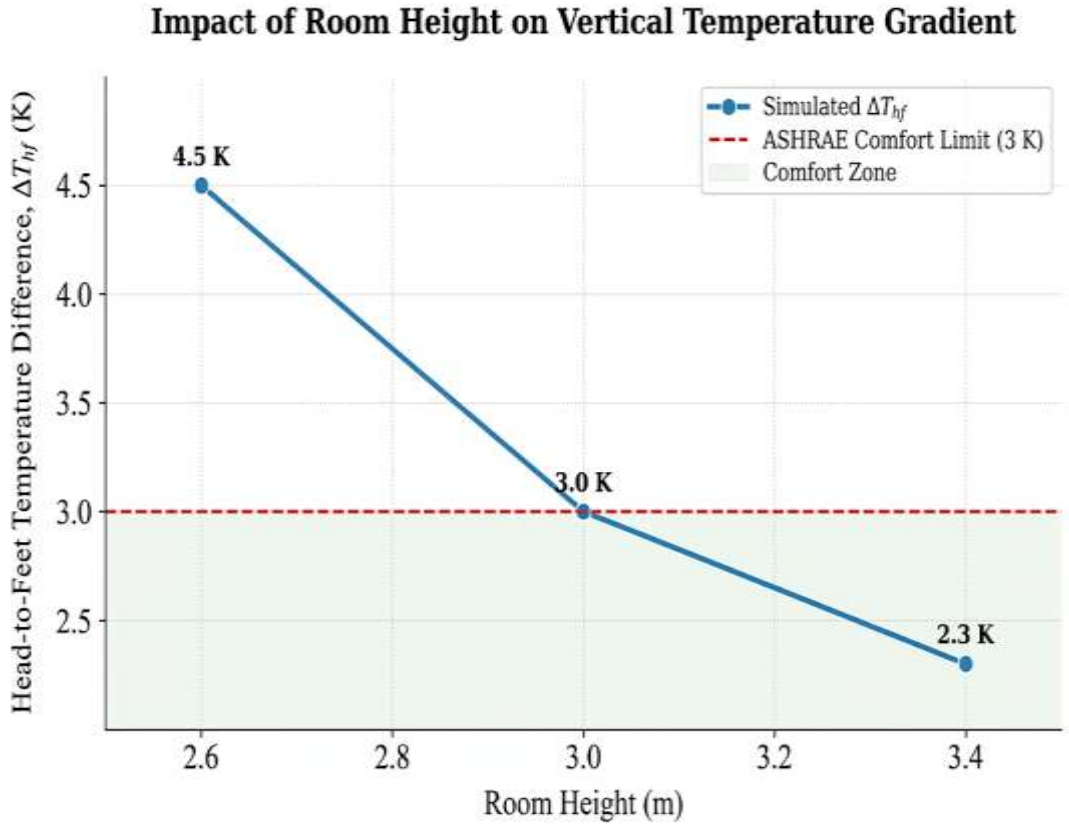

Figure 44: Temperature gradient vs ceiling height

Another way to look at the DV's sensitivity to envelope height is the vertical plot at the center of the room showing the age of air. The first case, with a height of 2.6 m, can be seen with an age profile with the blue zone reaching up to the ceiling. And there can also be seen numerous points with a high local mean age of air that are near the occupant zone. Under such a low ceiling height, the given amount of volumetric heat gain generates a thermal plume, which doesn't get enough vertical height for stratification. This causes localized mixing, which destroys the overall stratification layers of air, thus decreasing both thermal comfort and IAQ perfromance in DV (Villafruela et al., 2019). On moving to the cases with higher ceiling height, like 3m and 3.4 m, the local mean age of air profile can be seen as much more stable. This can be attributed to more vertical space above the occupant zone, where the thermal plume generated from the lower zone can get stably stratified. Thus, the local mean age of air profile can be seen

as the most stable for the case with a 3.4 m envelope height, as given in Figure 45. This sort of stratification pattern can also be seen for the CO_2 concentration, velocity, etc.

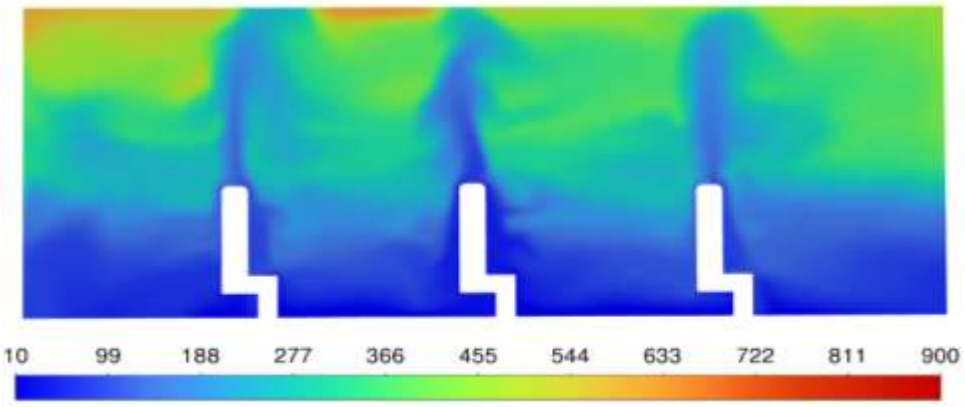

Age of air profile at 2.6 m Height

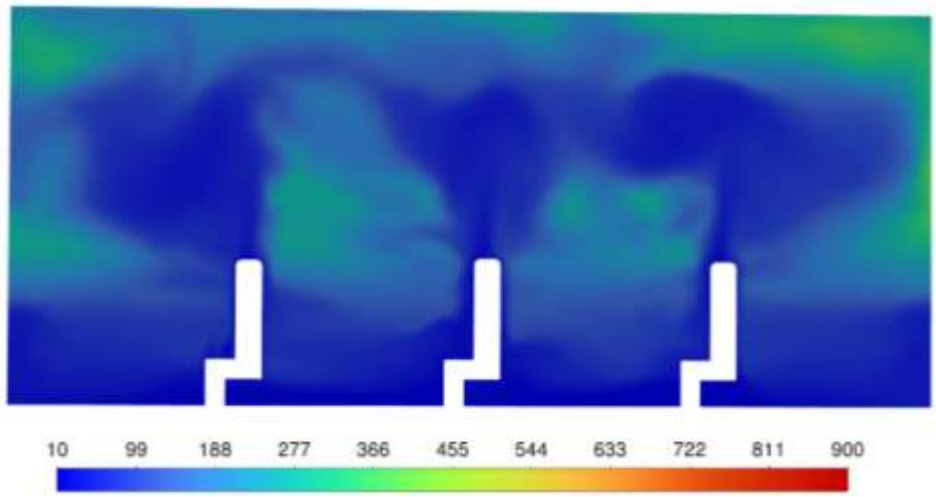

Age of air profile at 3 m height

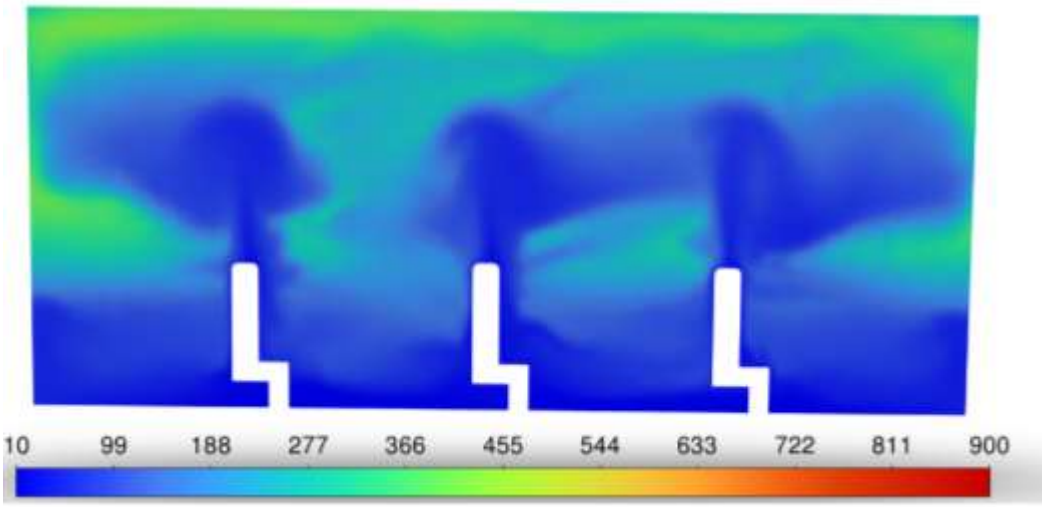

Age of air profile at 3.4 m Height

Figure 45: Mean age of air contour under different ceiling heights

4.8 Discussion

The results from the simulation and numerical analysis of two types of MV and a DV were briefly studied using different parameters related to thermal comfort and IAQ. The thermal comfort study included two parameters, namely, the thermal sensation and thermal effectiveness of ventilation. The value of thermal sensation under a given type of ventilation system was found to remain unchanged, regardless of where the cooling load is concentrated. Meanwhile, the other parameter for thermal comfort, which is the thermal effectiveness, is found to be somewhat affected by the cooling load concentration. Talking about the parameters related to IAQ, which in this case are contaminant removal effectiveness and age of air, they can be seen as affected by both the ventilation system and where the majority of the cooling load is coming from. The results from the simulation showed DV with the best performance among the three if looked along with the basic parameters like thermal effectiveness and contaminant removal effectiveness. But, if looked at with the more sophisticated air quality number, the mixing ventilation with the ceiling outlet is seen with the highest air quality number. That can be attributed to the uniform mixing MV with the ceiling outlet provides, thus keeping a minimal mean age of air, which gives a higher air quality number despite the contaminant removal efficiency slightly behind. Talking about the thermal comfort number which is a combination of both the thermal sensation and thermal effectiveness of ventilations sytem, DV is seen with the highest value. This lies with the fact that DV is based on thermal stratification, where the air in the upper space near the outlet is substantially hotter than that at the lower occupant space and inlet. This gives a higher value for the thermal effectiveness, thus giving a high thermal comfort number.

Looking at the result attained from the simulation performed under different envelope heights, DV was seen performing better as the envelope height increased. On the contrary, the two MV arrangements were seen with decreasing performance when the envelope height was increased. This was attributed to the fact that MV relies on turbulent mixing to achieve a uniform thermal environment. With a higher envelope height, MV may not be able to deliver perfect mixing, as in such a case, the incoming air often gets recirculated towards the outlet without reaching all the stagnant zones and pockets. This also indicated MV requires more CFM to facilitate a uniform thermal environment as the envelope height increases, despite the internal heat gain remaining

the same. On the contrary, DV was seen performing better under cases with higher envelope height, with very high values for IAQ parameters compared to MV.

Thus, DV was seen as suitable for spaces that have a substantial amount of occupant-level or floor-dominant heat gains. Also, DV was seen as suitable for spaces with substantial vertical height enough to develop strong stratification. Meanwhile, MV was seen as suitable for spaces with uniform heat gain and lower envelope height. However, MV can still perform under higher envelope height, but with extra CFM required, which implies a fall in its energy efficiency for such spaces. Another crucial parameter for selection between MV and DV was the type of ventilation system desired. In some cases, IAQ parameters like mean age or air, air exchange, contaminant removal, etc., may fall under higher priority, whereas in other cases, thermal comfort may be the priority. In cases that require better IAQ parameters, DV was seen as suitable, as the stratification-based ventilation strategy was seen as very effective in contaminant removal. This was attributed to the thermal plume-driven displacement of contaminants that creates a stratified region separating the contaminants from the occupant zone.

Chapter 5: CONCLUSIONS AND RECOMMENDATIONS

5.1 Conclusions

The following conclusions have been drawn from the simulations and numerical analysis done for the different types of ventilation systems.

I. The localized concentration of heat gain within the envelope space affects both thermal comfort and IAQ parameters. Though the effects weren't seen as vital when looked at with basic indices like temperature and velocity field, the advanced thermal comfort and IAQ parameters were found useful in analyzing the effects.

II. DV was seen as more affected by localized heat gain, as its thermal comfort and air quality numbers fluctuated by 4% and 20% under different heat distribution cases. Likewise, the overall ADI value fluctuated around 13.7%. DV relies on thermal plume for stable stratification, which directly depends on the location of the heat source; it generally requires more heat gain in the occupant space.

III. MV was seen as less affected by localized heat gain, as its thermal comfort and air quality numbers fluctuated by 4.35% and 7.55% under different heat distribution cases. Likewise, the overall ADI value fluctuated around 6 %. MV relies on a turbulent mixing-based uniform environment, which directly depends on the uniformity of the heat source; it generally requires more uniform heat gain throughout the envelope space.

IV. MV with floor outlet was seen as moderately affected by localized heat gain, as its thermal comfort and air quality numbers fluctuated by 5% and 16.87 % under different heat distribution cases. Likewise, the overall ADI value fluctuated around 10.5 %. The system's sensitivity to heat distribution, despite being based on turbulent mixing, was attributed to its near-floor outlet, which often comes with the risk of a short circuit.

V. The vertical envelope height directly affects the performance of the ventilation system despite the same internal heat gain value. This was the reason DV was seen performing better under higher vertical envelope height, whereas MV was seen failing short to deliver with the same CFM value.

VI. In DV, the effect can be studied in more detail using the dimensionless numbers like Archimedes' number (Ar) or even Richardson number (Ri).For the given heat

gain, a minimal height of 3m was determined for a stable Ri number, leading to stable DV.

VII. DV was found effective for spaces that require better IAQ parameters and energy efficiency ventilation system. But its sensitivity to envelope height or geometry and heat gain characteristics of the envelope was to be considered as well to get the best out of DV.

VIII. MV was seen working well, maintaining a uniform thermal environment, but its application in spaces with higher envelope height may sometimes be seen as less energy efficient compared to its DV counterpart. Also, MV may not be suitable for spaces that require an IAQ-centered ventilation system, like labs, special care units, etc., as it works towards mixing the overall room air, creating uniform diffusion of contaminants in the space.

5.2 Recommendation

I. CFD-based method can be applicable towards designing a ventilation system with desired thermal comfort and IAQ characteristics.

II. The current study can be extended by including a more detailed dimensionless approach towards studying the effects of space geometry, heat concentration on thermal comfort, and IAQ parameters. Local Ar, Ri, and Gr numbers can be used to determine the different critical flow zones within the envelope space.

III. Displacement ventilation was found to be working best under moderate cooling loads, like major cities of Nepal, Kathmandu, Pokhara, to name a few. The moderate summer and humidity across such cities make DV highly effective. With the increasing focus of energy efficient building, DV can be a way to go ahead. However, critical factors like ceiling height, space restriction, etc., should always be taken care of to exploit DV at optimal effectiveness.

IV. Displacement ventilation, though mainly used for cooling, a precise integration of DV and radiant floor heating or preheated air-based controlled mixing can allow the ventilation strategy to become more versatile for climate conditions like Kathmandu. However, if it is about limited space and optimal thermal comfort, then mixing ventilation will always be ahead of displacement ventilation.

REFERENCES

Almesri, I., Awbi, H. B., Foda, E., & Sirén, K. (2013a). An Air Distribution Index for Assessing the Thermal Comfort and Air Quality in Uniform and Nonuniform Thermal Environments. *Indoor and Built Environment*, *22*(4), 618–639. https://doi.org/10.1177/1420326X12451186

Almesri, I., Awbi, H. B., Foda, E., & Sirén, K. (2013b). An Air Distribution Index for Assessing the Thermal Comfort and Air Quality in Uniform and Nonuniform Thermal Environments. *Indoor and Built Environment*, *22*(4), 618–639. https://doi.org/10.1177/1420326X12451186

An, I.-H., Park, S.-H., Lee, Y.-H., Lee, C.-H., Seo, S.-B., Cho, S.-H., Lee, H.-W., & Yook, S.-J. (2024). Comparison of Local Mean Age of Air between Displacement Ventilation System and Mixing Ventilation System in Office Heating Conditions during Winter. *Buildings*, *14*(1), 115. https://doi.org/10.3390/buildings14010115

Aziz, M. A., Gad, I. A. M., Mohammed, E. S. F. A., & Mohammed, R. H. (2012). Experimental and numerical study of influence of air ceiling diffusers on room air flow characteristics. *Energy and Buildings*, *55*, 738–746. https://doi.org/10.1016/j.enbuild.2012.09.027

Causone, F., Baldin, F., Olesen, B. W., & Corgnati, S. P. (2010). Floor heating and cooling combined with displacement ventilation: Possibilities and limitations. *Energy and Buildings*, *42*(12), 2338–2352. https://doi.org/10.1016/j.enbuild.2010.08.001

Chen, H., Zhou, X., Feng, Z., & Cao, S.-J. (2022). Application of polyhedral meshing strategy in indoor environment simulation: Model accuracy and computing time. *Indoor and Built Environment*, *31*(3), 719–731. https://doi.org/10.1177/1420326X211027620

Dominguez Espinosa, F. A., & Glicksman, L. R. (2017). Determining thermal stratification in rooms with high supply momentum. *Building and Environment*, *112*, 99–114. https://doi.org/10.1016/j.buildenv.2016.11.016

Dos Reis, A. S., Vaquero, P., Dias, M. F., & Tavares, A. (2022). Passive Discomfort Index as an alternative to Predicted Mean Vote and Predicted Percentage of Dissatisfied to assess occupant's thermal discomfort in dwellings. *Energy Reports*, *8*, 956–965. https://doi.org/10.1016/j.egyr.2022.07.128

Foda, E., & Sirén, K. (2012). A thermal manikin with human thermoregulatory control: Implementation and validation. *International Journal of Biometeorology*, *56*(5), 959–971. https://doi.org/10.1007/s00484-011-0506-6

Franco, A., & Schito, E. (2020). Definition of Optimal Ventilation Rates for Balancing Comfort and Energy Use in Indoor Spaces Using CO2 Concentration Data. *Buildings*, *10*(8), 135. https://doi.org/10.3390/buildings10080135

Javed, S., Ørnes, I. R., Dokka, T. H., Myrup, M., & Holøs, S. B. (2021). Evaluating the Use of Displacement Ventilation for Providing Space Heating in Unoccupied Periods Using Laboratory Experiments, Field Tests and Numerical Simulations. *Energies*, *14*(4), 952. https://doi.org/10.3390/en14040952

Jiang, Z., & Haghighat, F. (1993). Ventilation Effectiveness in a Partitioned Office with Displacement Ventilation Determined by Computer Simulation. *Indoor Environment*, *2*(5–6), 365–373. https://doi.org/10.1177/1420326X9300200517

Khan, M. A. H., Bennia, A., Lateb, M., & Fellouah, H. (2022). Numerical investigation of thermal comfort using the mixing and displacement ventilation systems within a fitting room. *International Journal of Heat and Mass Transfer*, *198*, 123379. https://doi.org/10.1016/j.ijheatmasstransfer.2022.123379

Khan, M. A. H., Mboreha, C. A., & Abdelrahman, H. (2022). A Comparison of Mixing and Displacement Ventilation System in an Office Environment Using Computational Fluid Dynamics. In A. N. R. Reddy, D. Marla, M. N. Favorskaya, & S. C. Satapathy (Eds), *Intelligent Manufacturing and Energy Sustainability* (Vol. 265, pp. 95–105). Springer Singapore. https://doi.org/10.1007/978-981-16-6482-3_10

Lastovets, N., Kosonen, R., Mustakallio, P., Jokisalo, J., & Li, A. (2020). Modelling of room air temperature profile with displacement ventilation. *International Journal of Ventilation*, *19*(2), 112–126. https://doi.org/10.1080/14733315.2019.1579486

Li, H., Liu, R., Lan, Y., Kong, X., Jia, J., & Fan, M. (2025). *Threshold-Driven Ventilation Strategy Selection for Public Buildings: Quantifying Ceiling Height Effects on Energy, Comfort, and Infection Control*. SSRN. https://doi.org/10.2139/ssrn.5377086

Liu, S., Koupriyanov, M., Paskaruk, D., Fediuk, G., & Chen, Q. (2022). Investigation of airborne particle exposure in an office with mixing and displacement

ventilation. *Sustainable Cities and Society*, *79*, 103718. https://doi.org/10.1016/j.scs.2022.103718

Makris, R., Kopic, C., Tawackolian, K., Schumann, L., & Kriegel, M. (2025). Experimental comparison of aerosol transmission in displacement ventilation and mixing ventilation in a meeting scenario. *International Journal of Ventilation*, *24*(1), 53–75. https://doi.org/10.1080/14733315.2024.2406153

Menchaca-Brandan, M. A., Dominguez Espinosa, F. A., & Glicksman, L. R. (2017). The influence of radiation heat transfer on the prediction of air flows in rooms under natural ventilation. *Energy and Buildings*, *138*, 530–538. https://doi.org/10.1016/j.enbuild.2016.12.037

Ning, M., Mengjie, S., Mingyin, C., Dongmei, P., & Shiming, D. (2016). Computational fluid dynamics (CFD) modelling of air flow field, mean age of air and CO2 distributions inside a bedroom with different heights of conditioned air supply outlet. *Applied Energy*, *164*, 906–915. https://doi.org/10.1016/j.apenergy.2015.10.096

Pan, C.-Y., Weng, K.-T., & Hsu, H.-C. (2024). Air change per hour improvement for positive and negative pressure mechanical ventilation facilities systems. *Journal of Building Engineering*, *83*, 108414. https://doi.org/10.1016/j.jobe.2023.108414

Qiu-Wang, W., & Zhen, Z. (2006). Performance comparison between mixing ventilation and displacement ventilation with and without a cooled ceiling. *Engineering Computations*, *23*(3), 218–237. https://doi.org/10.1108/02644400610652965

Rees, S. J., & Haves, P. (2013). An experimental study of air flow and temperature distribution in a room with displacement ventilation and a chilled ceiling. *Building and Environment*, *59*, 358–368. https://doi.org/10.1016/j.buildenv.2012.09.001

Ribeiro, A. S., Alves E Sousa, J., Cox, M. G., Forbes, A. B., Matias, L. C., & Martins, L. L. (2015). Uncertainty Analysis of Thermal Comfort Parameters. *International Journal of Thermophysics*, *36*(8), 2124–2149. https://doi.org/10.1007/s10765-015-1888-1

Sinopoli, J. (2010). What Is a Smart Building? In *Smart Building Systems for Architects, Owners and Builders* (pp. 1–5). Elsevier. https://doi.org/10.1016/B978-1-85617-653-8.00001-6

Srebric, J., & Chen, Q. (2002). Simplified Numerical Models for Complex Air Supply Diffusers. *HVAC&R Research*, *8*(3), 277–294. https://doi.org/10.1080/10789669.2002.10391442

Villafruela, J. M., Olmedo, I., Berlanga, F. A., & Ruiz De Adana, M. (2019). Assessment of displacement ventilation systems in airborne infection risk in hospital rooms. *PLOS ONE*, *14*(1), e0211390. https://doi.org/10.1371/journal.pone.0211390

Wang, C., & Hong, J. (2023). Numerical investigation of airborne transmission in low-ceiling rooms under displacement ventilation. *Physics of Fluids*, *35*(2), 023321. https://doi.org/10.1063/5.0137354

Yadav, A., Samykano, M., Pandey, A. K., Natarajan, S. K., Vasudevan, G., Muthuvairavan, G., & Suraparaju, S. K. (2024). Sustainable phase change

material developments for thermally comfortable smart buildings: A critical review. *Process Safety and Environmental Protection*, *191*, 1918–1955. https://doi.org/10.1016/j.psep.2024.09.025

Yang, R., Ng, C. S., Chong, K. L., Verzicco, R., & Lohse, D. (2022). Do increased flow rates in displacement ventilation always lead to better results? *Journal of Fluid Mechanics*, *932*, A3. https://doi.org/10.1017/jfm.2021.949

Yuan, J., Wang, L., He, Z., & Liu, X. (2013). The Research of Performance Comparison of Displacement and Mixing Ventilation System in Catering Kitchen. *Journal of Environmental Protection*, *04*(06), 638–646. https://doi.org/10.4236/jep.2013.46073

Zhao, W., Mustakallio, P., Lestinen, S., Kilpeläinen, S., Jokisalo, J., & Kosonen, R. (2022). Numerical and Experimental Study on the Indoor Climate in a Classroom with Mixing and Displacement Air Distribution Methods. *Buildings*, *12*(9), 1314. https://doi.org/10.3390/buildings12091314

ANNEXES

Annex-1: Cooling load calculation

Parameter	**Values**
Total(Btu/hr)	21589.78
(Tons)	1.80
Calculation for the Required CFM for cooling	
Desired Indoor Temperature(DBT)	74.00
Desired Indoor Humidity(RH)	50.00
Inlet Supply Temperature(DBT)	64.40
Desired Indoor Temperature	
Cooling Load (Q) (Kw)	6.33
Sensible Cooling Load (Q_s) (BTU/hr)	13979.41
Latent Cooling load (Q_l) (BTU/hr)	7610.37
Difference between supply and indoor air (degree Celcius)	
Using the Sensible heat formula to get the CFM	
CFM	1348.32314
Humidity Difference(W)(lb water/lb dry air)	0.001166182
Supply Air Relative Humidity (Psychometric Chart)	42%
Calculation for Diffuser	
Desired CFM per Diffuser	337.080785
Face velocity Desired (m/s)	3
Size of Diffuser (l*b)	9 in *9in
Return Outlet Sizing	
CFM	1348.32314
Targeted Face Velocity(m/s)	2.5
Required Area(m^2)	0.254509476
Size of Square Return Grille (I*l) (m)	0.504489322

Parameter	**Values**	
Room Dimensions	23'-0"x12'-6"	
Height (m)	3	
Lehght(m)	7	
Width(m)	3.8	
Floor Area(m^2)	26.6	
Room Volume(Cubic meter)	79.8	
Floor Area per Person(m^2 /Person)	4.43333333	
Total Sensible Heat (W)	4095.97	
DV Requires Heat load separation into those located in occupied (Qoc)and unoccupied(Qmx) zones		
Aoc	0.295	
Amx	0.132	
Air Change Rate (n)		
Numerator(Qoc(W)*Aoc+(Qmx)(W)*Amx)	1008.01782	
Qoc(W)	2867.17788	
(Qmx)(W)	1228.79052	
Maximum Tmeperature Difference between head and foot(T)(F)	5	ASHRAE Standard 55-1192,
ACH(n) (3600*Numerator/T*ρ*Cp*H*A)	3.4	
Volume Flow Rate (meter cube per second)(ACH*H*A/3600)	0.075	
Design Temperature(F)	74	
Temperature at Floor(F)	69	
Dimensionless temperature at the floor	0.42	
Supply Temperature(F)	65.4	

Annex-2: Important formulas

$$\Delta T_{hf} = \frac{(a_{oc}Q_{oc} + a_{mx}Q_{mx})}{\rho C_p V} \qquad (5.2)$$

where

a_{oc} and a_{mx} = the coefficients for the fraction of the cooling loads entering the space between the head and feet of a sedentary person

Values for a_{oc} and a_{mx} are 0.295 and 0.132 respectively, based on empirical data that represents most U.S. buildings with the exception of large atria and theaters (Chen & Glicksman, 2003).

$$n = \frac{3600}{\Delta T_{hf}\ \rho C_p H\ A}(a_{oc}Q_{oc} + a_{mx}Q_{mx}) \qquad \frac{T_f - T_s}{T_e - T_s}$$

θ_f can be represented by the following [REHVA, 2002]:

$$\theta_f = \frac{1}{\frac{(\rho\ C_p)}{A}\left(\frac{1}{\alpha_r} + \frac{1}{\alpha_{cf}}\right) + 1} \qquad (5.7)$$

where

α_r = the heat transfer coefficient due to radiation (≈ 5 W/m^2 • K, 1 Btu/h • ft^2 • °F)

α_{cf} = heat transfer coefficient at the floor due to convection ($\approx$5 W/m^2 • K, 1 Btu/h • ft^2 • °F)

Annex-3: Breathing zone ventilation rates

TABLE 6-1 MINIMUM VENTILATION RATES IN BREATHING ZONE
(This table is not valid in isolation; it must be used in conjunction with the accompanying notes.)

Occupancy Category	People Outdoor Air Rate R_p		Area Outdoor Air Rate R_a		Notes	Default Values			Air Class
						Occupant Density (see Note 4)	Combined Outdoor Air Rate (see Note 5)		
	cfm/person	L/s·person	cfm/ft^2	L/s·m^2		#/1000 ft^2 or #/100 m^2	cfm/person	L/s·person	
Correctional Facilities									
Cell	5	2.5	0.12	0.6		25	10	4.9	2
Dayroom	5	2.5	0.06	0.3		30	7	3.5	1
Guard stations	5	2.5	0.06	0.3		15	9	4.5	1
Booking/waiting	7.5	3.8	0.06	0.3		50	9	4.4	2
Educational Facilities									
Daycare (through age 4)	10	5	0.18	0.9		25	17	8.6	2
Daycare sickroom	10	5	0.18	0.9		25	17	8.6	3
Classrooms (ages 5–8)	10	5	0.12	0.6		25	15	7.4	1
Classrooms (age 9 plus)	10	5	0.12	0.6		35	13	6.7	1
Lecture classroom	7.5	3.8	0.06	0.3		65	8	4.3	1
Lecture hall (fixed seats)	7.5	3.8	0.06	0.3		150	8	4.0	1
Art classroom	10	5	0.18	0.9		20	19	9.5	2
Science laboratories	10	5	0.18	0.9		25	17	8.6	2
University/college laboratories	10	5	0.18	0.9		25	17	8.6	2
Wood/metal shop	10	5	0.18	0.9		20	19	9.5	2
Computer lab	10	5	0.12	0.6		25	15	7.4	1
Media center	10	5	0.12	0.6	A	25	15	7.4	1
Music/theater/dance	10	5	0.06	0.3		35	12	5.9	1
Multi-use assembly	7.5	3.8	0.06	0.3		100	8	4.1	1

Annex-4: IOE GC acceptance letter

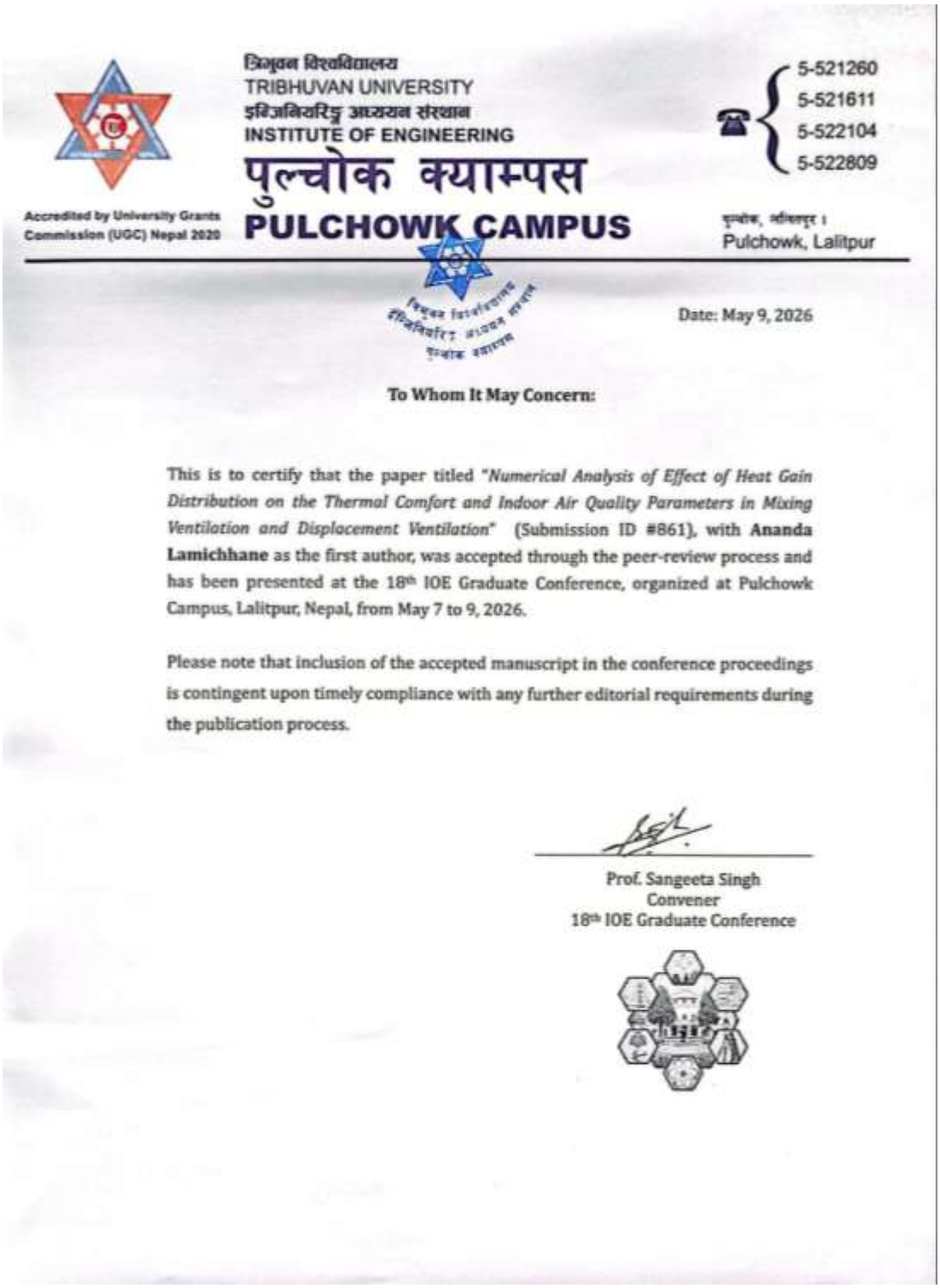

त्रिभुवन विश्वविद्यालय
TRIBHUVAN UNIVERSITY
इन्जिनियरिङ्ग अध्ययन संस्थान
INSTITUTE OF ENGINEERING
पुल्चोक क्याम्पस
PULCHOWK CAMPUS

Accredited by University Grants Commission (UGC) Nepal 2020

5-521260
5-521611
5-522104
5-522809

पुल्चोक, ललितपुर ।
Pulchowk, Lalitpur

Date: May 9, 2026

To Whom It May Concern:

This is to certify that the paper titled "*Numerical Analysis of Effect of Heat Gain Distribution on the Thermal Comfort and Indoor Air Quality Parameters in Mixing Ventilation and Displacement Ventilation*" (Submission ID #861), with **Ananda Lamichhane** as the first author, was accepted through the peer-review process and has been presented at the 18th IOE Graduate Conference, organized at Pulchowk Campus, Lalitpur, Nepal, from May 7 to 9, 2026.

Please note that inclusion of the accepted manuscript in the conference proceedings is contingent upon timely compliance with any further editorial requirements during the publication process.

Prof. Sangeeta Singh
Convener
18th IOE Graduate Conference

Annex-5: Plagiarism check

Influence Of Internal Heat Loads and Ceiling Heights on The Effectiveness Of Displacement and Mixing Ventilation for a Room

Ananda Lamichhane

080MSMDEThesis (1).docx

Tribhuvan University

Document Details

Submission ID
trn:oid:::3117:587802005

Submission Date
May 8, 2026, 6:56 AM GMT+5:45

Download Date
May 8, 2026, 7:03 AM GMT+5:45

File Name
080MSMDEThesis (1).docx

File Size
14.3 MB

102 Pages

19,344 Words

103,858 Characters

iThenticate Page 1 of 114 - Cover Page Submission ID trn:oid:::3117:587802005

iThenticate Page 2 of 114 - Integrity Overview Submission ID trn:oid:::3117:587802065

12% Overall Similarity

The combined total of all matches, including overlapping sources, for each database

Filtered from the Report

- Bibliography
- Quoted Text
- Cited Text
- Small Matches (less than 8 words)

Custom Section Exclusions

(titlesCount) Section Titles, (keywordsCount) Keywords

Section title	No. of Section Starters	Section Starters
"Acknowledgements"	4	Acknowledgements Acknowledgement Acknowledgment Acknowledgments

Match Groups

- 210 Not Cited or Quoted 12%
  Matches with neither in-text citation nor quotation marks
- 0 Missing Quotations 0%
  Matches that are still very similar to source material
- 0 Missing Citation 0%
  Matches that have quotation marks, but no in-text citation
- 0 Cited and Quoted 0%
  Matches with in-text citation present, but no quotation marks

Top Sources

9% Internet sources
10% Publications
0% Submitted works (Student Papers)

Integrity Flags

1 Integrity Flag for Review

Replaced Characters
28 suspect characters on 4 pages
Letters are swapped with similar characters from another alphabet.

Our system's algorithms look deeply at a document for any inconsistencies that would set it apart from a normal submission. If we notice something strange, we flag it for you to review.

A Flag is not necessarily an indicator of a problem. However, we'd recommend you focus your attention there for further review.

iThenticate Page 2 of 114 - Integrity Overview Submission ID trn:oid:::3117:587802065